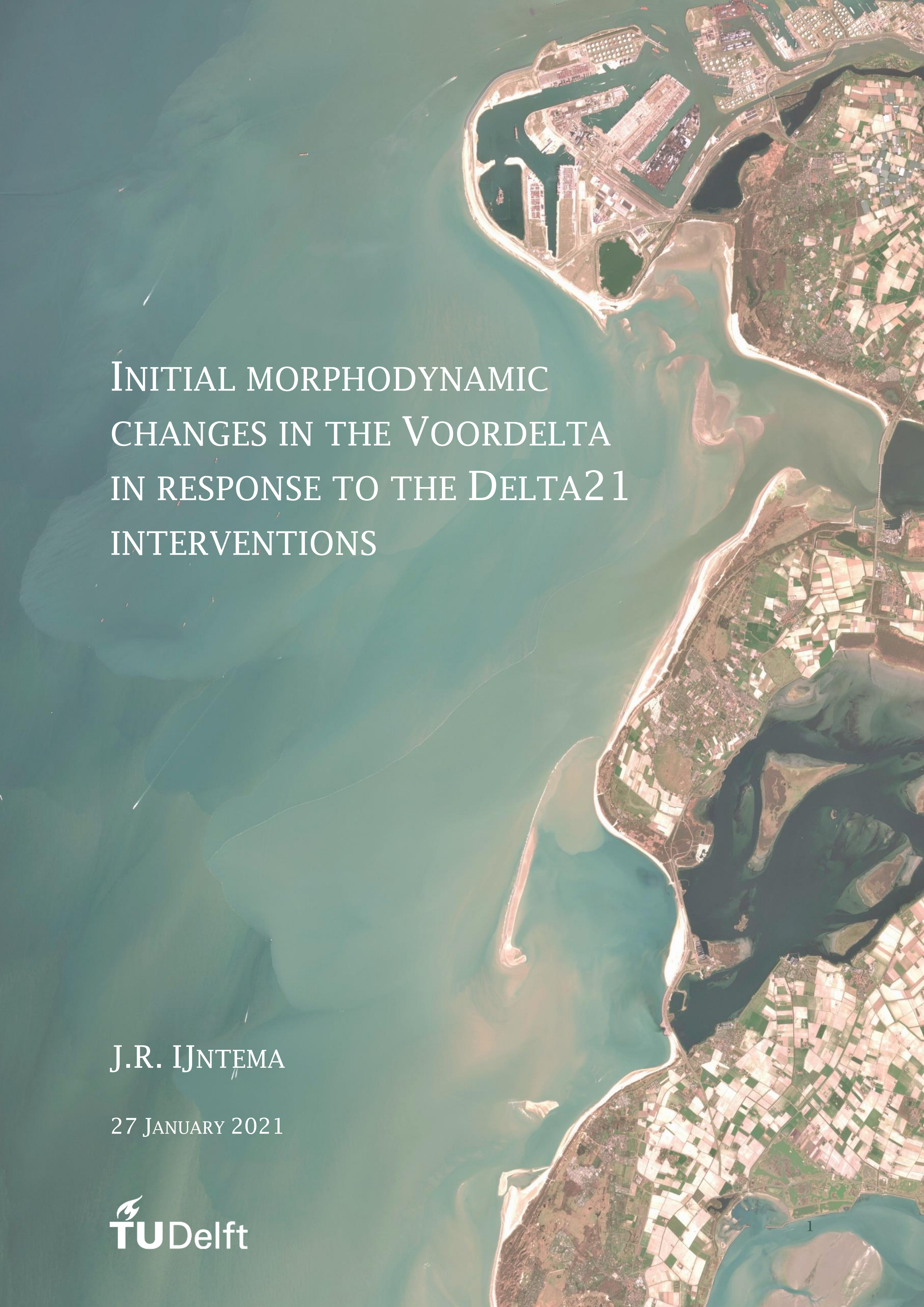

# Initial morphodynamic changes in the Voordelta in response to the Delta21 interventions

J.R. IJntema

27 January 2021

# INITIAL MORPHODYNAMIC CHANGES IN THE VOORDELTA IN RESPONSE TO THE DELTA21 INTERVENTIONS


By

J.R. (Jelmer) IJntema

student number: 4744373


In partial fulfilment of the requirements for the degree of:

**Master of Science**

in Civil Engineering


Delft University of Technology
27 January 2021


| | | | |
|---|---|---|---|
| Thesis committee: | Prof. Dr. Ir. S.G.J. (Stefan) Aarninkhof | *Chairman* | TU Delft |
| | Ir. M. (Martijn) Onderwater | *First supervisor* | Arcadis |
| | Dr. Ir. A.P. (Arjen) Luijendijk | *Second supervisor* | TU Delft |
| | Dr. Ing. M.Z. (Mark) Voorendt | *Third supervisor* | TU Delft |

In collaboration with:

| | | |
|---|---|---|
| | Ir. H.A. (Huub) Lavooij | Delta21 |
| | Drs. L. (Leen) Berke | Delta21 |

*Cover: Modified Sentinel data retrieved from EO Browser, Sinergise Ltd.*

# ACKNOWLEDGEMENTS

This thesis concludes my journey of the Master of Science program in Hydraulic Engineering at Delft University of Technology. This research was conducted as part of the Delta21 initiative in collaboration with the multidisciplinary Delta Futures lab network of Delft University of Technology. I am grateful for the opportunity to work on such an innovative and ambitious project within an open minded and interdisciplinary group of researchers.

This study would not have been possible without the critical feedback, support and time of my graduation committee. Therefore, I would like to thank the committee members, Stefan Aarninkhof, Martijn Onderwater, Arjen Luijendijk and Mark Voorendt. Stefan Aarninkhof, thank you for your positive criticism and your thorough insights that made me question my choices and at the same time kept me on the right track. Martijn Onderwater, thank you for all your time and guidance. Especially during all the model simulations when you even asked the expertise of some of your colleagues at Arcadis to help me out. Arjen Luijendijk, thank you for your expertise during the setup of the Delft3D model. Thanks for challenging me to create a model that fitted the purpose of this research. I learned a great deal. Mark Voorendt, thank you for looking at this research from another point of view. You helped me to overlook my report in order to discover the parts that might be unclear for people other than myself. Also, I would like to thank Jan van Overeem who helped me starting up my research even though he was already working towards his retirement.

Additionally, I want to thank the Delta21 initiators Huub Lavooij and Leen Berke for conceiving the project. I would like to express my gratitude for your open mindset despite the challenges such an initiative brings. You helped me by using your great network of companies which led me to Anne de Beer and Jasper Leuven from Royal Haskoning DHV. Anne and Jasper, thank you for your time during the COVID pandemic in which you, from a distance, provided me with useful feedback, advice and site information that helped me during all stages of my research.

Further, I would like to thank all my Hydraulic friends who were always there during my time here in Delft for both on- and off-campus activities. You helped me through the difficult parts of my studies, but more importantly, you have been the perfect group to hang out with when it was needed.

Last but not least, I want to give my complete gratitude to my family. Thanks to my parents for their support, love and interest in my field of work. Thanks to my girlfriend Gali and my sister Femke, not only for their feedback and grammar check but mostly because of your listening ear. Mijn opa, oma en pake wil ik in het bijzonder bedanken voor het feit dat ze altijd hebben laten zien hoe trots ze zijn en me daarmee enorm hebben gesteund.

*Jelmer IJntema*
*Delft, January 2021*

# SUMMARY


In recent years, the awareness of climate change and sea level rise has grown. Especially in low lying countries like the Netherlands, with a large river delta with a high economical and natural value, extreme variations in water levels will have great impact. Former used solutions proofed to be expensive and in some cases disturbed the dynamics of nature. Consequently, the need of new solutions of flood protections grows in which the negative impact on nature environments should be limited.

The Delta21 plan proposes a future-proof design for the Dutch Southwest delta, that aims to tackle the growing need for flood protection, while contributing to nature and storing energy all at once. However, the coastal structure, located in the Haringvliet mouth, is likely to produce large disturbances in the environment. Since the Haringvliet mouth is located in the 'Voordelta', a Natura2000 area, it is essential to study the initial response of the proposed interventions to the hydraulics and morphodynamics that shape the system. Hence, the objective of this research is to determine the initial impact of the Delta21 plan on the large scale multi-year average hydro- and morphodynamics of the Northern Voordelta.

To this end, a literature review was performed to analyse the evolvement of the Northern Voordelta since the closure of the Grevelingen and Haringvliet estuaries by the Delta Works in 1970. This study showed that the closure caused the tidal prisms to reduce strongly resulting in the tidal propagation to change from cross-shore to longshore. The remaining ebb tidal deltas started to follow the characteristics of a short basin, in which water levels offshore and nearshore are in phase. Flow velocities reduced strongly and channels started to fill up, at the foreshore waves started to dominate the morphodynamics. Waves began to 'bulldoze' the former ebb-tidal deltas onshore, creating shore parallel sandbars like the Bollen van de Ooster and the Hinderplaat. Besides, the construction of the Maasvlakte 2 triggered further sedimentation of the Haringvliet mouth, landward of the Hinderplaat, by sheltering the area from NW waves.

The initial response of the system to Delta21 has been studied using a short-term morphostatic 2DH computational model simulation. The complexity of the processes inside the study area caused the need of the process based model Delft3D, in which flow, waves and sediment transport computations can be carried out. To reduce computational times, the applied modelling setup made use of reduction techniques and schematisations of the hydraulic forcing, while maintaining the natural character of the system. The computed flow and sediment transport patterns were used as indicators, in order to predict and compare the feedback of the system of the various scenarios.

Model results showed that the tidal propagation inside the Haringvliet estuary, which is opened in the Delta21 scenario, changes to cross-shore again. Similar to the situation prior to the closing, the area will start to follow the characteristics of a long-basin. This implies that water levels in the estuary are out of phase with the offshore water levels. A cross-shore tide dominated flow prevails in the area, while the Grevelingen delta remains unchanged in the Delta21 scenario. The cross-shore action influences the offshore wave- and setup-driven residual currents. In the same offshore area, the Delta21 pump discharge develops a similar cross-shore acting influence area. Model results further showed that the Delta21 geometry causes a 'tidal squeeze', similar to the present-day processes around Maasvlakte 2. Altogether, the large disturbances to the hydrodynamic forcing, triggers morphodynamic activity. Concluding from literature and the model results, this leads to the erosion and formation of ebb and flood channels in the Haringvliet mouth and the formation of an ebb- and flood-tidal delta around the inlet. Processes in and around the ebb-tidal delta adjust towards a balance between the wave and tidal action. These findings agree with the known processes of a mixed-energy tidal inlet system that is adjusting towards a dynamic equilibrium. Conceptualised results are shown in Figure 1.

Concluding, the analysis on the initial response of the system, as well as the expected initial dynamic behaviour, provides useful insight and a good basis for future optimisation studies on the Delta21 design. This study reveals the disturbed areas caused by the presence of Delta21 and relates it to the contribution of the various hydrodynamic processes. Furthermore, the development of this type of study can be significantly relevant to the evaluation of other preliminary studies on solutions to sea level rise.

# SAMENVATTING

In de afgelopen jaren is het bewustzijn van klimaatverandering en zeespiegelstijging gegroeid. Zeker in laag gelegen landen zoals Nederland, met een grote rivier delta dat een hoge economische waarde en natuurwaarde heeft, zullen extreme variaties in water standen grote impact hebben. Voorheen gebruikte oplossingen waren duur en verstoorden in sommige gevallen de dynamiek van de natuur. Als gevolg groeit de vraag naar nieuwe oplossingen voor hoog water bescherming.

Het Delta21 plan is een toekomst gericht voornemen voor de zuidwestelijke delta van Nederland, dat in gaat op de groeiende vraag naar oplossingen voor hoog water bescherming en tegelijkertijd streeft naar natuur herstel en energie opslag. Echter zal de voorgenomen constructie, gelegen in de Haringvliet monding, waarschijnlijk voor grote verstoringen van de natuurlijke dynamiek zorgen. Omdat de Haringvliet monding onderdeel is van de 'Voordelta', een Natura 2000 gebied, is het essentieel om de initiële reactie van de hydro- en morfodynamiek op de voorgenomen constructie te onderzoeken. Vandaar dat het doel van dit onderzoek is om vast te stellen wat de initiële impact van het Delta21 plan is op de grootschalige, meerjarig gemiddelde hydro- en morfodynamiek van de noordelijke Voordelta.

Om die reden is er een literatuuronderzoek gedaan om de ontwikkeling van de noordelijke Voordelta te onderzoeken, sinds het sluiten van de Grevelingen en Haringvliet estuaria in 1970 als onderdeel van de Deltawerken. Dit onderzoek heeft aangetoond dat de sluiting zorgde voor een flinke reductie van de getijde prisma's wat vervolgens resulteerde in een verandering van een kust dwarse naar een kust parallelle voortplanting van het getij. De overgebleven eb-getijdendelta's begonnen de karakteristieken van een kort bassin te volgen, waarin waterstanden op de Noordzee en aan de kust in fase zijn. De stroomsnelheden verminderden sterk en de geulen begonnen te sedimenteren, terwijl aan de zeewaartse kant van de eb-getijdendelta's de golven de morfodynamiek begonnen te domineren. De golven 'duwden' de voormalige eb-getijdendelta's kustwaarts waardoor kust parallelle zandbanken zoals de Bollen van de Ooster en de Hinderplaat ontstonden. Daarnaast zorgde de bouw van Maasvlakte 2 voor verdere sedimentatie van de Haringvliet monding, door het gebied te beschutten voor noordwestelijke golven.

De initiële reactie van de kust dynamiek op Delta21 is bestudeerd door middel van een korte-termijn simulatie van een morfostatisch 2DH numeriek model. De complexiteit van de processen in het onderzoeksgebied riep de vraag op voor het process-based model Delft3D, waarin stromingen, golven en sediment transport berekeningen uitgevoerd kunnen worden. Om de rekentijd te reduceren, zijn input reductie technieken toegepast en zijn processen geschematiseerd met behoud van het natuurlijke karakter van het systeem. De berekende stroom en sediment transport patronen zijn gebruikt als indicatoren om zo de feedback van het systeem op verschillende scenario's te voorspellen.

De model resultaten lieten zien dat het getij in het Haringvliet estuarium, dat geopend is in het Delta21 scenario, zich weer kust dwars voortplant. Vergelijkbaar met de situatie voor de sluiting begint het gebied de karakteristieken van een lang bassin te volgen. Dit betekent dat waterstanden in het estuarium uit fase zijn met de waterstanden op de Noordzee. Een kust dwarse stroom domineert in het Haringvliet gebied terwijl de Grevelingen monding juist onveranderd blijft in het Delta21 scenario. De kust dwarse processen van het getij beïnvloeden de offshore golf- en opzet-gedreven reststroming. In hetzelfde zeewaartse gebied zorgt de Delta21 pomp afvoer voor een vergelijkbare kust dwarse stroming. Model resultaten lieten verder zien dat de Delta21 geometrie voor een 'tidal squeeze' zorgt, vergelijkbaar met de processen rond Maasvlakte 2. Alles samengenomen, zorgen de grote veranderingen aan de hydrodynamiek voor een verhoging van de morfodynamische activiteit in de Haringvliet monding. Concluderend vanuit de literatuur en de model resultaten, leidt deze verhoging tot de verdieping en vorming van eb- en vloed-geulen in de Haringvliet monding met daarbij de vorming van een eb- en vloed-getijdendelta rond de inlaat. Processen in en rond de eb-getijdendelta passen zich aan naar een balans tussen de golf en getij energie. Deze bevindingen komen overeen met de bekende processen van een gemengd-energie getijde systeem dat zich aanpast naar een dynamisch evenwicht. De resultaten zijn geconceptualiseerd weergegeven in Figure 1.

Concluderend, de analyse van de initiële reactie van het systeem, met daarbij het verwachtte initiële dynamische gedrag, biedt nuttige inzichten en een goede basis voor toekomstige optimalisatie studies van het Delta21 plan. Deze studie onthult de verstoorde gebieden als gevolg van Delta21 en relateert het aan de bijdrage van de verscheidene hydrodynamische processen. Daarnaast, de ontwikkeling van dit type onderzoek kan significante relevantie hebben voor de evaluatie van andere preliminaire onderzoeken naar oplossingen voor zeespiegel stijging.

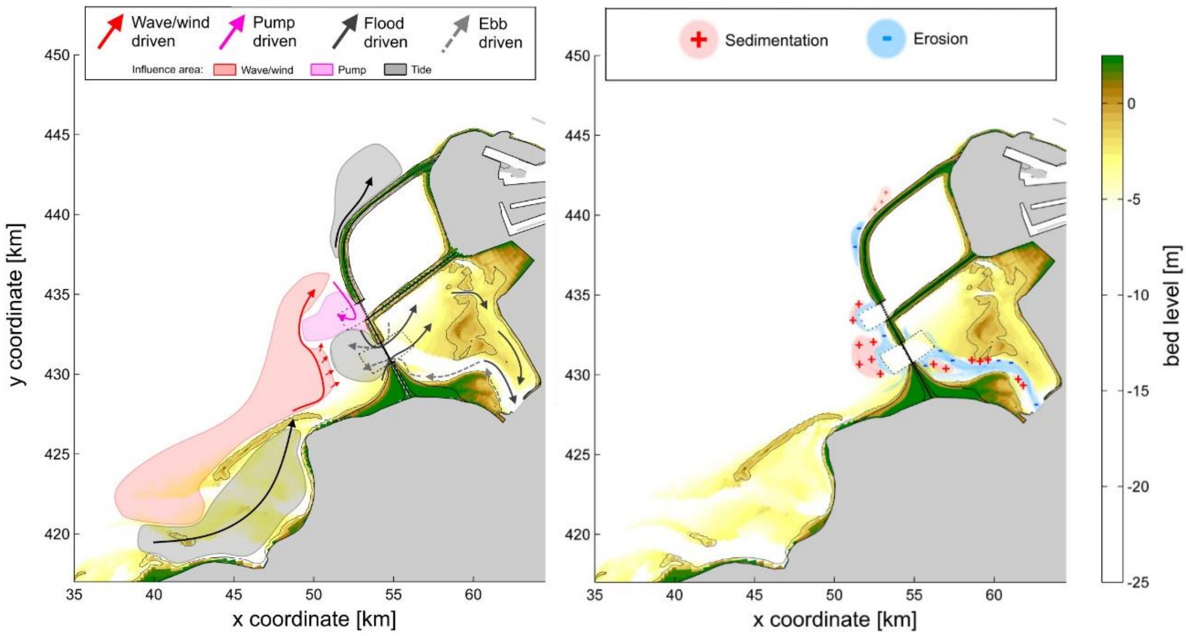


FIGURE 1: CONCEPTUALISED INITIAL HYDRAULICS (LEFT) AND MORPHODYNAMICS (RIGHT) IN PRESENCE OF DELTA21

# TABLE OF CONTENTS

Acknowledgements ..... iii
Summary ..... iv
Samenvatting ..... v
Chapter 1 Introduction ..... 1
1.1 Coastal structures in the Dutch delta ..... 1
1.2 Delta21: an integrated solution ..... 1
1.3 Natura 2000, The Voordelta ..... 4
1.4 Problem description ..... 6
1.5 Objective and research question ..... 6
1.6 Methodology and thesis outline ..... 8
Chapter 2 The Northern Voordelta ..... 9
2.1 Introduction ..... 9
2.2 The evolvement of the Northern Voordelta ..... 9
2.3 The hydrodynamic drivers ..... 14
2.4 The morphodynamics ..... 20
2.5 Concluding remarks ..... 22
Chapter 3 Model selection & framework ..... 24
3.1 Introduction ..... 24
3.2 Modelling study method ..... 24
3.3 Model software selection ..... 24
3.4 Model setup ..... 25
Chapter 4 Model input ..... 26
4.1 Introduction ..... 26
4.2 Delft3D setup ..... 26
4.3 Boundary conditions ..... 27
4.4 FLOW and WAVE module setup ..... 29
4.5 Calibration and validation ..... 29
Chapter 5 Model results and analyses ..... 30
5.1 Introduction ..... 30
5.2 Flow characteristics ..... 30
5.3 Residual currents ..... 39
5.4 Sediment transport characteristics ..... 41
Chapter 6 Conceptual model ..... 46
6.1 Introduction ..... 46
6.2 Conceptualising the expected response to Delta21 ..... 46

Discussion ........ 52
Model limitations ........ 52
Result interpretation ........ 53
Conclusions ........ 54
Recommendations ........ 58
Future research ........ 58
References ........ 59
Appendices ........ 62
Appendix A ........ 63
A.1 Introduction ........ 63
A.2 Wind roses ........ 63
Appendix B ........ 64
B.1 Introduction ........ 64
B.2 Wave conditions ........ 64
B.3 Main model parameter settings ........ 65
B.4 Water level dataset comparison ........ 66
Appendix C ........ 67
C.1 Introduction ........ 67
C.2 Residual flow pattern of simulation I. Tide only ........ 67
C.3 Residual currents of simulation III. All processes ........ 69
C.4 Additional flow patterns ........ 71
C.5 Residual flow magnitudes ........ 72
Appendix D ........ 74
D.1 Introduction ........ 74
D.2 Additional results regarding sediment transport ........ 74
D.3 Additional results regarding sedimentation/erosion patterns ........ 76
Appendix E ........ 78
E.1 Introduction ........ 78
E.2 Additional plots regarding the conceptual model ........ 78

# CHAPTER 1

# INTRODUCTION

## 1.1 COASTAL STRUCTURES IN THE DUTCH DELTA

In the Dutch delta, many large coastal engineering projects have been carried out. The purposes of these projects differ from expanding industrial and marina areas to flood protection. Examples of land reclamation projects are the Maasvlakte in 1964, the Slufter in 1986 and the Maasvlakte 2 in 2013. These large scale projects affected the hydraulics and therefore the morphology of the Dutch Southwest delta (Aarninkhof and Van Kessel 1999). In order to mitigate the impact of these projects on the morphology of the surrounding area, it is necessary to study and understand the morphological development caused by these interventions (Tönis, Stam et al. 2002).

Further, many of the coastal structures done in the Netherlands are related to flood defence. For many years, the Dutch fought against the rising water. About 25 percent of The Netherlands lies below mean sea level and 65 percent is vulnerable for flooding from sea and rivers (Wesselink, Bijker et al. 2007). For every new flood event the Dutch tried to find a better solution to protect their delta. The area below sea level is protected by dikes, dunes and dams.

Concerning flood protection, the IPCC Panel (IPCC 2014) reports the anthropogenic cause of sea-level rise. Extreme events like storm surges, drought and heavy rainfall have a bigger probability of occurrence in the near future. In low lying countries like the Netherlands, with a large river delta that has a high economical and natural value, extreme variations in water levels will have great impact. Projected sea level rise of 0.5 to 1.0 m and increased probability of peak discharges in the Dutch rivers threatens the Dutch flood defence system. However, former used solutions like the construction of large hydraulic structures like the Delta Works or the reinforcement of dikes are very expensive. More importantly, in some cases the nature environment has been disturbed by these constructions. Seen the projected sea level rise caused by global warming, the need of new solutions of flood protection grows.

Lavooij and Berke (2019) initiated the Delta21 plan. Delta21 is a future-proof plan for the Dutch Southwest delta, that aims to tackle the growing need for new solutions for flood protection. Delta21 is located in the Haringvliet mouth and surrounded by the delta of the rivers Rhine and Meuse, see Figure 2. Besides, the Haringvliet mouth is part of the Natura2000 area called 'The Voordelta', a highly important area to nature.

## 1.2 DELTA21: AN INTEGRATED SOLUTION

### 1.2.1 INTRODUCTION TO DELTA21

This research focusses on the interventions of the Delta21 project. Delta21 is a spatial design proposal for three ambitions: 1) flood protection, 2) energy storage, and 3) nature restoration. Primarily, Delta21 focusses on flood safety to provide an alternative for expensive dike reinforcement projects. The first key mindset behind the Delta21 project is maintaining a low water level in the downstream area of the Dutch rivers. With the pump capacity, that is needed to achieve this goal, opportunities for large scale energy storage become available. Delta21 provides this energy storage by means of a large lake. Beside the energy storage lake, the plan provides space for other sources of green energy like solar panels and

FIGURE 2: LOCATION OF DELTA21

wind farms. The third part of the Delta21 plan is restoring nature by reopening the Haringvliet estuary and bringing back the tidal motion in the area. Together with the return of brackish water, this creates opportunities for new habitats and the migration of fish will be restored.

Delta21 consists of an Energy Storage Lake (ESL) (A in Figure 3) with a pumping station (D in Figure 3). The ESL is connected via siphons (E in Figure 3) to a tidal lake (B in Figure 3). The tidal lake is the connection between the North Sea with a barrier (C in Figure 3) and the Haringvliet gates (F in Figure 3).

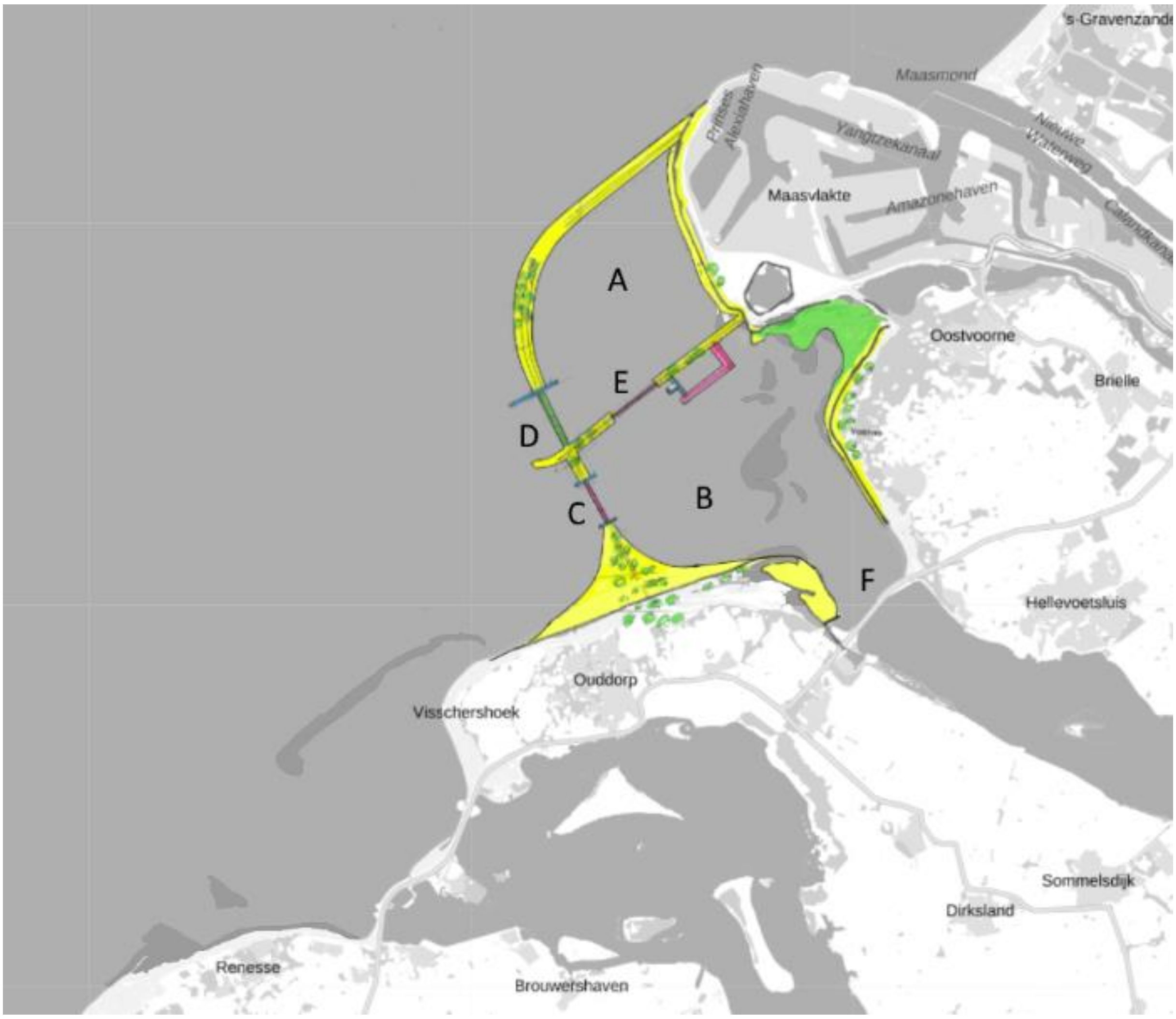


FIGURE 3: DELTA21 DESIGN (ADJUSTED FROM: LAVOOIJ AND BERKE (2020))
A: ESL, B: TIDAL LAKE, C: BARRIER, D: PUMPING STATION E: SIPHONS, F: HARINGVLIET GATES

### 1.2.2 FUNCTIONING UNDER NORMAL CONDITIONS

Under normal conditions the main function of Delta21 is discharging river water into the North Sea. The Haringvliet estuary is chosen to be recovered as being the main discharge route for the rivers Rhine and Meuse. Fully opening the Haringvliet gates will introduce the tidal movements in- and outside the estuary. Fish migration can be restored and nature may be enhanced.

Outside the estuary, in front of the Haringvliet gates (F in Figure 3), the tidal lake (B in Figure 3) provides a buffer area to control water levels between the Haringvliet estuary and the North Sea. The tide leaves and enters the lake through a barrier (C in Figure 3) and the incoming North Sea water reaches far into the opened Haringvliet estuary (Lavooij and Berke 2019). Simultaneously, the river flow coming from the Haringvliet gates leaves the lake via the barrier. The left plot in Figure 4 (left) provides a visualisation of the functioning under normal conditions.

North of the tidal lake another lake will be constructed, the ESL (A in Figure 3). The ESL system is used to flatten daily peaks of the Dutch energy demand and supply. Under normal conditions, the function of the ESL is to store energy over night, when there is a surplus of energy due to a low demand, by creating gravitational potential energy. Gravitational potential energy is created when the ESL is emptied by the pumping station (D in Figure 3) and a water level difference arises between the North Sea and the ESL. Energy can be generated during the day when the energy demand is high. The energy is generated by turbines that will be installed in the pumping station, when the water flows from the North Sea back into the emptied ESL. The ESL will have a storage capacity of 400 million $m^3$ and a working capacity of 17.5 m water head. The pumping station is used to empty the ESL and is able to store 1860 MW in water power by pumping water into the North Sea with 10,000 $m^3/s$ in 12 hours. The ESL can be filled with water from the North Sea through the turbines with a discharge of 10,000 $m^3/s$ in 12 hours.

### 1.2.3 FUNCTIONING UNDER EXTREME CONDITIONS

During high river discharges the main discharge route is still via the barrier. Under these conditions, as a backup system, siphons (E in Figure 3) allow excess water to flow from the tidal lake into the ESL. The pumping station of the ESL system, pumps the excess river water into the North Sea. This backup system is used when the water level in Dordrecht is close to reaching NAP +2.5 m. For an illustration see Figure 4 (middle). These extreme conditions affect the energy storage working of the ESL, the exact impact depends on the severity of the condition. When this backup system is used, water flows from the tidal lake into the ESL via the siphons with a maximum capacity of 10,000 $m^3/s$. The pumping station, with the same capacity, then pumps it into the North Sea. The barrier is still open, it can be closed during high water when the water level in Dordrecht is close to reaching NAP +2.5 m. The barrier will be opened again when this threat is gone, presumably during low water. When the barrier is closed, the complete river discharge route will be via the ESL system which is illustrated in Figure 4 (right).

During a large storm surge, the ESL can be emptied within 12 hours to act as a buffer for outgoing river water. The barrier can be closed when needed and the river discharge route will be via the ESL system. For an illustration see Figure 4 (right). The same method is used in the extreme case of both high river discharges and high storm surge levels (Lavooij and Berke 2019).

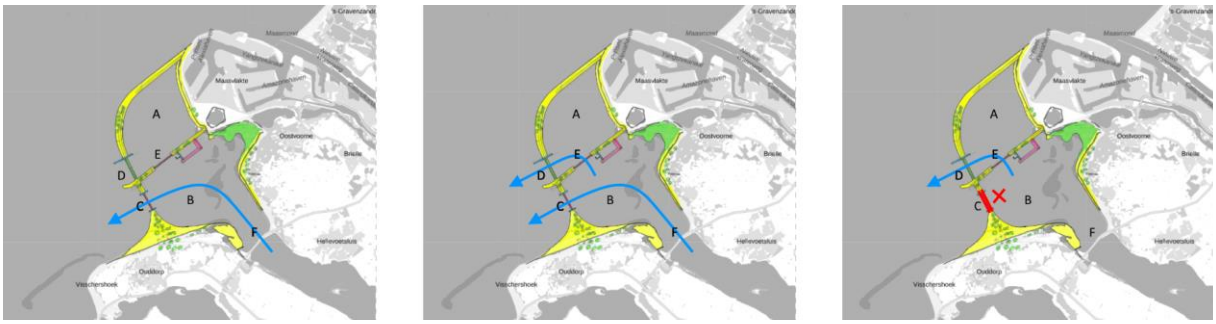


FIGURE 4: NORMAL CONDITIONS (LEFT), HIGH DISCHARGE (MIDDLE), HIGH WATER LEVEL AT NORTH SEA (RIGHT) (ADJUSTED FROM: LAVOOIJ AND BERKE (2020))

## 1.3 NATURA 2000, THE VOORDELTA

The coastal area of the Dutch Southwest delta is called the Voordelta, see Figure 5. The area is characterised by a dynamic environment of coastal waters, inter-tidal sand banks and beaches that together form a sheltered transition zone between (former) estuaries and the North Sea. The Voordelta is highly important to nature since many animals and plants find their habitats in the area. The Voordelta is one of the Natura 2000 areas in the Netherlands, which means that it is under strict regulatory protection measures (Rijkswaterstaat 2020). Management of the Natura 2000 areas are prescribed in a management plan as is done for the Voordelta. This management plan follows from European regulations and the Dutch Nature Conservation act of 2017. Activities in and changes to the Natura 2000 areas is regulated by permits. Natura 2000 authorities decide whether permits are given, following the policy given in the Voordelta management plan (Rijkswaterstaat 2016).

The morphology of the Natura2000 habitats changes over time by erosion and sedimentation processes. In the Voordelta the morphodynamics are driven by the wave and tidal currents, where the tide has been the dominant forcing between the two in the past. However, since the construction of the Delta Works, the coastal processes have changed from a mixed energy regime towards a wave-dominated regime. Because waves became more important, a new equilibrium was formed. This was especially the case for the two northern estuaries, the Haringvliet and Grevelingen, that were closed off almost completely. The new equilibrium demanded more landward sediment transport, therefore the offshore sandbanks migrated landward (Elias, Lazar et al. 2016). Furthermore, the construction of the Maasvlakte in 1964 changed the Voordelta by taking up a large part of inter-tidal sandbanks. In 2013, the construction of Maasvlakte 2 again took up a large important shallow area of the Voordelta. Consequently, compensations in the design were demanded by Natura 2000 authorities. The construction of these large land reclamations caused a shadowing effect of the Haringvliet mouth. The land reclamations sheltered the area from NW waves which had a significant influence on its development. An extensive research on the evolution of the Voordelta, with the combination of all human activities in the area, is elaborated in Chapter 2.

Morphological changes affect the habitats inside the Natura 2000 area. Therefore, it is important to note the following habitats that are of particular interest for this research and prescribed in the Voordelta management plan:

- H1110 Permanently flooded sandbanks
- H1140 Inter-tidal silt and sandbanks

Figure 5 shows the present-day distribution of both habitats inside the Voordelta. The main changes in the past years are caused by the construction of Maasvlakte 2. Habitat type H1110 faced large reduction in surface area. Compensation for this loss of surface area was demanded in the permit that was given before construction. It was demanded that a protected area of 24,550 ha should experience distinct quality improvement.

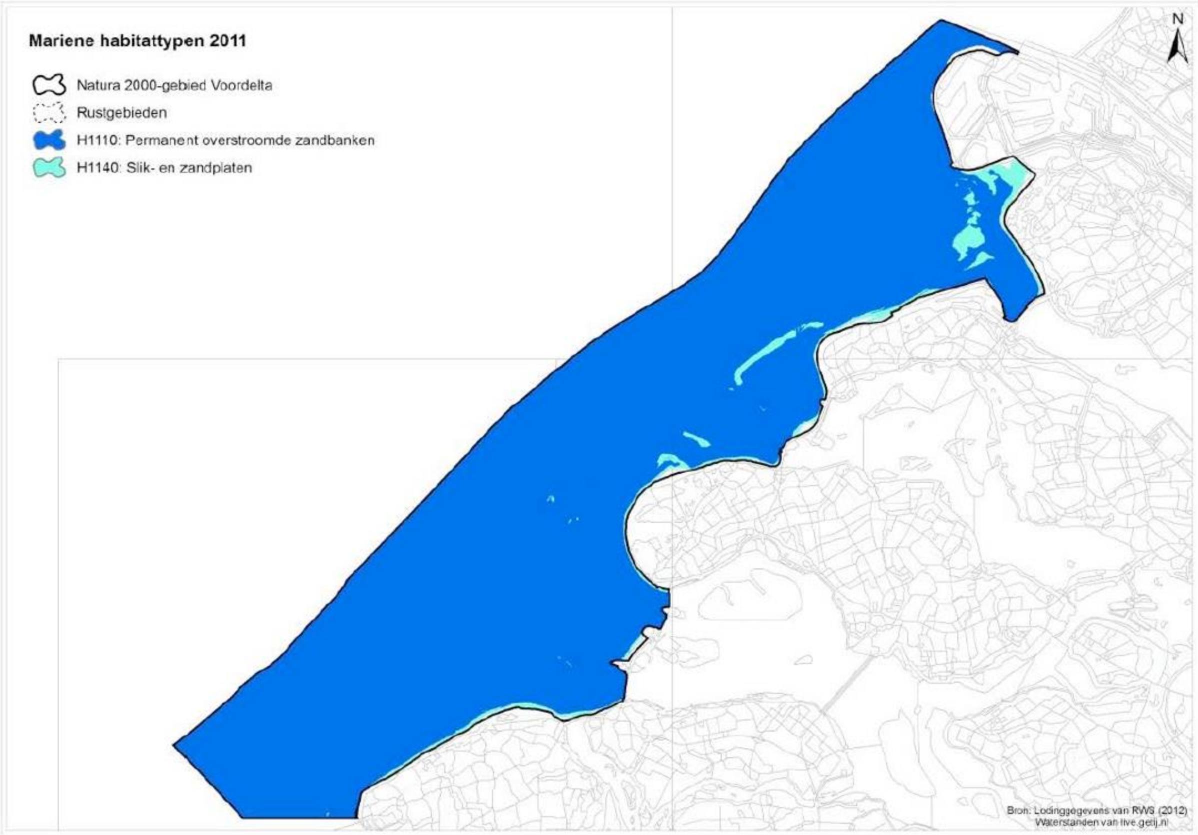


FIGURE 5: SPATIAL DISTRIBUTION OF HABITAT TYPES IN THE VOORDELTA.
DARK BLUE: H1110, LIGHT BLUE: H1140 (SOURCE: RIJKSWATERSTAAT (2016)).

In the northern part of the Voordelta, where Delta21 is located, a so-called seabed-protection-area is found. This area contains the habitats of seals, birds, sea ducks, the big stern, the common tern and the red-throated diver. As a result of the protection, the seabed is exposed to the dynamics of the nature only.

Inside the research area the following important sub-areas consisting of permanently flooded- and inter-tidal silt and sandbanks are found (see Figure 6):

- Middelplaat
- Bollen van de Ooster
- Coastline of Goeree and Kwade hoek
- Hinderplaat
- Slikken van Voorne


FIGURE 6: NATURA 2000 SUB-AREAS INSIDE THE RESEARCH AREA

## 1.4 PROBLEM DESCRIPTION

### 1.4.1 LAND RECLAMATIONS

Large land reclamations like the Maasvlakte influenced the surrounding area significantly. Research showed that morphodynamic changes are related to the scale of an intervention (Elias and Van der Spek 2014, Bosboom and Stive 2015). The damming of the Haringvliet resulted in strong shoreface erosion and a shift from a mixed wave-tide regime to a wave dominated regime. Furthermore, the construction of the Maasvlakte caused the Westplaat, a large sandbank in the Voordelta, to disappear. In conclusion, interventions caused changes to the morphology in the Voordelta; sandbanks disappeared, other grew bigger and sandbars developed due to a changing regime (Elias, Lazar et al. 2016). To understand, predict and eventually prevent negative impact to coastal morphology from happening, it is important to perform research before building structures like the Maasvlakte, the Delta Works and Delta21.

### 1.4.2 NATURA 2000 REGULATION

The Delta21 design must follow the legal requirements prescribed in the Natura 2000 management plan of the Voordelta (Rijkswaterstaat 2016). This management plan follows from European regulations and the Dutch Nature Conservation Act of 2017 (*Natuurbeschermingswet*). Activities in and changes to the Natura 2000 areas is regulated by permits. Natura 2000 authorities decide whether permits are given, following the policy given in the Voordelta management plan. Natura 2000 regulations demand that projects to be implemented in Natura 2000 areas aim to conserve or contribute towards the targets stated in the site's management plan. If changes to Natura 2000 areas might happen due to projects, permits can still be given if negative impacts are mitigated and compensations will be made like it was the case for Maasvlakte 2.

## 1.5 OBJECTIVE AND RESEARCH QUESTION

As previous studies on similar cases showed, the Delta21 contour together with the significant pumping discharge and the reopening of the Haringvliet estuary, can have a severe impact on hydraulics and morphodynamics in the surrounding area. Based on its relevance, the objective of this research is to determine the initial impact of the Delta21 plan on the large scale multi-year average morphodynamics of the Northern Voordelta. Further, to study to what extent Delta21 changes the morphological trend initially and which drivers are dominant in the initial change of the large scale (e.g. basins, estuaries, deltas) multi-year average hydraulic and morphodynamic characteristics in the system. The research area covers the Northern Voordelta, shown in Figure 7. The area runs from Maasvlakte 2 along the coastline, the Haringvliet sluices and the Brouwersdam until the head of Schouwen-Duiveland with the seaward boundary being the Voordelta boundary (NAP -20m). This area covers the important habitats of the Voordelta as shown in Figure 6.

The objective has resulted in the following general research question:

***What is the initial morphodynamic impact of the proposed Delta21 plan on the northern part of the Voordelta?***

To find the answer on this question, the following sub-questions have been specified:

1. What hydraulic and morphodynamic processes caused the evolution of the Northern Voordelta since the closure of the Haringvliet and Grevelingen estuaries?
2. What are the present-day characteristics of the large scale multi-year average hydraulics and morphodynamics and what mechanisms are dominant inside the research area?
3. What will the initial large scale multi-year average characteristics of the hydraulic and morphodynamics be and what mechanisms will initially be dominant inside the research area in the presence of Delta21?
4. To what extent will Delta21 initially change the morphological trend, in response to the initial change of the large scale and multi-year average processes?

An overview of the objective of each sub-question, together with the used methodology is shown in Table 1. The methodology is explained in Section 1.6.

TABLE 1: RESEARCH OBJECTIVES

| Research question | Objective | Methodology |
|---|---|---|
| **1** | Understand the hydraulic and morphodynamic behaviour of the system in the period just after the closure of the estuaries, in order to compare it with the behaviour of the Delta21 system, in which the Haringvliet will be reopened. | Literature review and data analysis |
| **2** | Identify the dominant drivers of the presently acting large scale multi-year average hydraulic and morphodynamic processes inside the research area. | Literature review and data analysis |
| **3** | Understand the large scale hydraulic and morphodynamic processes and identify the dominant drivers in the presence of Delta21. | Modelling study |
| **4** | Conceive an expectation of the trend change of the morphology as a result of the initial changes to the large scale hydraulic and morphodynamic processes in presence of Delta21 | Modelling study and conceptual model |

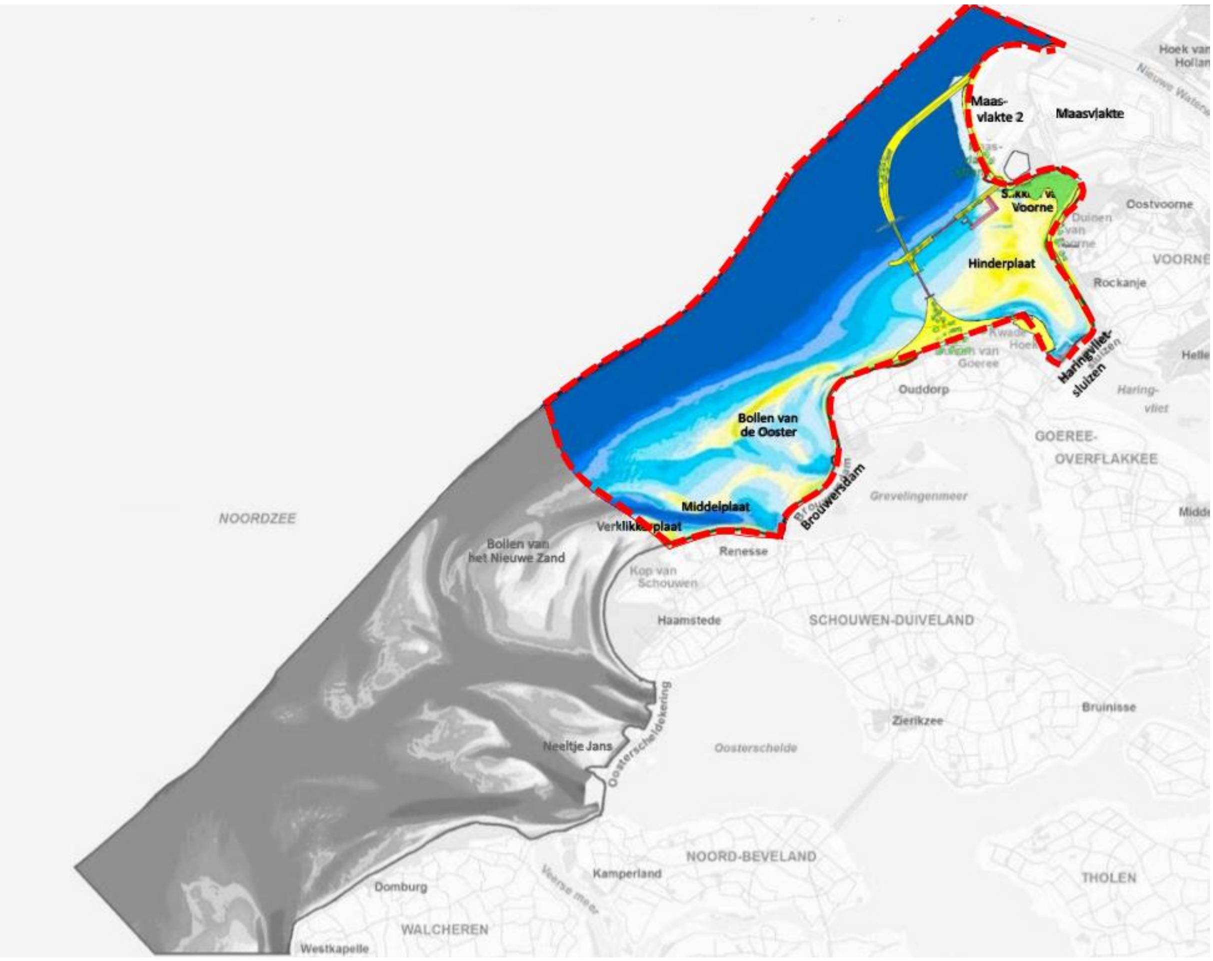


FIGURE 7: RESEARCH AREA (ADJUSTED FROM: RIJKSWATERSTAAT (2016) AND LAVOOIJ AND BERKE (2019))

## 1.6 METHODOLOGY AND THESIS OUTLINE

In order to reach the objectives and to answer the general research question, a combined literature and modelling study has been carried out. The methodology of this research is divided in several stages:

- Perform a literature review (sub-questions 1 and 2)
  To predict the initial impact on the morphodynamic system caused by the Delta21 plan, a deeper understanding of the characteristics of the research area is needed.
  - To exclude the impact caused by Delta21 from other, already existing processes, the evolution of the hydraulics and morphodynamics in the area have been studied (Section 2.2). The evolution of the area is studied using the available literature, site specific studies from Elias and Van der Spek (2019), De Vries (2007), De Winter (2008), Colina Alonso (2018) Reintjes (2002), De Boom (2016), Groenewegen (2019), Terwindt (1964) and Tönis, Stam et al. (2002) have been used.
  - Further, the present-day hydraulic and morphodynamic processes are studied (Sections 2.3 and 2.4). Some of the previously named studies also provided information about the present-day processes in the research area. The analysis of these studies treat the hydraulic characteristics of the area such as tidal data, wind data, wave data and terrestrial information. Further, it addresses the present-day state and trend of the morphology and the morphodynamics behind it. The literature review is of high importance to the understanding of the coastal system. The literature review is elaborated in Chapter 2.

- Perform a modelling study (sub-question 3)
  To eventually predict and understand the hydraulic and morphodynamic changes caused by Delta21, a modelling study is performed. The findings of the literature review are used to compare the model results. The aim of the model study is to determine how and to what extent the large scale multi-year hydraulics and morphodynamics will be changed by Delta21. Further, to identify the dominant drivers. Along with the fact that Delta21 is still in the design stage it is not necessary to reproduce the exact coastal evolution. Nevertheless, the complexity of the processes inside the study area causes the need of a process based model instead of conceptual or semi-empirical models. For this study, a former developed process-based Delft3D model is used, this model was developed to study the effects of Maasvlakte 2 and is expanded to cover the scope of this research.
  - First the modelling framework is explained in Chapter 3 in which the model software choice and the study method are elaborated. Further, choices regarding the setup of the modelling study are clarified.
  - Then, the model input is described in Chapter 4. The chapter starts with background information about the used model and thereafter treats the input of the different model components.
  - Following, the results and corresponding analysis are processed in Chapter 5. The chapter exists of the results regarding the hydrodynamics and subsequently the morphodynamics. The analysis examines the differences between various model scenarios and relates it to the findings of the literature review.

- Conceptualize the results (sub-question 4)
  Based on the findings of the modelling study in Chapter 5, a conceptual model is established in which the dynamic behaviour of the Delta21 system is analysed. The analysis presented via the conceptual model is done using the knowledge from literature combined with model results of several scenarios. The conceptual model is elaborated in Chapter 6.

# CHAPTER 2

# THE NORTHERN VOORDELTA

## 2.1 INTRODUCTION

To predict the impact on the hydraulic and morphodynamic system, caused by the Delta21 plan, a deeper understanding of the characteristics of the research area, 'the Northern Voordelta', is needed. To distinguish the impact of Delta21 from other, already existing processes, the evolvement of the hydraulics and morphology in the area along with the present-day processes must be studied.

In order to have a better comprehension of the research area, this chapter will first introduce the Voordelta and will elaborate on the history and evolution of the research area, which contains only the Northern Voordelta as explained in Chapter 1, and gives an answer on the following sub-question:

*What hydraulic and morphodynamic processes caused the evolution of the Northern Voordelta since the closure of the Haringvliet and Grevelingen estuaries?* (Section 2.2)

Secondly, the present-day hydraulic and morphodynamic characteristics of the area will be analysed. This part answers the following sub-question:

*What are the present-day characteristics of the large scale multi-year average hydraulics and morphodynamics and what mechanisms are dominant inside the research area?* (Sections 2.3 and 2.4)

## 2.2 THE EVOLVEMENT OF THE NORTHERN VOORDELTA

### 2.2.1 THE DUTCH VOORDELTA

The Dutch Southwest delta is made up of six estuaries, from north to south; 1) Nieuwe Waterweg, 2) Brielse Maas, 3) Haringvliet, 4) Grevelingen, 5) Eastern Scheldt, and 6) Westers Scheldt. The Western Scheldt is the distributary of the river Scheldt while all other estuaries are distributaries of the rivers Rhine and Meuse. These distributaries changed tremendously over the years due to both natural processes and human interventions. Extension of the port of Rotterdam and damming of the Brielse Maas resulted in a contiguous ebb-tidal delta of the Haringvliet, Grevelingen, Eastern Scheldt, and Western Scheldt estuaries (Elias, Lazar et al. 2016). Further changes to the delta happened after the 1953 storm surge. Sequential to this disaster, the Delta Project was realized which included the (semi-) closing of the Eastern Scheldt, the Haringvliet- and the Grevelingen estuary. The joint ebb-tidal deltas of the (former) estuaries now form the Voordelta. The Voordelta consists of the shallow North Sea part of the Zeeuwse and Zuid-Hollandse Delta extending 10 km offshore with a coastline of approximately 90 km (Elias, Lazar et al. 2016). It contains a dynamic coastal area of inter-tidal sand banks and the connection between the (former) estuaries and the North Sea.

### 2.2.2 HISTORY AND MORPHOLOGICAL EVOLUTION

The Delta Project contained several closings of the six estuaries (all activities since the start in 1950 are shown in Table 2). It started with the closing of the Brielse Maas in 1950. The damming of this estuary caused drastic changes to the morphology of its ebb-tidal delta. The channels were filled in and their orientation changed. Terwindt (1964) concluded that the changes were caused by the reduction in tidal prism of the estuary. In 1957 the closure of the Haringvliet estuary started, in which a large part of the estuary was closed off by discharge sluices. These sluices were built to regulate the river discharge of the rivers Rhine and Meuse. The former Haringvliet estuary became a fresh water lake until in 2018 the Kierbesluit policy was implemented. This policy states that the Haringvliet sluices should be partly opened. Consequently, a part of the lake is now brackish (Noordhuis 2017, Colina Alonso 2018). In 1965 the first section of the Brouwersdam was finished and the Grevelingen estuary was closed off completely in 1971. In 1986 the Eastern Scheldt was closed off by a storm surge barrier, which allowed the tidal motion to stay in the estuary.

While the Western Scheldt and the Eastern Scheldt remained (semi-) open, the situation of the two northern estuaries, the Haringvliet and Grevelingen estuaries, was completely different due to their closing (Elias and Van der Spek 2019). The different closing situations between north and south started an entirely different morphological regime between the two.

Prior to the start of the Delta Project, the morphology in the area was influenced by waves and tidal currents, the tide being the dominant factor of the two. Following the classification of Davis and Hayes (1984), the northern part of the Voordelta (all locations in this area are shown in see Figure 10) could be classified as a mixed-energy regime changing towards a tide dominated regime in the Southern Voordelta. After the construction of the Delta Works, the coastal processes changed from a mixed energy regime towards a wave-dominated regime. Nowadays there is a clear difference between the two northern closed estuaries (Haringvliet and Grevelingen) and the two southern open estuaries (Western- and Eastern Scheldt). Because waves became more important, a new equilibrium was formed. Especially in the two northern estuaries (Haringvliet and Grevelingen), that were closed off completely, the shift towards a new equilibrium was noticeable. Before closure, tidal currents perpendicular to the coast shaped the outer deltas. After closure the tidal currents changed their orientations parallel to the coast. The new equilibrium demands more landward transport due to the 'bulldozing' waves, therefore the offshore sandbanks moved landward and many other morphological changes happened to the two northern estuaries in the years after closure (Elias, Lazar et al. 2016).

TABLE 2, OVERVIEW ACTIVITIES INSIDE THE RESEARCH AREA AFTER THE START OF THE DELTA PROJECT (ADJUSTED FROM: COLINA ALONSO (2018))

| Activities | Year |
|---|---|
| **Major activities:** | |
| Damming Brielse Maas | 1950 |
| Closing Haringvliet: River discharge regulation | 1957-1970 |
| Construction Maasvlakte and Europoort | 1964-1976 |
| Closing Grevelingen by the Brouwersdam | 1971 |
| Construction Slufter | 1986-1987 |
| Construction Maasvlakte 2 | 2008-2013 |
| Kierbesluit: Haringvliet sluices partly open | 2018 |
| **Maintenance activities:** | |
| Nourishment coast of Goeree | 1969-1985 |
| Nourishment cost of Voorne | 1973-1993 |
| Dredging operations Slijkgat | 1983-now |
| Dredging operations Hindergat | 1986-1987 |
| Dynamic Maintenance policy Voorne and Goeree | 1991 |
| Nourishment Slufterdam | 1991-2005 |

### THE HARINGVLIET ESTUARY

The Haringvliet closing finished in 1970. The size of the estuary decreased and with it the tidal prism. In the remaining ebb-tidal delta, outside the Haringvliet sluices, the outgoing tide disappeared due to the closing and the waves became the dominant forcing for morphological changes. The entire ebb-tidal delta was pushed landward as a result of the increased wave dominance (see Figure 10). After the closure, the seaward front of the ebb-tidal delta eroded and the shallow parts faced sedimentation (Aarninkhof and Van Kessel 1999). The landward push could have been expected since a decrease in tidal prism means a decrease in offshore directed ebb-driven sand transport and a smaller cross-sectional area of the ebb- and flood channels (Wang, De Ronde et al. 2009). The surface area of the seaward part of the ebb-tidal delta decreased along with the average depth in that area. After the closure, flow velocities decreased with 35-80% (De Vries 2007). The channels in the ebb-tidal delta filled up, predominantly with mud, due to the decrease of the in and out going tidal currents. Only the channels Slijkgat, north of the head of Goeree, and the Gat van de Hawk, in front of Slikken van Voorne, remained. The Slijkgat remained to serve as the only discharge channel of the Haringvliet sluices and the fairway to Stellendam.

During this period, the closing of the Grevelingen estuary also finished (see Table 2). As well as the Haringvliet estuary, the tidal prism decreased considerably which resulted in the size reduction of its ebb-tidal delta front. The erosion of the seaward edge of the Grevelingen ebb-tidal delta fed the large south-west running sediment supply for the coast of Goeree (Reintjes 2002). Along with the northly directed longshore sediment transport, the shoreface of Goeree accreted and the spits at Kwade Hoek expanded (Elias and Van der Spek 2019).

Between 1986 and 1987 the Slufter was built, extending the Maasvlakte and the shoreline of the island of Rozenburg seaward. Along with the completion of Maasvlakte 2 in 2013, a step-by-step seaward extension increased the sheltered part of the Haringvliet ebb-tidal delta from NW waves (Tönis, Stam et al. 2002). The erosion of the seaward part of the ebb-tidal delta continued, reducing the seaward extent of it. The area landward of the Hinderplaat silted up and the channels continued to fill in. The Hinderplaat increased in height but became more narrow leading to a breach around 1995 during an extreme discharge event (Colina Alonso 2018, Elias and Van der Spek 2019). Since then the Hinderplaat is no longer a distinct bar but rather a dynamic system of shoals and channels (see Figure 10). Further, the intertidal shoals in the south part of the ebb-tidal delta merged with the Hinderplaat since 2001. The spit at Kwade Hoek turned out to be flourishing and the shoreface of Goeree accreted rapidly since the mid-1990s (Reintjes 2002). However, the accretion comes together with erosion at the eastern tip of Goeree.

In conclusion, during its closure the Haringvliet estuary reduced in size changing the tidal prism which caused a sharp decrease in ebb-driven sand transport. The landward wave-driven sand transport became the dominant factor for the morphological evolvement in the area. This resulted in the landward push of the ebb-tidal delta. Longshore sediment transport from the alongshore tidal- and wave-driven currents, together with the erosion of the seaward edge of the Grevelingen ebb-tidal delta, created a large sediment supply for the Haringvliet mouth (see Figure 9). Consequently, a large scale sedimentation pattern became present in the Haringvliet outer delta after closure (Aarninkhof and Van Kessel 1999). The rapid infilling of the remaining Haringvliet delta is partly due to mud deposition that is enhanced by the outflow of freshwater and suspended mud through the sluices. The increased shelter from northwest waves caused by the large land reclamations north of the ebb-tidal delta, contributed to this sedimentation. It is expected that the reduction of the seaward front of the ebb-tidal delta will continue until the part behind the Hinderplaat is filled completely and merges with the coast (Elias and Van der Spek 2019).

### The Grevelingen estuary

Before completion of the Brouwersdam in 1971, the hydraulics and morphodynamics were dominated by cross-shore tidal currents in and out the Grevelingen estuary. In the channel Kous the ebb-driven current was dominant while the flood-driven current was dominant in the Brouwershavense Gat (Aarninkhof and Van Kessel 1999). The channels and sandbars in the area were all cross-shore orientated (see Figure 8). Similar to the Haringvliet delta, after closure of the Grevelingen estuary the cross-shore tidal current change towards an alongshore tidal current which caused a circulation pattern in the ebb-tidal delta. The in and out going currents in the channels of the ebb-tidal delta decreased in strength with 50-90%, causing the related sand transport to disappear. The abrupt disappearance of the cross-shore tidal currents caused the ebb-tidal delta to change (Aarninkhof and Van Kessel 1999). As was the case for the Haringvliet ebb-tidal delta, the seaward edge started to erode and coastline parallel sandbanks started to form in the former Grevelingen estuary mouth (Elias and Van der Spek 2019). These sandbanks were found especially in the northern part and moved landwards (see Figure 8). Their speed slowed down from a few 100 meters per year to about 10 meters per year in 1978, after that they stabilized. In the nineties the morphological activity in the whole ebb-tidal delta slowed down, currently the effect of the closure has seemingly disappeared and a new equilibrium is reached (Aarninkhof and Van Kessel 1999).

Similar to the Hinderplaat, the Bollen van de Ooster were formed. A part of the sand from the ebb-tidal delta shoreface was bulldozed upwards creating this longshore bar in the northern part of the Grevelingen mouth. Over the years, the Bollen van de Ooster grew in size and moved along the coast merging with smaller shoals. In 1996 the Bollen van de Ooster became one distinct sandbar. The sandbar became longer and stretched towards the coast of Goeree. Where the Gat van de Hawk separated the Hinderplaat from the coast, the Schaar separates the Bollen van de Ooster with the western tip of Goeree. Due to the change in tidal currents and a shift in phase lag the currents in the Schaar increased after closure leading to erosion of the Westhoofd at Goeree. The erosion leads to the need of coastal maintenance in that area and for several years nourishments have been executed (Groenewegen 2019). The eroding Westhoofd and seaward edge of the Grevelingen outer delta transported sediment in northeast direction, feeding the coast of Goeree.

Further, the Middelplaat, one of the largest sandbars before closure, eroded after closure due to the increased wave activity. The sandbar, just seaward of the Brouwersdam, moved landwards onto the dam. The sand from this shoal created a beach along the Brouwersdam (Elias and Van der Spek 2019).

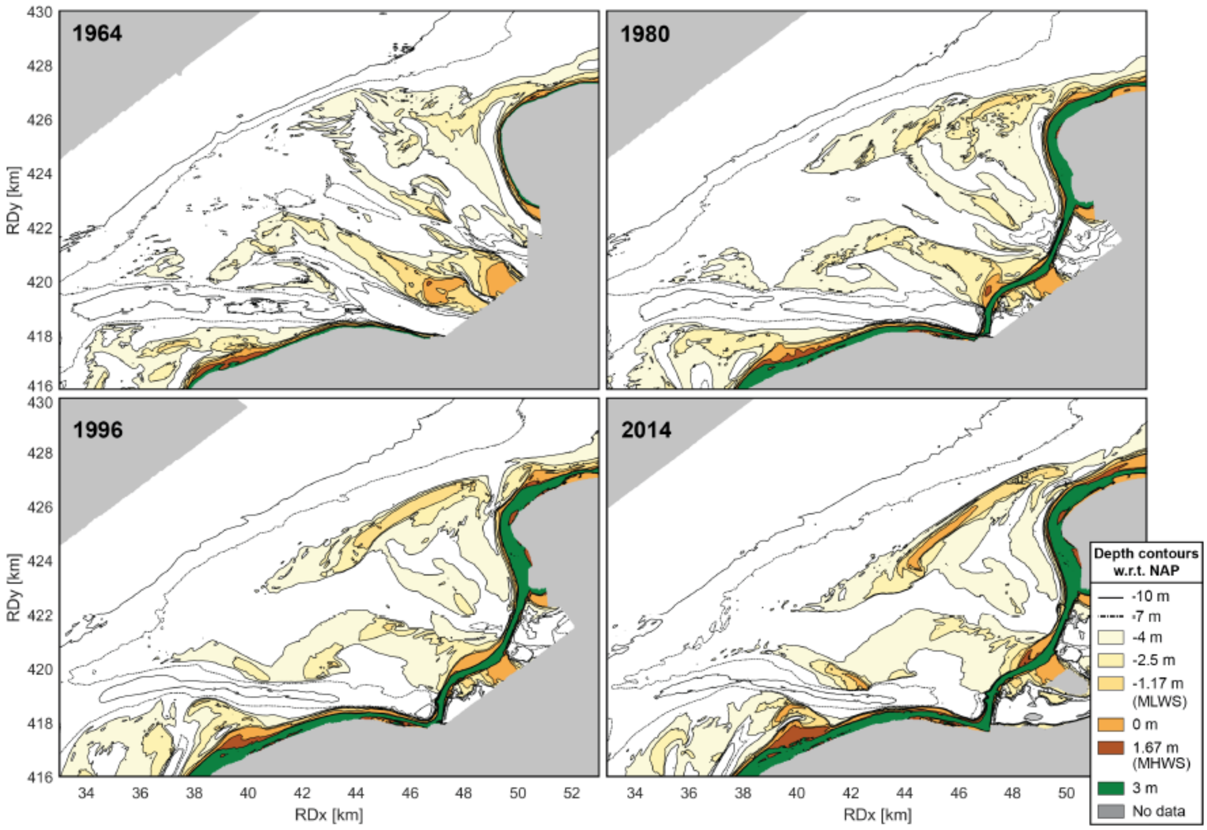


FIGURE 8: EVOLUTION OF THE GREVELINGEN EBB-TIDAL DELTA (SOURCE: GROENEWEGEN (2019))

Concluding from the literature, in the Grevelingen ebb-tidal delta, changes happened on a slower adaption time scale than the Haringvliet ebb-tidal delta (see Figure 9). This may be explained by the fact that morphological changes in this area are less influenced by large land reclamations and due to the larger size of the area. Moreover, the south-north directed tidal flow is sustained, possibly delaying the breach of shore-parallel bars like the Bollen van de Ooster. At the Grevelingen ebb-tidal delta, the Bollen van de Ooster is currently still present and even growing in longshore direction (Elias and Van der Spek 2019).

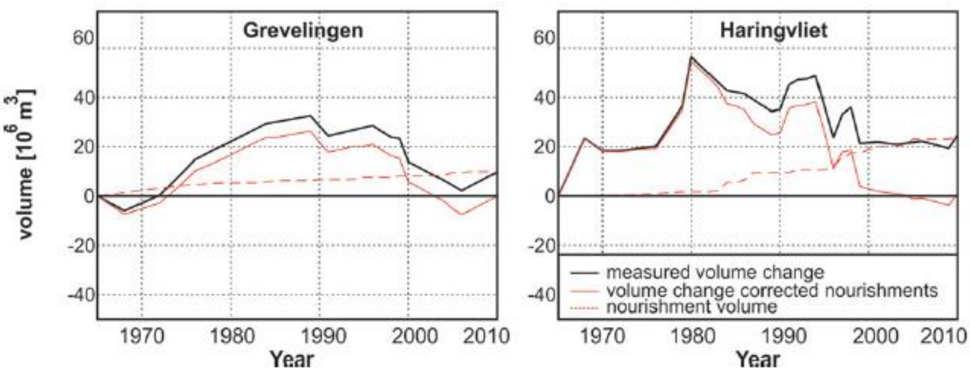


FIGURE 9: VOLUME CHANGE OF THE GREVELINGEN AND HARINGVLIET EBB-TIDAL DELTAS AFTER CLOSURE (SOURCE: ELIAS, LAZAR ET AL. (2016))

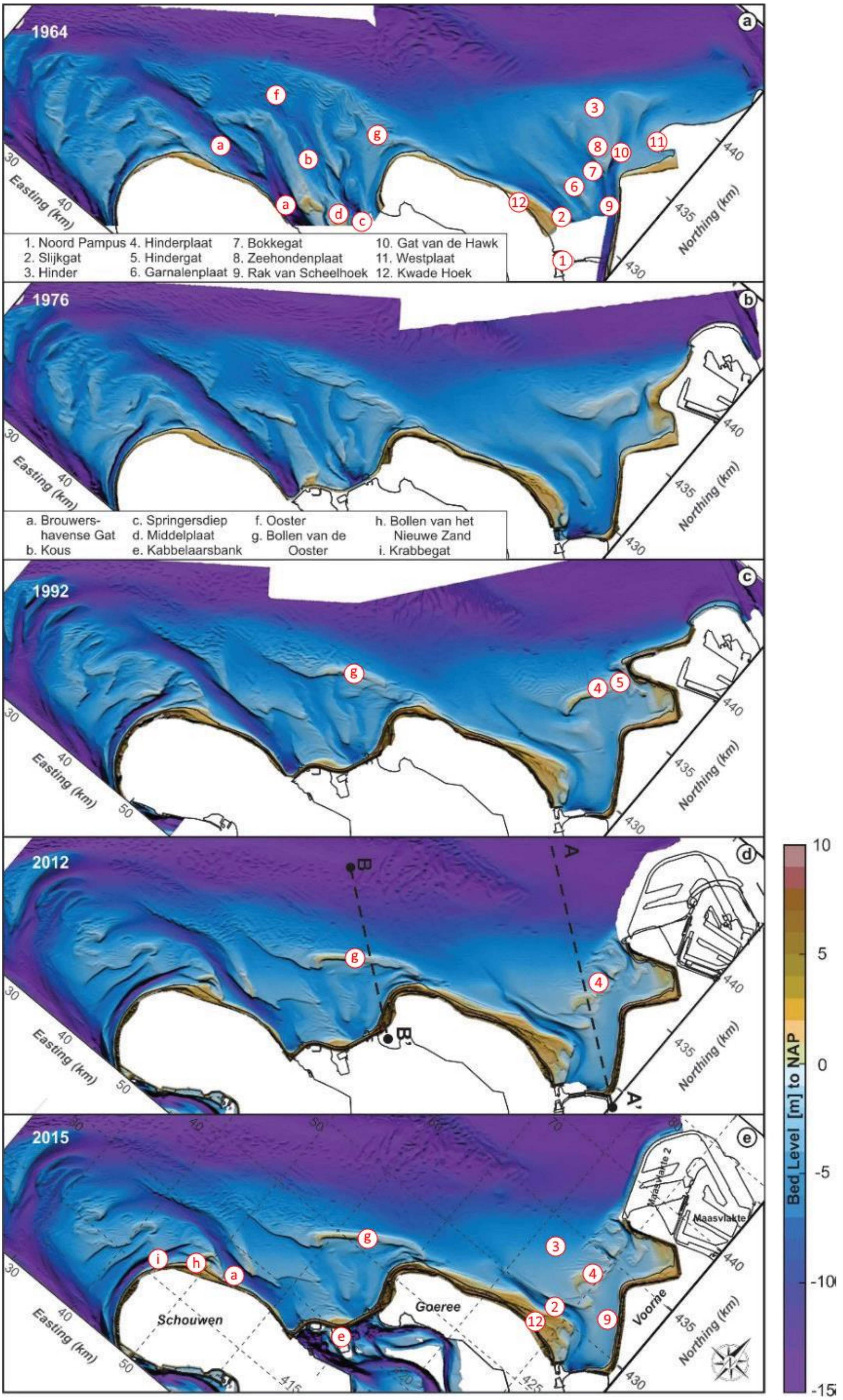


FIGURE 10: MORPHOLOGICAL EVOLVEMENT OF THE GREVELINGEN AND HARINGVLIET EBB-TIDAL DELTAS (ADJUSTED FROM: ELIAS AND VAN DER SPEK (2019))

## 2.3 THE HYDRODYNAMIC DRIVERS

The literature review of the historical evolution showed that the coastline and its profile are shaped by many processes. This research addresses the following hydrodynamic drivers on morphodynamics:

- Marine forces (waves, tides, currents)
- Atmospheric forces (wind and climate)
- Terrestrial forces (river outflow)

A coastal system is shaped by its drivers. Looking at the equilibrium concept of Bosboom and Stive (2015), a morphological system tries to find an equilibrium with the present forcing. However, if there is not an equilibrium, morphological adjustments start to take place immediately. Changes to the forcing or the morphodynamic system itself lead to a new equilibrium. The morphological system can be changed by changing the (underwater) topography, some examples are:

- Anthropogenic factors(revetments, groynes, breakwaters, harbours, etc.)
- Variations in coastline orientation
- Vegetation, difference in sediment characteristics

Delta21 changes this (underwater) topography and thus might interfere with the hydrodynamic drivers like the tidal propagation and the characteristics of waves. This section focusses on the hydrodynamic drivers in order to compare and understand the impact of Delta21.

### 2.3.1 TIDE

In the northern hemisphere the entering semi-diurnal tide moves counter-clockwise around amphidromic points (see Figure 11). In the North Sea basin this results in the tide entering from the North and turning counter clockwise around the amphidromic point between the Dutch and the British coast (De Winter 2008). Hence, this means that the tidal wave propagates from south to north along the Dutch coast. Further, there is a large variation in amplitude along the coast as a result of the North Sea topography. De Winter (2008) remarks that there is a phase lag of 20 minutes between the coast of Goeree and the Hoek van Holland. The net currents in the area, especially around the Hinderplaat, were also found to turn counter-clockwise.

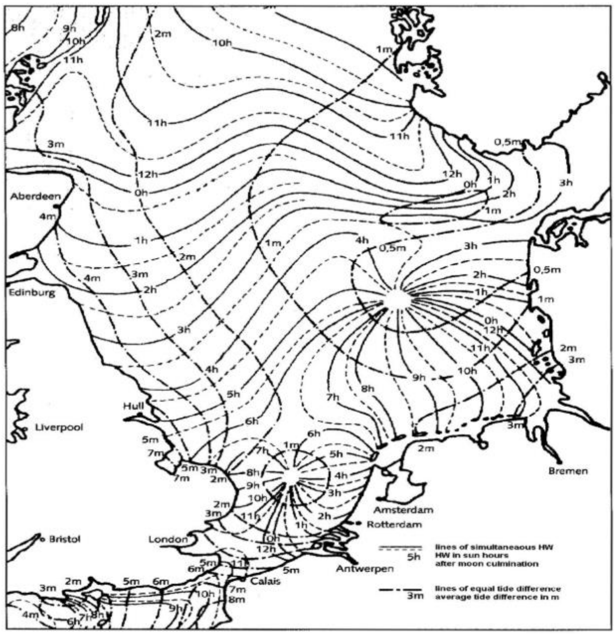

FIGURE 11: PROPAGATION OF THE TIDE AROUND THE AMPHIDROMIC POINTS (SOURCE: BOSBOOM AND STIVE (2015))

The semi-diurnal tide is characterised by the fact that there are two high and low waters each day. In the southwest Netherlands it is found that there is a daily inequality between the two high waters. From south to north the tidal amplitude decreases from 3.8 m at Vlissingen to 2.5 m at Grevelingen, 2.1 m at Haringvliet and 1.4 m in Den Helder (De Boom 2016, Colina Alonso 2018). Besides the daily inequality, Colina Alonso (2018) found that the tidal signal in front of the coast of Goeree shows significant spring-neap variations (see Figure 12).

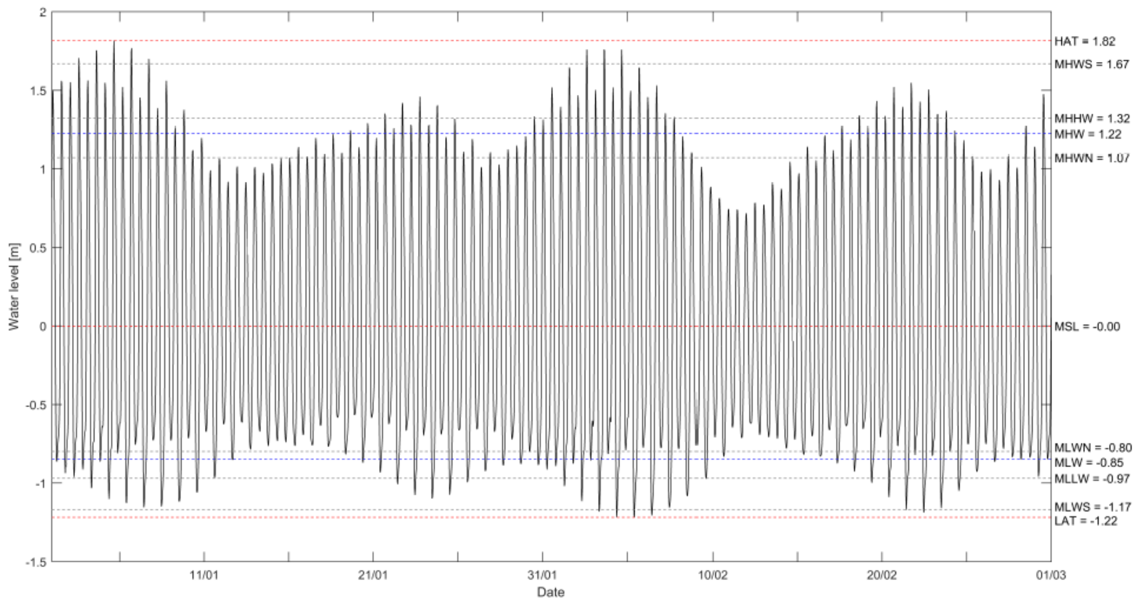


FIGURE 12: TIDAL SIGNAL IN FRONT OF GOEREE, INCLUDING FOUR SPRING-NEAP TIDAL CYCLES (SOURCE: COLINA ALONSO (2018))

Before and after closure

Before closure the horizontal tide lagged 3 hours behind the vertical tide due to the large difference in tidal amplitudes. This resulted in the cross-shore flow in and out the estuary to be out of phase with the longshore North Sea flow. When these currents are in phase they amplify each other which is the case for the estuaries in the Wadden Sea. There the asymmetric ebb-tidal deltas are rotated against the dominant wave direction. The morphology in the southwest delta is symmetric since the flow velocities are out of phase. During maximum cross-shore flow, the longshore flow is minimum resulting in channels fanning in all directions and landward pointing shoals (Aarninkhof and Van Kessel 1999). This theory is in line with the observed bathymetry before closure (see Figure 10).

The closure of the Haringvliet and Grevelingen estuaries changed the tidal propagation in the area considerably. The orientation of the tidal propagation in the estuary mouth changed from cross-shore to longshore. This change in orientation is illustrated in Figure 15. The figure shows the isolines for the phase of the M2 tide. Before closure the tide entered the Grevelingen estuary, creating a cross-shore orientation while after closure the coastal boundary caused the propagation of the tide to be orientated alongshore. The change in orientation changed the flow patterns in the area significantly. De Boom (2016) showed that in the Grevelingen ebb-tidal delta the phase lag mechanism became of less importance after closure. The perpendicular flow changed to a somewhat shore parallel circular flow, which is visualised in Figure 13.

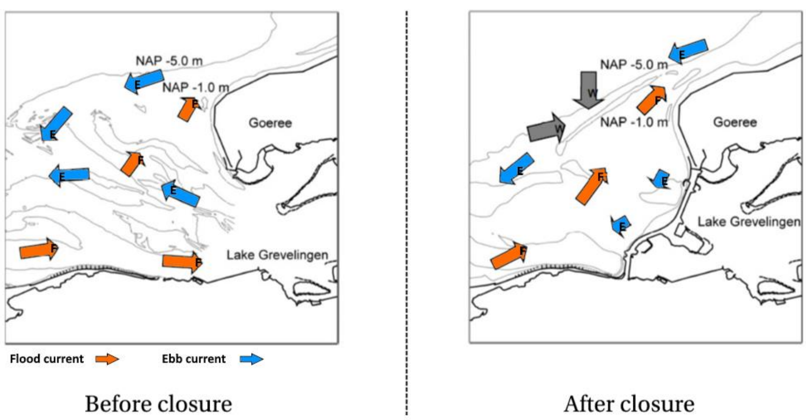


FIGURE 13: FLOW PATTERNS BEFORE AND AFTER CLOSURE OF THE GREVELINGEN ESTUARY (ADJUSTED FROM: DE BOOM (2016))

Tönis, Stam et al. (2002) studied the difference between the situation before and after closure of the Haringvliet estuary. The closure caused a change in the flow pattern which was linked to the shape change of the estuary. Before closure the estuary was long and the water level was out of phase with the water level at the North Sea. The closure caused the estuary to shorten, following the characteristics of a short basin, and the water level is now approximately in phase with the water level at sea (see Figure 14). This figure from Tönis, Stam et al. (2002) shows the phases of the flow patterns during a tidal cycle together with the change in phase lag from less than $90^0$ before and $90^0$ after closure. Tönis, Stam et al. (2002) found that the channels are flood dominant meaning that the current velocities reached their maximum in flood direction, this did not change after closure. Since the flow is a function of the water level, the flow pattern changed too as visualised in Figure 14.

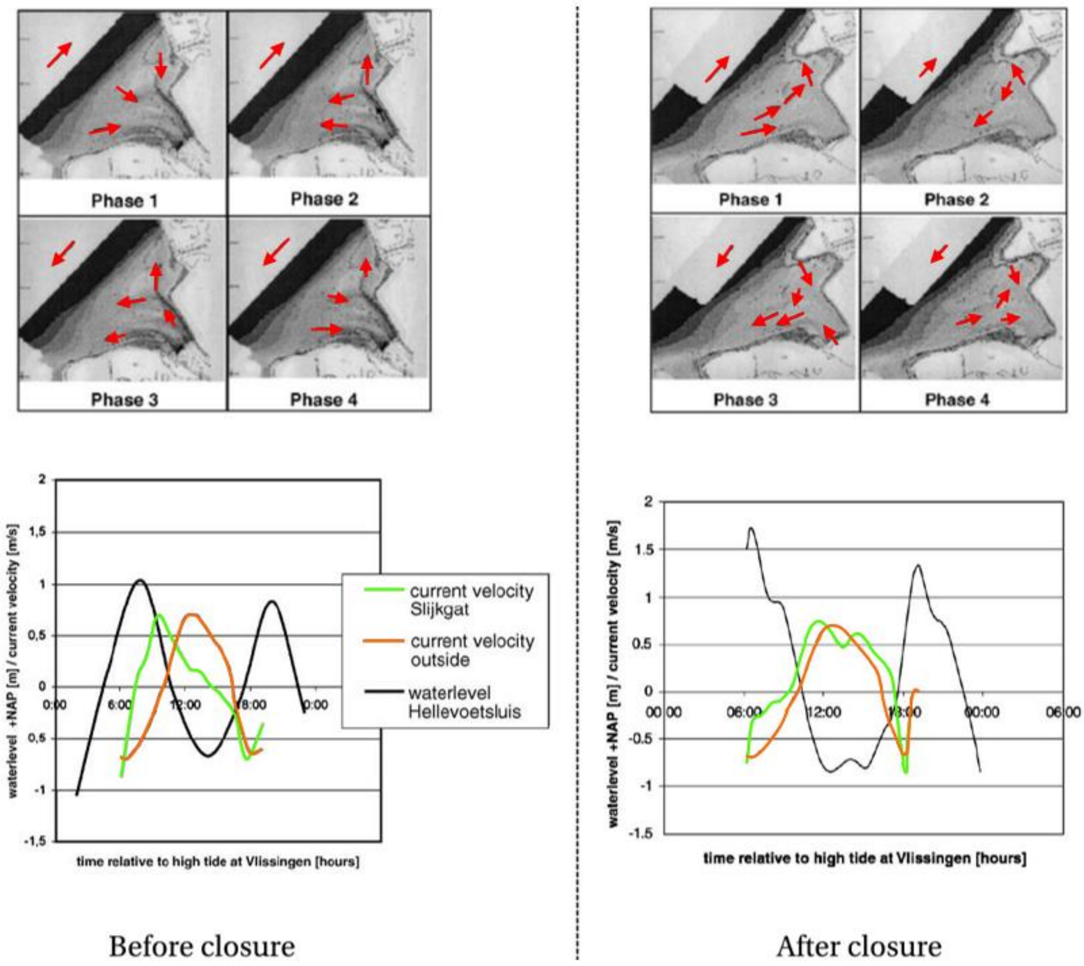


FIGURE 14: CHANGE IN FLOW PATTERN AND PHASE LAG IN THE HARINGVLIET MOUTH (ADJUSTED FROM: TÖNIS, STAM ET AL. (2002))

The main difference in flow pattern between before and after closure is the change from cross-shore directed flow to a more or less alongshore directed flow. The stages after closure are described as follows (De Winter 2008):

Stage 1: at high water, the flow enters the estuary at the south side and leaves the estuary via the north side.

Stage 2: about 3 hours after high water, the flow inside the estuary is in ebb direction.

Stage 3: at low water, the flow enters the estuary at the north side and leaves via the south side.

Stage 4: the flow at sea is in ebb direction and inside the estuary in flood direction.

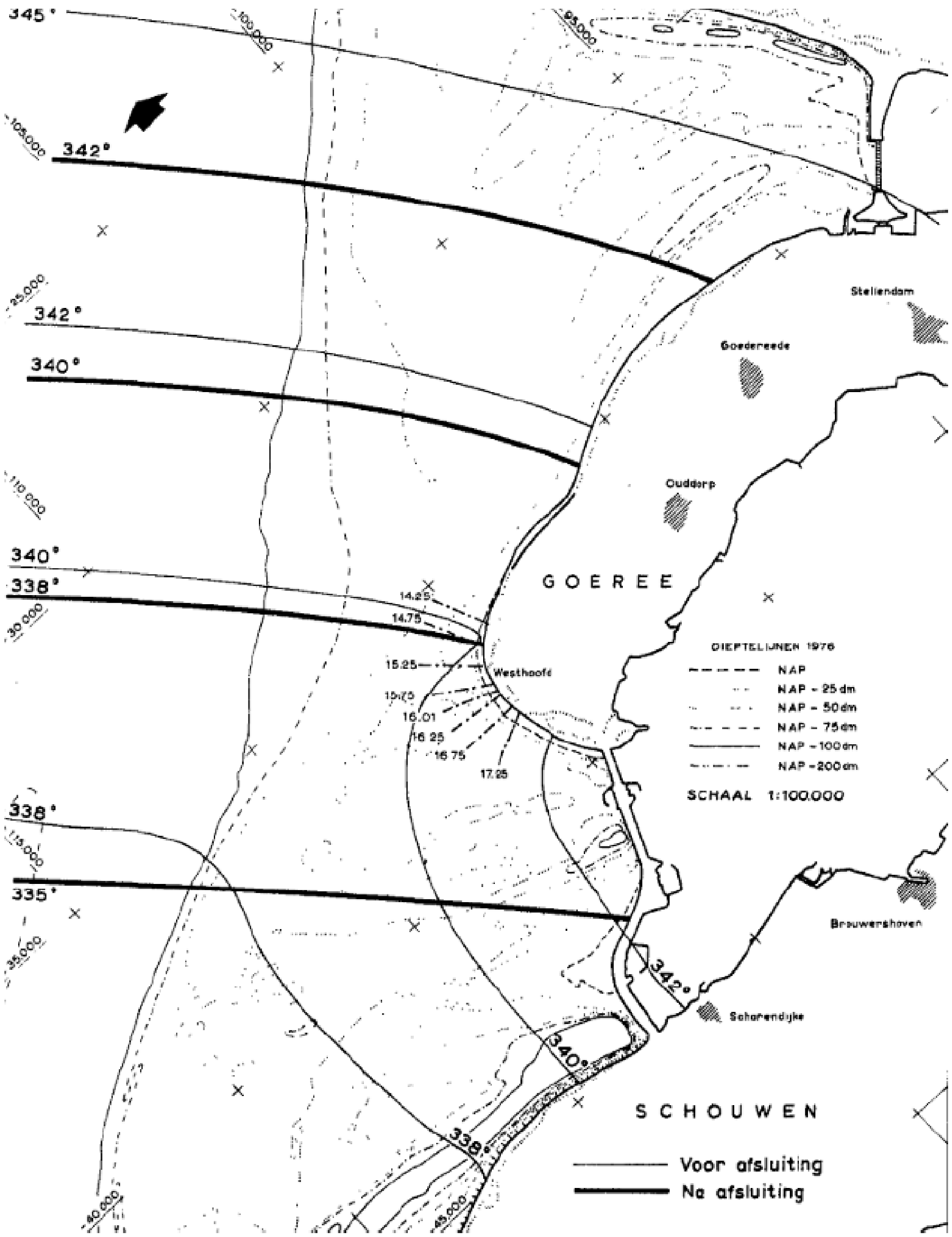


FIGURE 15: ORIENTATION OF THE TIDAL PROPAGATION BEFORE CLOSURE (THIN LINE) AND AFTER CLOSURE (THICK LINE) (SOURCE: GROENEWEGEN (2019))

### 2.3.2 Wind

The wind is one of the driving forces for water motion since it exerts stress on the water surface creating water level set-up and waves. Continuity requires a return current, resulting in the indirect influence of wind on flow patterns (De Vries 2007). Wind affect the residual currents in an area and residual currents control the net sediment transport in shallow areas.

Huibregtse (2013) and Colina Alonso (2018) studied the wind climate at the Brouwershavense Gat and Europlatform respectively. The wind data at the Brouwershavense Gat, which is in front of the Brouwersdam, shows a prevailing wind direction between west and south (see Appendix A.2 Wind roses). The most common wind direction is southwest, while wind between the direction south and east are very scarce. A second dataset containing only wind speeds above 20 m/s, representing storm conditions, shows roughly the same results (Huibregtse 2013). The Europlatform dataset shows a wider range of wind directions. The prevailing wind direction at Europlatform is also southwest. The mean wind speed is 7.5 m/s, while extreme storms show wind speeds up to 30 m/s generating waves of over 6m (Colina Alonso 2018).

### 2.3.3 Waves

Historical research, as described in Section 2.2.2, showed that waves are a dominant driving force for water motion and morphodynamics in the area. Wave forces generate cross- and longshore currents in the coastal area. Wave action inside the surf zone also causes an increase of bed shear stress and sediment can be stirred up. The longshore currents by waves and tides transport the suspended sediment along the coasts. Cross-shore transport can be induced by wave-asymmetry (De Vries 2007, Bosboom and Stive 2015).

De Winter (2008) studied the waves in the Haringvliet area and in front of the coast of Goeree. The offshore generated waves propagate towards the coast and change mainly by shoaling, refraction and wave breaking. The offshore waves (nr. 1 in Figure 16) are the largest since they did not yet face these depth induced characteristic changes. The offshore waves originate from two main directions, namely the North by North West and the South West which is also visible in the wave rose taken at the Europlatform in Figure 17. The highest waves at Haringvliet come from the North West (up to 3.2m), probably caused by the larger wind fetch in that direction. The waves become smaller and change to a prevailing WNW direction while approaching the Haringvliet mouth due to the different depth induced processes as named before. Location nr. 2 in Figure 16 shows a smaller directional sector which indicates refraction. Location nr. 3 perfectly shows the shelter effect of the Maasvlakte as described in Section 2.2.2.

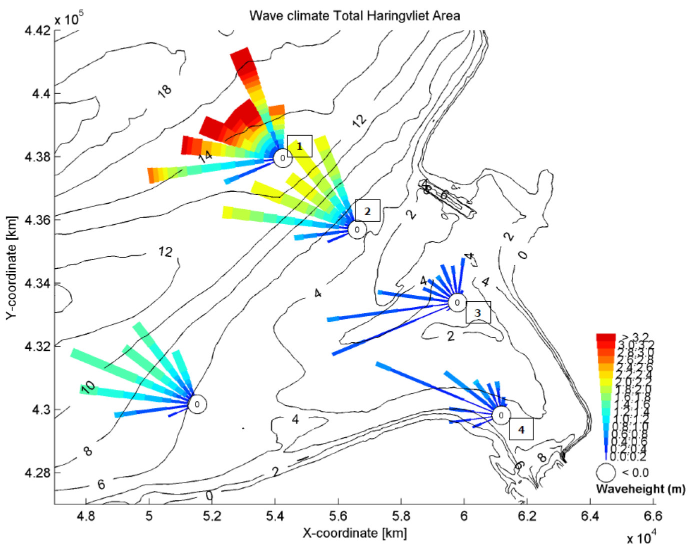


FIGURE 16: WAVE CLIMATE IN THE HARINGVLIET AREA (SOURCE: DE WINTER (2008))

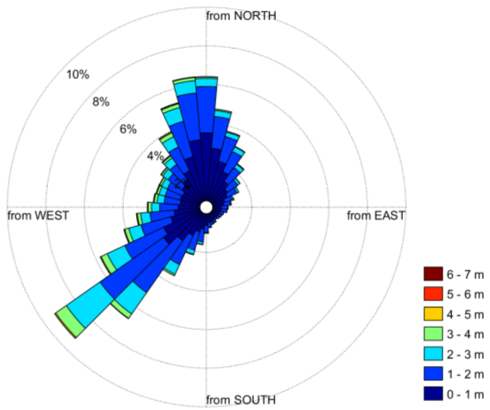


FIGURE 17: WAVE CLIMATE MEASURED AT EUROPLATFORM (SOURCE: GROENEWEGEN (2019))

### 2.3.4 TERRESTRIAL

The river discharge through the Haringvliet sluices is another driving force for water motion in the area. Before closure of the Haringvliet estuary the rivers Rhine and Meuse could discharge naturally. After closure the discharge is managed by the Haringvliet dam by means of sluice gates. These sluices are opened 3.5 hours before low tide and closed 3.5 hours after (De Vries 2007). Fresh water enters the Haringvliet mouth and is released into the North Sea via the Slijkgat (see Figure 10). The sluices have a maximum discharge capacity of 25,000 $m^3/s$ (Colina Alonso 2018). In reality only 1.3% of the year the discharge exceeds 4,000 $m^3/s$, when this happens the entire Haringvliet mouth can be flooded (De Winter 2008). 89.9% of the time, the discharge is smaller than 2,000 $m^3/s$ and only small velocities of 0.2 m/s are induced. The other 8.8% of the time, discharges between 2,000 and 4,000 $m^3/s$ are present and velocities of 0.4 m/s can be found near the sluices (Colina Alonso 2018). While under normal discharge conditions, only the Slijkgat acts as discharge route. Above 2,000 $m^3/s$ also other channels are used. De Vries (2007) concluded that high discharges at the sluices can lead to large morphological changes in the ebb-tidal delta of the Haringvliet. During high discharges, a landward directed sediment transport can be induced due to a salinity gradient caused by the fresh water run-off. In 2018 the Kierbesluit policy is implemented which concerns the partly opening of the sluices. The partly opening means that during high water, salt water can enter the Haringvliet mouth and a transition area between salt and fresh water will be created. When Rhine discharges at Lobith are lower than 1,100 $m^3/s$ during ebb or lower than 1,500 $m^3/s$ during flood, the sluices will be closed. This results in an average of 90-100% being open during ebb from January till August reducing to 70% in October. During flood the average is 80-90% from January till August reducing to 45% in October (Noordhuis 2017).

Colina Alonso (2018) studied the yearly average discharges at the Haringvliet sluices and found a mean discharge of about 1,000 to 2,000 $m^3/s$. Figure 18 shows the daily and yearly mean discharge in the period 1971-2012. A maximum daily mean discharge of 9015 $m^3/s$ is found during the 1995 flooding of the Southeast Netherlands. Colina Alonso (2018) concluded that, after implementing the Kierbesluit policy, no significant morphological changes to the outer Haringvliet delta are to be expected and any possible change will only happen to the Slijkgat area. Noordhuis (2017) too concluded that, seen the details of the Haringvliet sluice management programme, the impact after implementation will be very low.

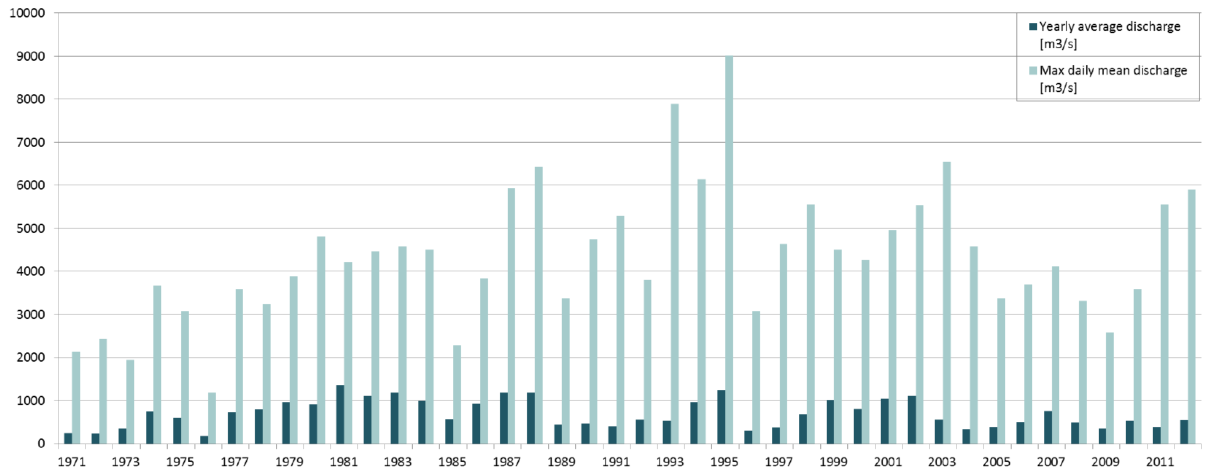


FIGURE 18: DISCHARGE AT HARINGVLIET SLUICES IN THE PERIOD 1971-2012 (SOURCE: COLINA ALONSO (2018))

## 2.4 THE MORPHODYNAMICS

In the research area, bed load as well as suspended load transport are important for sediment transport. Bed load transport is mainly related to morphological changes because suspended load cannot settle easily due to their small-grain size and high mobility under hydrodynamic forcing. This section describes the bed composition, the sediment transport and the sedimentation and erosion patterns in the area.

### 2.4.1 BED COMPOSITION

Figure 19 shows the spatial distribution of median grainsize of the bed in the Haringvliet ebb-tidal delta. Most of the sediment in this area was disposed during the formation of the estuary (Colina Alonso 2018). After closure, only a small part of the sediment came from the rivers Rhine and Meuse while most of the sediment supply came from the Grevelingen ebb-tidal delta. Longshore sediment transport by tides and waves moved sediment on and off the southern coast of Goeree, the Bollen van de Ooster and the seaward edge with the North Sea like explained in Section 2.2.2. While most of the Haringvliet and Grevelingen ebb-tidal deltas consist of sand, especially in the Haringvliet delta high percentages of mud are present in the channels (Colina Alonso 2018). De Vries (2007) remarks that about 10% of the entire Haringvliet outer delta consists of mud and that mud can be found in the channels and on flats. The characteristic values for the main diameter are listed as follows:

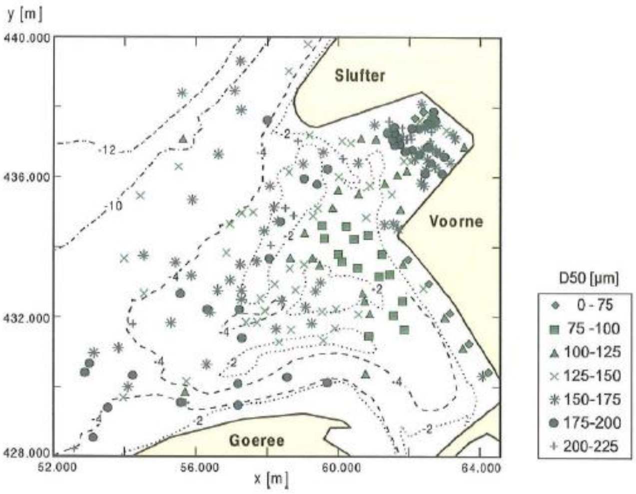


FIGURE 19: SPATIAL DISTRIBUTION OF THE MEDIAN GRAIN SIZE AT THE HARINGVLIET OUTER DELTA IN 1994 (SOURCE: DE VRIES (2007))

- channels: $d_{50} < 150 \mu m$
- flats: $d_{50} = 150 - 200 \mu m$
- coastline: $d_{50} < 125 \mu m$

### 2.4.2 SEDIMENT TRANSPORT

De Vries (2007) listed the following transport processes important for sediment transport in the area:

- tide-driven transport;
- cross-shore transport induced by waves;
- long-shore transport induced by waves;
- water level gradient return currents along shoals;
- stirring up of sediment by waves;
- density-driven transport

The tidal current at the North Sea generates a net sediment transport in northern direction due to a flood dominant character. This flood dominance is also present in the tidal currents at the Haringvliet ebb-tidal delta and consequently induce eastward directed sediment transport. This net eastward directed transport is in line with the observed sediment supply from the Grevelingen outer delta (De Vries 2007). The tidal currents shaped the breaker bars, e.g. the Bollen van the Ooster, in the Grevelingen outer delta. During low water the southward directed ebb-current is present at the seaward side of the bar and results in the expansion at the south side of the Bollen van de Ooster (see Figure 20). During high water, current directions are reversed and result in a northward directed sediment transport at the landward side of the bars, partly over the bars, and cause expansion at the north side. Overall the tidal currents are responsible for a seaward migration. However, cross-shore wave processes, especially during storms, cause a landward migration which prevails in the area (De Boom 2016).

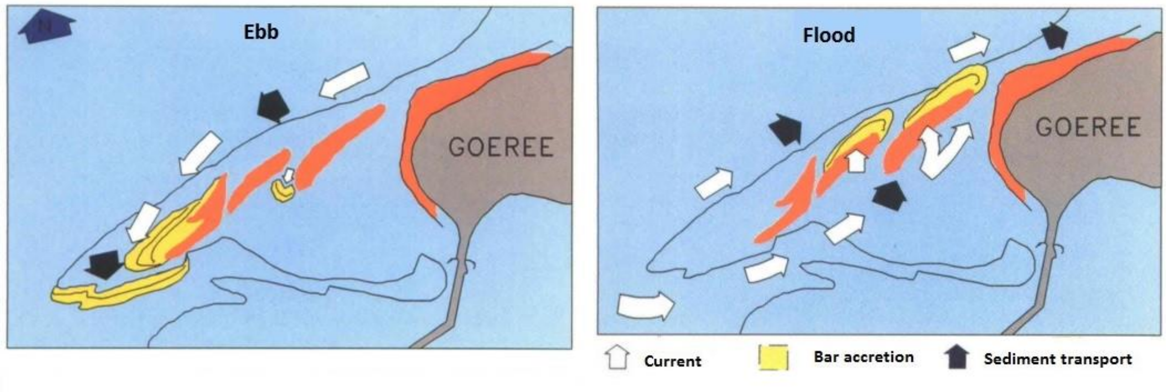


FIGURE 20: TIDE-DRIVEN MIGRATION OF THE BOLLEN VAN DE OOSTER (SOURCE: DE BOOM (2016))

Cross-shore wave-driven currents are mainly induced by wave-asymmetry and an undertow. Wave-asymmetry is the phenomenon where the wave crest faces higher onshore directed velocities than the offshore directed wave through velocities. A pitched forward wave shape is the result and sediment is brought up higher in the water column. Similar to the morphology at Grevelingen, the Haringvliet bars are influenced by cross-shore processes. Nowadays, cross-shore transport processes and water level gradient induced return currents influence the Hinderplaat and cause an eastward migration. During flood, water level gradients induce a flow that transport sediment at the leeside of the Hinderplaat extending it landward (De Vries 2007).

Long-shore wave-driven currents are induced by the cross-shore gradient of the shear component of the radiation stress of obliquely incoming waves (Bosboom and Stive 2015). A longshore current is present at the Grevelingen ebb-tidal delta, the Bollen van de Ooster, the coast of Goeree, the Hinderplaat and the Maasvlakte 2. The net sediment transport is in NE direction and gradients are present along the coast of Goeree. Sediment is picked up at the Bollen van de Ooster and deposited at the Kwade Hoek, where wave influence is reduced (De Vries 2007, Colina Alonso 2018).

To resume, at Haringvliet the transport through the channel Slijkgat is mainly determined by the river discharge combined with the tide. Waves stir up the western part of the Slijkgat while the tidal and river currents transport it. Through the channel Hindergat, both wave-driven- and tide-driven currents dominate. While in the Hindergat there is an equal transport in both directions, a net eastward transport is observed in the Slijkgat (De Vries 2007). Nevertheless, it's the wind that dominates most of the currents and the related sediment transport in the area according to a study from Colina Alonso (2018)

*Intermezzo*

---

Scha and Van den Berg (1993) studied the relative importance of the tide compared to the waves and its influence on the shape of ebb-tidal deltas. They found that the phase difference between the longshore tidal flow and the cross-shore flow at the inlet influence the ebb-tidal delta geometry. If both are in phase, the ebb-tidal delta will be asymmetric. The cooperating flows enhances tidal currents in ebb-direction and pushes the ebb-tidal delta channels in that direction. If the flow patterns are out of phase, the geometry will be symmetric since the flow can run-off in all directions. However, in both cases the relative influence of the waves play a big role. This relative influence of waves increases for smaller tidal prisms, in that situation the cross-shore tidal currents will be small compared to the longshore wave-driven currents at sea. This results in the ebb-tidal delta channels to bend in downdrift direction. For large tidal prisms the cross-shore tidal currents dominate and the phase difference becomes more important again. Figure 21 shows the model of Scha and Van den Berg (1993). Situations A, B and C refer to a situation without phase difference. In these situations the waves only affect the symmetry of the delta if its relative importance is high enough, e.g. for small tidal prisms. Situations D, E and F refer to a situation with phase difference where in all situations the waves only have minor effect to the shape of the symmetric ebb-tidal delta.

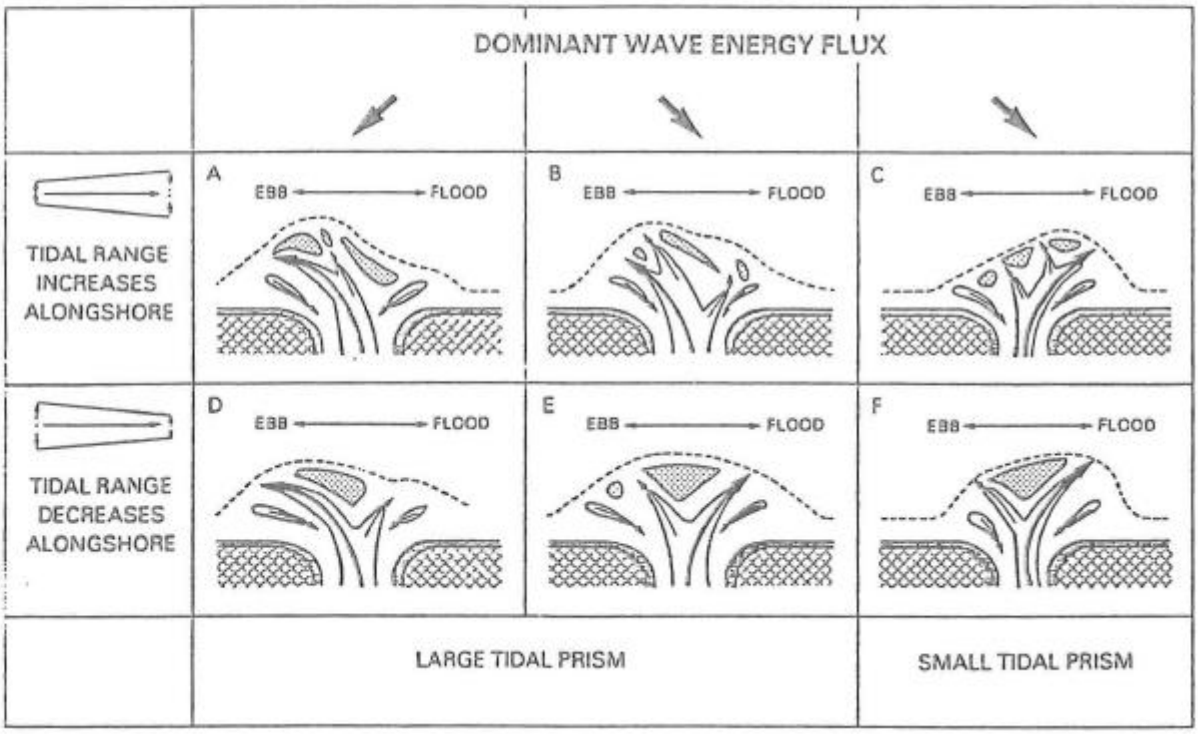


FIGURE 21: MODEL OF VARIATION IN EBB-TIDAL DELTA GEOMETRY OF SCHA AND VAN DEN BERG (1993).

## 2.5 Concluding remarks

In conclusion, the most important morphodynamic processes are listed using the sedimentation and erosion patterns:

1. General erosion of the delta front in the whole Northern Voordelta, this is clearly observable in the sedimentation and erosion patterns as visualised in Figure 22.
2. Sand from the eroded delta front is pushed landward by bulldozing waves, creating shore-parallel sand bars like the Bollen van de Ooster, Middelplaat and the Hinderplaat.
3. These sandbars face erosion on the seaward side and sedimentation on the landward side which is clearly visible in Figure 22. This results in a landward migration of the sandbars, the Middelplaat already reached the coastline and formed a beach along the Brouwersdam.
4. Sedimentation of the landward part of the ebb-tidal deltas, i.e. landward of the large sandbars Bollen van de Ooster and Hinderplaat.
5. Infilling of the former ebb- and flood channels, clearly visible in the Haringvliet delta in Figure 22.
6. Erosion/deepening of the channel Schaar at the Westhoofd due to the new longshore tidal currents.
7. Elongation of the Bollen van de Ooster in north-eastern direction due to the new longshore tidal currents.
8. Sedimentation at the coast of Goeree expanding the coast towards Kwade Hoek due to an increasing shelter from NW waves.
9. A net sedimentation pattern is present in both former estuaries.

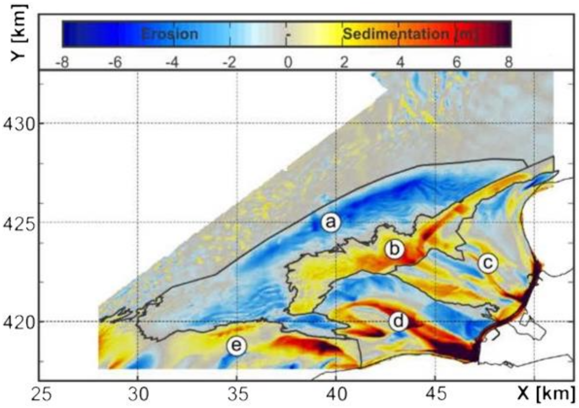


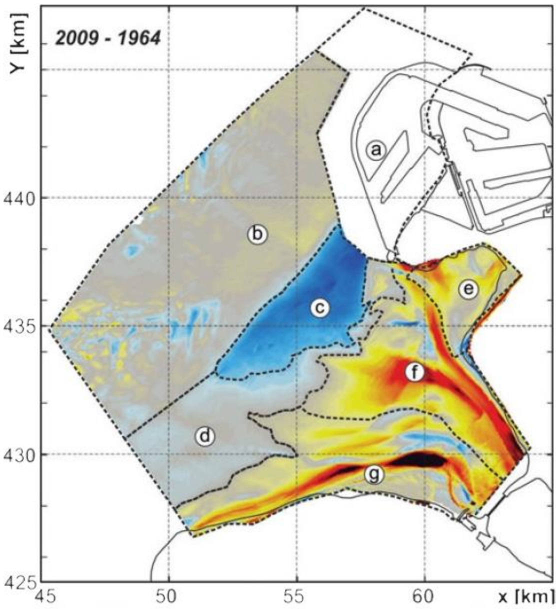


| Volume changes (million m$^3$): | | | |
|---|---|---|---|
| Location | Sed | Erosion | Net |
| a. Bollen vd Ooster front | 0.3 | -89.1 | -88.8 |
| b. Bollen van de Ooster | 38.6 | -0.4 | 38.2 |
| c. Aardappelenbult | 28.1 | -10.5 | 17.6 |
| d. Brouwershavense Gat | 52.6 | -22.6 | 30.0 |
| e. Banjaard Noord | 34.9 | -6.7 | 28.1 |
| Totals | 154.4 | -129.3 | 25.1 |

| Volume changes 1964-2009 (million m$^3$): | | | |
|---|---|---|---|
| Location | Sed | Erosion | Net |
| a. Maasvlakte2 | 14.7 | -33.7 | -18.5 |
| b. Coast (offshore) | 5.8 | -20.3 | -14.5 |
| c. Hinderplaat | 0.2 | -50.2 | -50.2 |
| d. Coast (nearshore) | 0.0 | -15.4 | -15.0 |
| e. Brielse Gat | 0.4 | -0.9 | 9.6 |
| f. Scheelhoek | 10.5 | -2.2 | 64.5 |
| g. Coast Goerree/Slijkgat | 66.6 | -4.4 | 50.2 |
| Total | 98.2 | -127.1 | 26.1 |

FIGURE 22: SEDIMENTATION AND EROSION PATTERNS IN THE PERIOD 1964-2009 (SOURCE: ELIAS, LAZAR ET AL. (2016))

# CHAPTER 3

# MODEL SELECTION & FRAMEWORK

## 3.1 INTRODUCTION

The literature review in Chapter 2 provides the information for a deeper understanding of the processes inside the research area. This chapter first presents the method of the modelling study in Section 3.2. The modelling study is used to predict and understand the possible change of the existing processes in presence of Delta21. It is further used to investigate the underlying mechanisms behind the changes and their relation to the different Delta21 interventions. Subsequently to the method, the selection of the used model software is addressed in Section 3.3. The chapter ends addressing important in- and exclusion regarding the setup of the model in Section 3.4.

## 3.2 MODELLING STUDY METHOD

The modelling study method is based on the comparison of different scenarios. To understand the impact of the Delta21 plan, two scenarios have been studied. The first scenario is scenario 0. This scenario represents the present-day hydraulics and morphodynamics that followed from the literature review and data analysis (Chapter 2). Scenario 0 is modelled in Model0 and is used to serve as benchmark to the scenario where Delta21 is included. Scenario 1 represents the Delta21 plan and is studied using the model with other boundary conditions and a modified geometry that simulates the Delta21 plan. Scenario 1 is sub-divided into two models in order to distinguish the difference between the contribution of the ESL and the opening of the Haringvliet with the tidal lake (more on that in Section 1.2).

All three models have been run on three simulations. These simulations vary in forcing type, this is done to study the contribution of each forcing and the changes to that forcing. The simulations, using different processes, combined with the model scenarios gives a total of 9 computations as shown in the table below:

TABLE 3: MODEL SCENARIOS

| **Simulation** | **Processes** | | | | **Comparison** | | |
|---|---|---|---|---|---|---|---|
| | **Tide** | **Wave** | **Discharge** | **Wind** | **Model0** (present situation) | **Model1A** (Delta 21, no ESL) | **Model1B** (Delta21, full) |
| **I. Tide only** | Yes | No | Yes | No | N/A | I. Model 0<br>I. Model 1B<br>II.+III. Model 1A | I. Model 0<br>I. Model 1A<br>II.+III. Model 1B |
| **II. Wind** | Yes | No | Yes | Yes | N/A | II. Model 0<br>II. Model 1B<br>I.+III. Model 1A | II. Model 0<br>II. Model 1A<br>I.+III. Model 1B |
| **III. All processes** | Yes | Yes | Yes | Yes | N/A | III. Model 0<br>III. Model 1B<br>I.+II. Model 1A | III. Model 0<br>III. Model 1A<br>I.+II. Model 1B |

## 3.3 MODEL SOFTWARE SELECTION

Seen the variety of processes and scenarios, the modelling study makes use of a process-based depth-averaged (2DH) Delft3D model. A process-based model is required given the complexity of the bathymetry and the various processes acting in the research area. To add, in process-based models the equilibrium of a system follows from the balance of forces or transport contributions, which suits the study on Delta21 in which the equilibrium is not known in prior. Delft3D is able to describe waves, flow, sediment transport and bed level changes using a set of mathematical equations that are based on physical principles (De Vriend and Ribberink 1996). Furthermore, it was not the aim to reproduce the exact evolution of the research area. The model has only been used to, qualitatively, study the large scale multi-year average driving mechanisms and their relative influence on the hydraulic and morphodynamic processes.

## 3.4 MODEL SETUP

The model is focussed on the large scale multi-year average forcing mechanisms. The input for the Delft3D model thus consists of the multi-year average conditions. Therefore, storms, extreme discharge events and other extreme peaks in the hydraulic boundary conditions are not part of this modelling study. Further, the modelling study does not focus on 3D gravitational circulation effects since these effects are assumed to be less relevant in the study on large scale hydrodynamics of coastal cells and deltas compared to the more dominant two dimensional horizontal processes.

Modelling with Delft3D consists of several stages (see Figure 23). First, a grid has to be generated on which computations are executed. The grid requires information about the bathymetry and in order to solve the non-linear shallow water equations, boundary conditions have to be applied. In order to represent the Delta21 geometry as presented in Lavooij and Berke (2020), the bathymetry has been modified. This included:

- the deepening (to -10 m NAP) and extension of the Slijkgat towards the opening of the tidal lake;
- the formation of a sandy dune ring round the ESL and the tidal lake including an opening of 1500 m;
- the formation of a bed protection in the opening of the ESL and in front of the pumpstation.

Setting up a model is finding the balance between reliable results and short computation times. In order to find this balance, the model study consist of multiple 'morphostatic' simulations of each scenario (see Table 3). In a morphostatic simulation the feedback loop between morphological bed changes and hydrodynamic forcing does not exist. This means that the bathymetry is fixed and only the initial sedimentation/erosion (ISE) can be determined. This reduces the complexity of the model but also the reliability of long-term predictions.

Greater explanation on how these adjustments are processed in the Delft3D model and what input is used for each part of the model is further discussed in Chapter 4. This chapter also elaborates on the boundary conditions of each scenario.

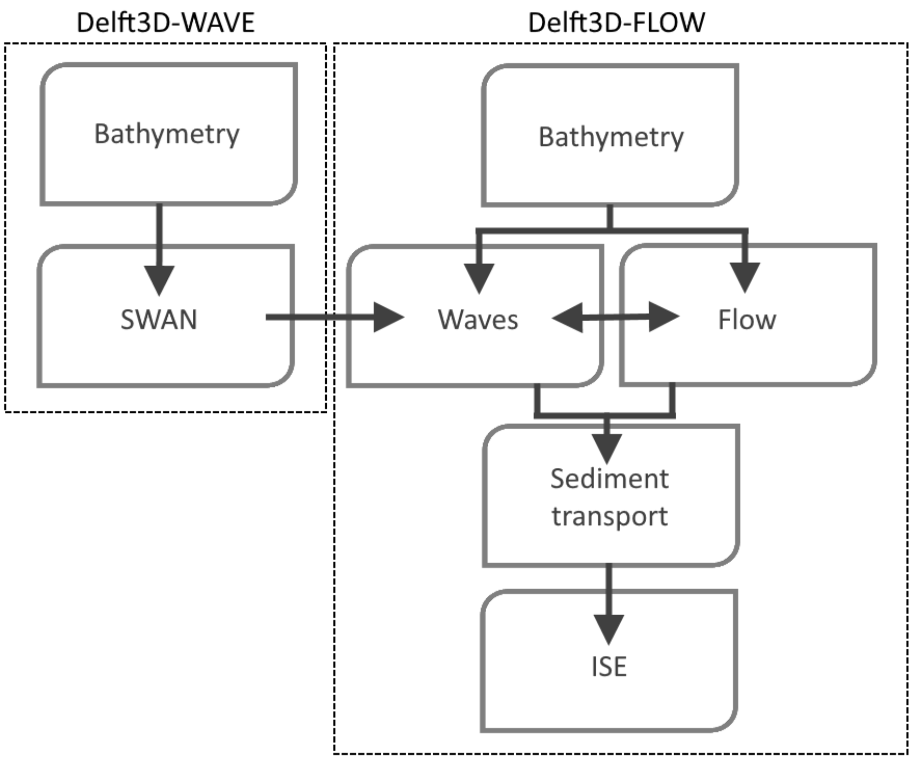


FIGURE 23: DELFT3D MORPHOSTATIC MODELLING FLOWCHART

# CHAPTER 4

# MODEL INPUT

## 4.1 INTRODUCTION

This chapter describes the input of the depth-averaged (2DH) Delft3D model, that fits the purpose of the model as proposed in the previous chapter. The chapter starts in Section 4.2 with a short background on Delft3D and the schematisation of the grid and the bathymetry. Subsequently, the imposed boundary conditions are derived in Section 4.3. Thereafter, the FLOW- and WAVE- module settings are described in Section 4.4.

## 4.2 DELFT3D SETUP

### 4.2.1 DELFT3D BACKGROUND

Delft3D is an integrated computer software suite for 3D computations of coastal, river and estuarine areas. The software, developed by Deltares, is able to carry out simulations of flows, waves, sediment transport, water quality, morphological developments and ecology. The Delft3D suite is composed of several modules, in this study the Delft3D-FLOW and Delft3D-WAVE modules have been used. Delft3D-FLOW calculates non-steady flow and transport phenomena on a curvilinear grid. The non-steady shallow water equations are solved in either 3D or in 2DH (depth-averaged) mode (Deltares 2014a). For this research the 2DH mode is used, meaning that the vertical momentum equation is reduced to the hydrostatic pressure relation. This is done under the assumption of small vertical accelerations compared to the gravitational acceleration. Further, Delft3D uses the Alternating Direction Implicit (ADI) time integration method for the shallow water equations. The ADI-method splits one time step into two stages, each consisting of half a time step.

Sediment transport calculations are performed simultaneously with the flow calculations in Delft3D-FLOW. For transport of non-cohesive sediment, like sand, the Van Rijn formula is used. Van Rijn's calculation formulas account for bedload transport, suspended transport and the effect of waves.

Delft3D-WAVE simulates the evolution of random, short-crested wind-generated waves using the third-generation SWAN model (Deltares 2014b). The numerical SWAN model is based on the discrete spectral action balance and is fully spectral. SWAN computes the evolution of waves by representing the natural processes of wave generation by wind and wave energy dissipation due to whitecapping, bottom friction, depth-induced wave breaking and non-linear wave-wave interactions. SWAN uses an implicit numerical scheme, making the computation unconditionally stable. The FLOW and WAVE modules interact during a simulation and work on the same curvilinear grid.

### 4.2.2 GRID AND BATHYMETRY SCHEMATISATION

The grid used for this study originates from a model developed by Van Holland (1997) and Steijn, Eysink et al. (2001), that was used particularly for effect studies of the Maasvlakte 2 construction on the Haringvliet outer delta. The grid for the FLOW-module extents from Noordwijk until Nieuw Haamstede. The resolution of the grid is highest around the Maasvlakte 2 and the Haringvliet outer delta and decreases both south- and northwards. In order to obtain reliable results the grid had to be extended and the resolution needed to be increased inside the research area. To prevent disturbances from entering the research area, the southern boundary has been extended southwards until Zeebrugge. Further, the resolution near Delta21 is increased to 120x120 $m^2$ while more offshore the resolution is 450x450 $m^2$. The grid for the WAVE-module is an extended version of the FLOW-grid, it has been enlarged at the seaward boundaries by 20 grid cells. This is done for two reasons: first, to prevent boundary disturbances due to waves from entering the FLOW-grid and second, to ensure fully developed waves at the boundaries of the FLOW-grid. The grids are shown in Figure 24.

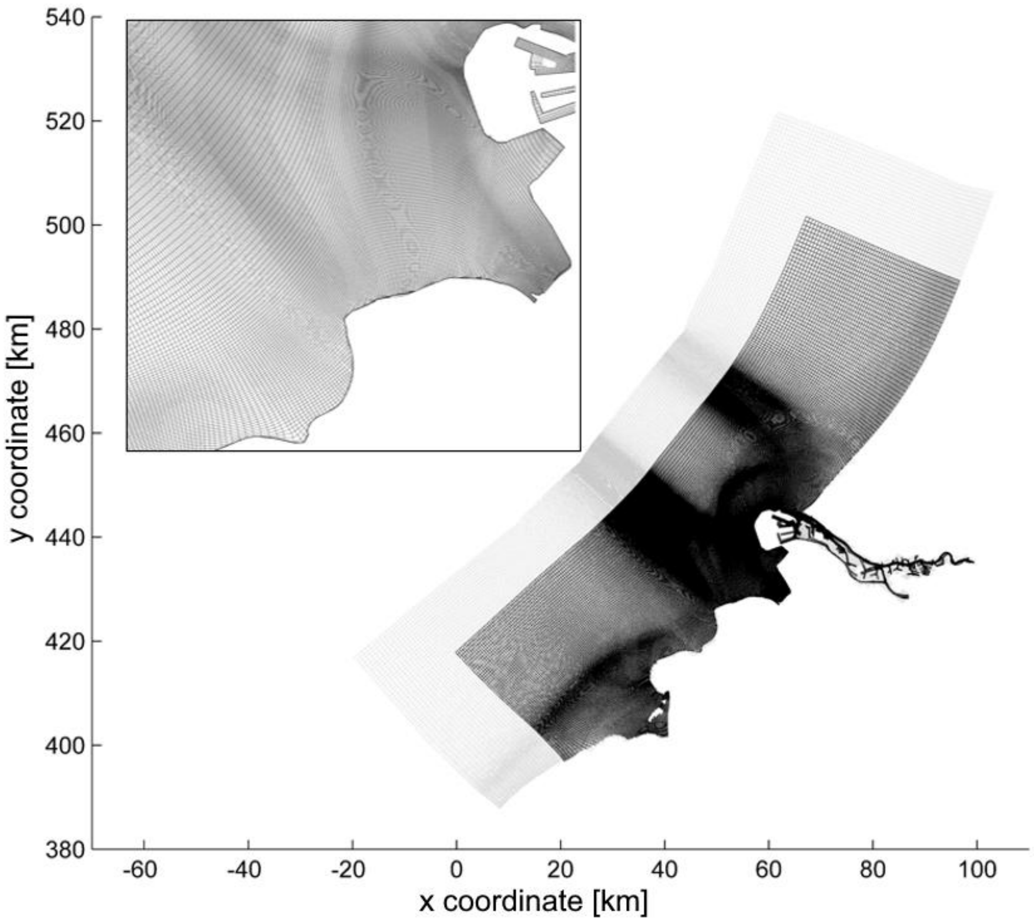


FIGURE 24: DELFT3D MODEL GRIDS FOR FLOW (BLACK) AND WAVE (LIGHT GREY), THE INSERT SHOWS THE GRID INSIDE THE RESEARCH AREA

The bathymetry used in the model is schematised using the 2015 Vaklodingen dataset of Rijkswaterstaat. However, the Vaklodingen dataset only covers the near-shore area up to -20 m NAP. Therefore the bathymetric data was supplemented by the offshore bathymetry of the North Sea model. Thereafter the depth has been specified on the corner of every grid cell using triangular interpolation at locations with a low density of datapoints and grid cell averaging at locations where the density was high. The resulting schematised bathymetry has been smoothened at locations with small-scale disturbances. Afterwards, the sediment characteristics were specified. Even though Section 2.4.1 stated that there is also a small amount of mud present in the research area, the sediment was schematised by only one layer of sand with a median grainsize of 160 μm. This is done because the focus of this study is on the Natura2000 habitats that mainly consists of sand only. Besides, mud transport calculations require information on initial mud concentrations which is not available for the simulated period.

## 4.3 Boundary conditions

The non-linear shallow water equations computed in the FLOW-module require boundary conditions. These boundary conditions have to be provided at all open boundaries. In Delft3D boundaries are closed by default, examples of other boundary conditions are: water level, discharge, current, waves, etc. This section treats the derivation and setup of the boundary conditions for both the FLOW and the WAVE module used in this study.

### 4.3.1 FLOW boundary conditions

The FLOW grid contains three different types of open boundaries. All open boundary conditions are prescribed by a time series of the period 01-08-2001 till 01-09-2001 such that it contains at least one full spring-neap tidal cycle. For the seaward NW and NE boundaries a water level boundary condition is applied. The SW-boundary is prescribed by a current boundary condition to prevent disturbances from entering. The time series for these boundary conditions are extracted from Arcadis' North Sea model. The modelled water levels have been verified using the online dataset of Rijkswaterstaat (2020), the comparison is shown in Appendix B.

The landward open boundaries of the Oude Maas, Nieuwe Waterweg and Eastern Scheldt are prescribed by a discharge condition. For the Oude Maas and Nieuwe Waterweg the time series of the old model of Van Holland (1997) and Steijn, Eysink et al. (2001) are used while for the Eastern Scheldt a time series has been obtained using measurement data from a study of Ministerie (2010). In model scenario 0, a discharge condition is set for the Haringvliet boundary. In model scenario 1 this condition is replaced by a time series of discharge conditions obtained from another Delft3D model that includes the upstream part of the Haringvliet estuary. This model, from a study of Piña (2020), uses the Delta21 scenario where the tide can freely enter and leave the open Haringvliet estuary, which corresponds to scenario 1 of this model study.

For morphodynamic calculations it is also necessary to specify the sediment concentration at the open inflow boundaries. In Delft3D-FLOW this is done by setting a zero concentration gradient at the boundaries, meaning that the concentration at the boundary is equal to the concentration just inside the model domain.

To resume, to represent the Delta21 processes in Model1, discharge points were used to simulate the ESL pump station. A total of 9 discharge points are used, each discharging 1111 $m^3/s$ to get to a total of 10,000 $m^3/s$ and changing direction linearly starting at 6 h and at 18 h every day. Further, a sediment thickness file was used to simulate the bed protection in front of the ESL pump station and in the inlet of the tidal lake by setting the thickness to zero at these locations. At last, the initial bathymetry has been adjusted in order to fit the Delta21 layout. This consisted of deepening the Slijkgat channel to -10m NAP starting at the Haringvliet sluices and ending at the tidal inlet, crossing the tidal lake in WNW direction. Further, adding dry points and applying a sandy slope to represent the Delta21 sandy dune contour. All adjustments correspond to the Delta21 plan as proposed in Lavooij and Berke (2020).

### 4.3.2 WAVE BOUNDARY CONDITIONS

Wave data has been gathered from the measurement station Europlatform (3.28$^0$E, 52.00$^0$N) for the period 01-01-2012 till 01-01-2019. The data contains the offshore significant wave height, peak period, peak direction and surge levels measured every 10 minutes. To schematise the wave climate, the dataset is sorted into bins. Each bin represents a class with respective class sizes of $\Delta H_s = 0.5$ m and $\Delta Dir_p = 15^0$. All waves are assigned to one of the bins, the number of waves in one bin divided over the total number of waves resulted in the probability of occurrence of each bin (see Appendix B).

In order to limit the computation time and complexity of the Delft3D model, the schematised wave climate is reduced from 229 to 12 conditions. De Queiroz, Scheel et al. (2019) tested the most common reduction methods on the dynamics of sandbars. They found that wave climate reduction by binning methods in general provide better results than clustering methods. The Sediment Transport Bins method performed best, however, this method requires sediment transport data which is not available for the same period as the wave data. Consequently, the fixed bins method resulted in the best reduction technique for this study. The fixed bins method uses the significant wave height and the wave direction as input and divides all wave conditions in pre-defined bins. De Queiroz, Scheel et al. (2019) furthermore suggested a higher resolution in wave direction bins than wave height bins. Additionally, weighting the wave height bins proportional to $H_s^{2.5}$ performs better than methods based on wave

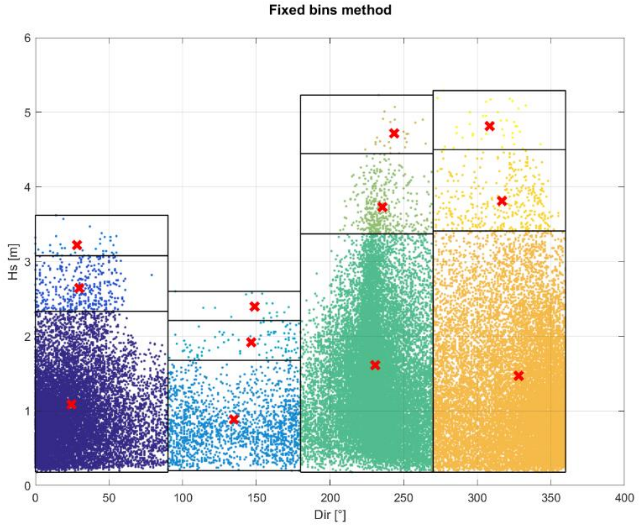


FIGURE 25: REDUCTION OF WAVE CONDITIONS USING THE FIXED BINS METHOD

statistics only. After defining and weighting the bins, the representative conditions were determined based on the centre of gravity of each block. The results are shown in Figure 25. The 12 wave conditions and their correspoding probability of occurence, wind characteristics and surge levels are shown in Table 4.

TABLE 4: REDUCED WAVE CLIMATE

| Condition | Hs [m] | Tp [s] | Wave dir. [º] | P[-] | Wind dir. [º] | Wind spd [m/s] | Surge [m] |
|---|---|---|---|---|---|---|---|
| **1** | 1.6142 | 4.2598 | 230.6426 | 0.3939 | 235.29 | 8.65 | -0.020 |
| **2** | 1.4674 | 4.5429 | 328.2644 | 0.3223 | 290.77 | 5.62 | 0.003 |
| **3** | 1.0853 | 4.1309 | 24.4642 | 0.2321 | 56.88 | 7.25 | -0.090 |
| **4** | 0.8838 | 3.4569 | 134.6984 | 0.0284 | 143.64 | 7.82 | -0.303 |
| **5** | 3.7308 | 6.1594 | 235.8058 | 0.0072 | 230.67 | 13.6 | 0.373 |
| **6** | 3.8115 | 6.3465 | 316.6577 | 0.0062 | 275.38 | 16.85 | 0.913 |
| **7** | 2.6409 | 5.5358 | 29.8359 | 0.0062 | 64.17 | 12.67 | -0.140 |
| **8** | 1.9152 | 4.5544 | 146.7197 | 0.0016 | 140 | 11.31 | -0.108 |
| **9** | 4.8163 | 6.9225 | 308.4861 | 7.02E-04 | 312.5 | 17.67 | 0.966 |
| **10** | 3.2171 | 5.92 | 28.0768 | 7.02E-04 | 62 | 12.9 | -0.240 |
| **11** | 4.7177 | 6.692 | 243.5045 | 4.39E-04 | 256.15 | 18.38 | 0.222 |
| **12** | 2.3962 | 4.9176 | 148.7735 | 2.98E-04 | 141.1 | 13.56 | -0.283 |

## 4.4 FLOW AND WAVE MODULE SETUP

The model scenarios have been running on 1 spring-neap tidal cycle, which is equal to 14 days. To take model spin-up into account the simulation time has been extended by 1 day. Scenario I. Tide only used a time step Δt of 1 min and after 1440 min spin-up time the sediment transport computations were initiated. For scenario III. All processes a time step  Δt of 0.5 min was used to ensure a stable simulation. The models in this scenario have run with the Parallel Online approach. With this approach all wave conditions are run simultaneously and share the same bathymetry. The results of each condition are weighted using the probability of occurrence as shown in Table 4 and summed to obtain the results of the complete reduced wave climate.

Further, a morphostatic model setup has been used, in which the bed level is fixed and initial sedimentation/erosion patterns are analysed via the bed composition update in Delft3D. When the composition update is turned on during the simulation, the initial sedimentation/erosion patterns can be calculated by comparing the bed composition of different timesteps. All other parameter settings of the different Delft3D modules are described in Appendix B.3 Main model parameter settings.

## 4.5 CALIBRATION AND VALIDATION

Setting up a model is aiming to reproduce the physical mechanisms as closely as possible. This calibration is done by tuning the models parameter settings. Validation is done by proving the accuracy of the model output using an additional dataset. A sensitivity analysis was performed on the original model of Van Holland (1997), the model was validated on hydrodynamic and morphodynamic results as well. The model was calibrated and validated by Steijn, Eysink et al. (2001) a view years later. The model was reviewed by De Vries (2007) and later used by Colina Alonso (2018) for a study on the evolution of the Hinderplaat using varying processes and a morphostatic approach. Because of the significant similarity of the approach in the same research area, their findings have been taken into account in this research by taking over these reviewed parameter settings. Although the focus of these previous studies somewhat differ from the focus of this study, further calibration and validation is yet considered to lie outside the scope of this study. Moreover, the model is considered to act as a tool to obtain insight in the Delta21 system. Therefore it is not the aim to optimize the existing model settings.

# CHAPTER 5

# MODEL RESULTS AND ANALYSES

## 5.1 INTRODUCTION

Three model scenarios have been simulated, each on three different simulations: I. Tide only, II. Wind and III. All processes (see Section 3.2). This chapter presents the most relevant results of the model experiments. Firstly the flow patterns are studied in Section 5.2. The flow patterns are divided in tide-driven currents and wave-driven currents, to understand the difference in contribution. Secondly, the morphodynamics are analysed in Section 5.4. Section 5.4 focusses on the sediment transport patterns of the different model scenarios, followed by the resulting initial sedimentation and erosion patterns.

## 5.2 FLOW CHARACTERISTICS

### 5.2.1 TIDAL PROPAGATION

In Section 2.3.1 the tidal characteristics inside the research area are discussed. It was concluded that after closure of both the Grevelingen and the Haringvliet estuary the tide changed from propagating cross-shore to propagating in alongshore direction. Figure 26 shows the orientation of the tidal propagation per scenario. Looking at Model0, which simulates the present-day scenario, the alongshore tidal propagation can be seen clearly. The Model1 scenarios, that include Delta21 and the opening of the Haringvliet estuary, show the same alongshore propagation until the entrance of the tidal lake. From this point on, the tide starts propagating in cross-shore direction into the tidal lake and the Haringvliet estuary. This change in propagation orientation is similar to the situation before closure of the Haringvliet estuary in 1957.

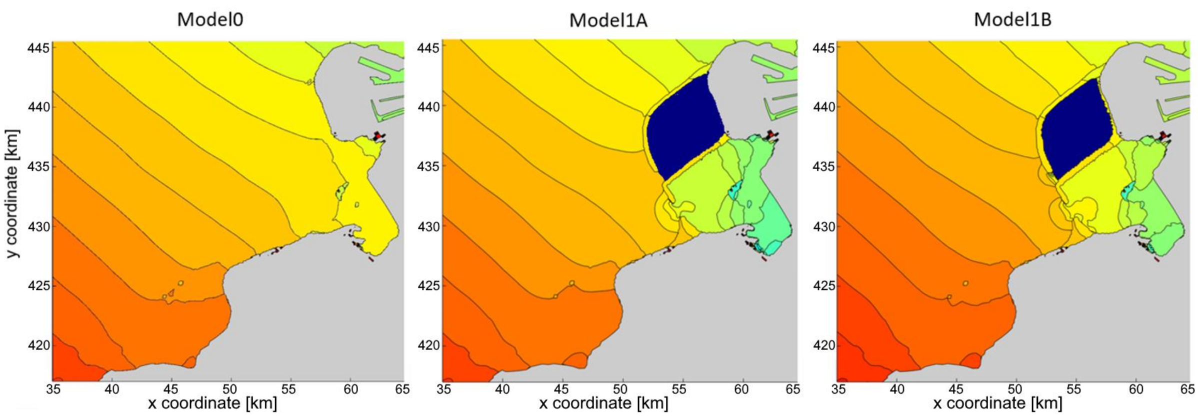


FIGURE 26: ORIENTATION OF THE TIDAL PROPAGATION PER SCENARIO, EQUAL COLOUR MEANS EQUAL TIDAL PHASE

In the situation before 1957 the water level in the Haringvliet estuary was out of phase with the water level at sea. This changed after closure to the water levels being more or less in phase. Figure 28 shows the difference between the water level offshore and at the Haringvliet sluices. The left picture, showing the Model0 scenario, presents the situation after closure with the water levels being in phase. The right picture however, illustrating the Model1 scenario, shows that the water levels are again out of phase. This change can be related to the shape change of the estuary. In Model0 the Haringvliet estuary ends at the Haringvliet sluices and has a tidal prism of 15 $Mm^3$. This results in the Haringvliet following the characteristics of a short basin. Whereas in Model1 the Haringvliet estuary is opened again, increasing the tidal prism up to 237 $Mm^3$ and following the characteristics of a long basin.

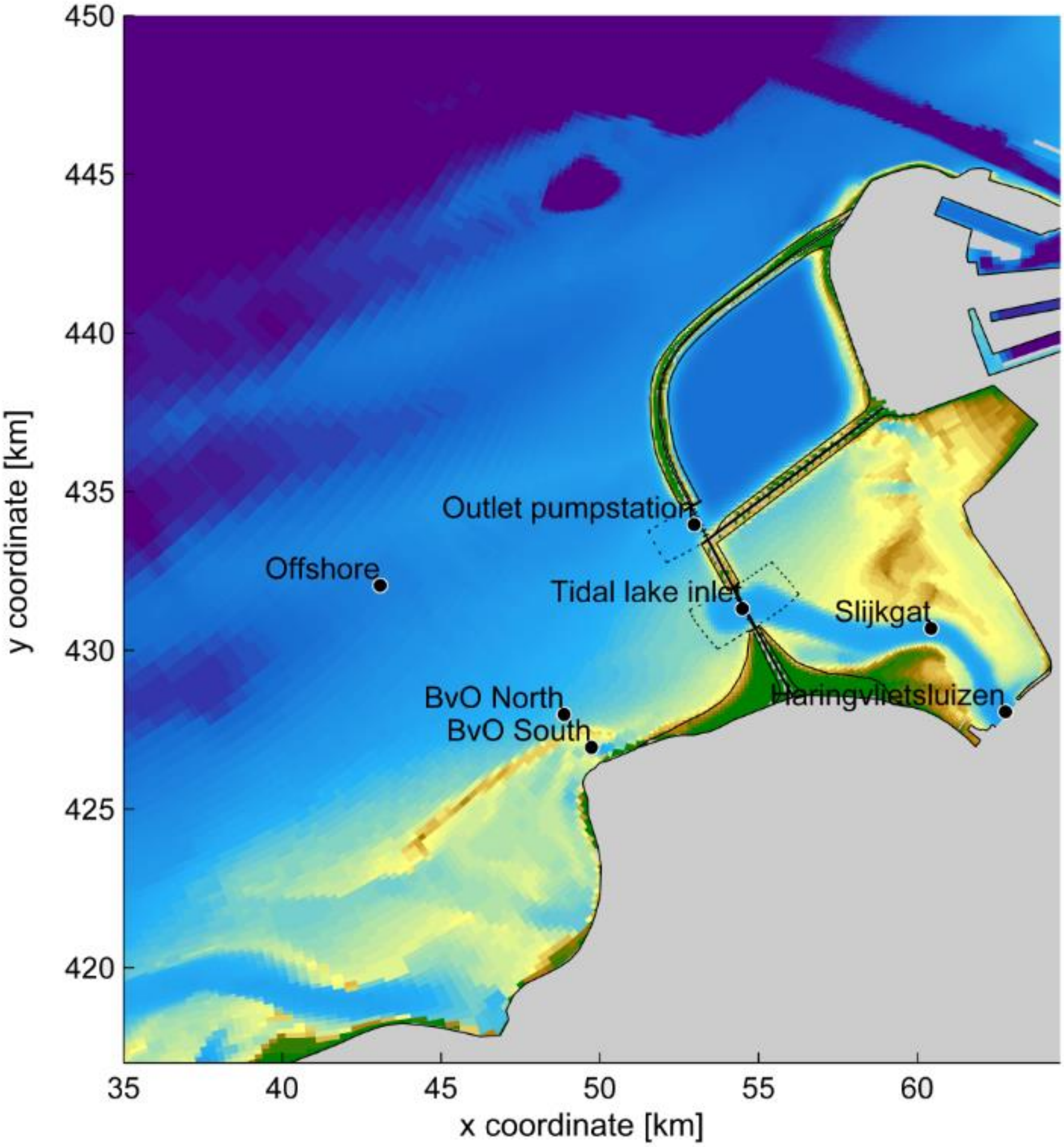


FIGURE 27: LOCATIONS OF THE OBSERVATION POINTS

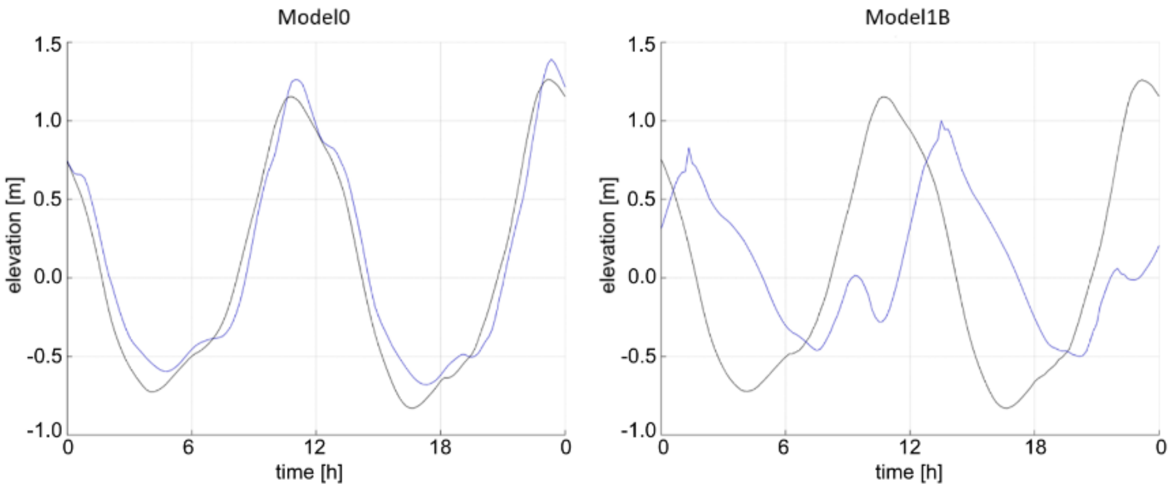


FIGURE 28: WATER LEVEL OFFSHORE (BLACK) AND AT THE HARINGVLIET SLUICES (BLUE), WITH AND WITHOUT DELTA21. THE LOCATIONS OF THE TIME SERIES ARE SHOWN IN FIGURE 27

### 5.1.1 TIDE-DRIVEN CURRENTS

As explained in Section 2.3.1, the tide-driven currents changed from cross-shore to longshore after the closure of the two estuaries. Inside the Haringvliet outer delta the flow patterns became complex due to the interaction of the tide-driven currents with the river discharge and the complicated delta bathymetry. In the Grevelingen outer delta the flow directions nowadays are parallel to the coast.

In the presence of Delta21 the tidal propagation in the Haringvliet changed from longshore to cross-shore again, which is related to the increase of the tidal prism. The change in propagation is likely to cause changes in flow patterns as well. The difference in tide-driven currents between the two model scenarios is described in this section.

#### 5.1.1.1 FLOW PATTERNS

I.Model0 simulated the present-day flow patterns. The flow patterns during four representative tidal stages are shown in Figure 29. These stages are marked with blue lines in the water level plot at the right side of the figure. The other four plots show the flow direction at each representative stage, illustrated by white and red arrows. The size of these arrows indicate the magnitude of the flow velocity.

At low water (*stage 1*), the flow velocities are highest at sea and in ebb direction. At the NW corner of Maasvlakte 2 the ebb-current is contracted and high velocities arise. The flow follows the curvature of the Haringvliet outer delta to the south. There river water flows seaward, through the Slijkgat. At low water the Bollen van de Ooster is exposed, blocking the flow coming into the Grevelingen outer delta. At the south, water leaves the outer delta in a shore-parallel direction.

During flood (*stage 2*), the flow velocities are highest along the coastline and directed north. The flow enters the Grevelingen outer delta at the south leaving it in the north, partly over the submerged Bollen van de Ooster. At the Haringvliet the flow enters via the Slijkgat where the river flow blocks the incoming flood current. At the north side water flows into the outer delta over the partly submerged Hinderplaat.

At high water (*stage 3*), the flow at sea is the strongest and in northern direction. The flow inside the Grevelingen outer delta decreased. The flow at the Haringvliet outer delta still enters via the south but now leaves the delta via the north. The Hinderplaat is completely submerged and water flows over it while leaving the part of the delta behind it. At the most western boundary of Maasvlakte 2 the flow is contracted again but now in opposite direction compared to *stage 1*.

During ebb (*stage 4*), the flow at sea decreased significantly but is still in flood direction while along the coast the flow already turned into ebb direction. The flow patterns inside the outer deltas are similar to *stage 1* but since flow velocities at sea are relatively low the outgoing flow is more cross-shore directed.

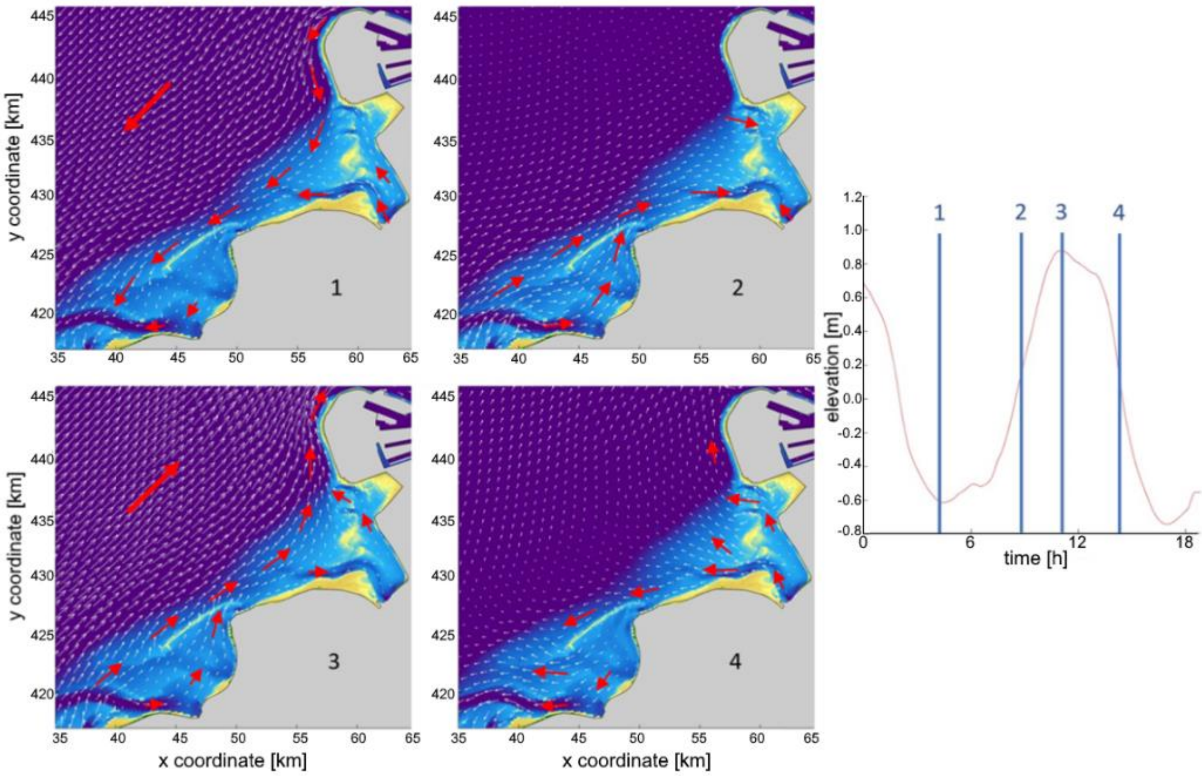


FIGURE 29: I.MODEL0 FLOW PATTERN OF FOUR TIDAL STAGES

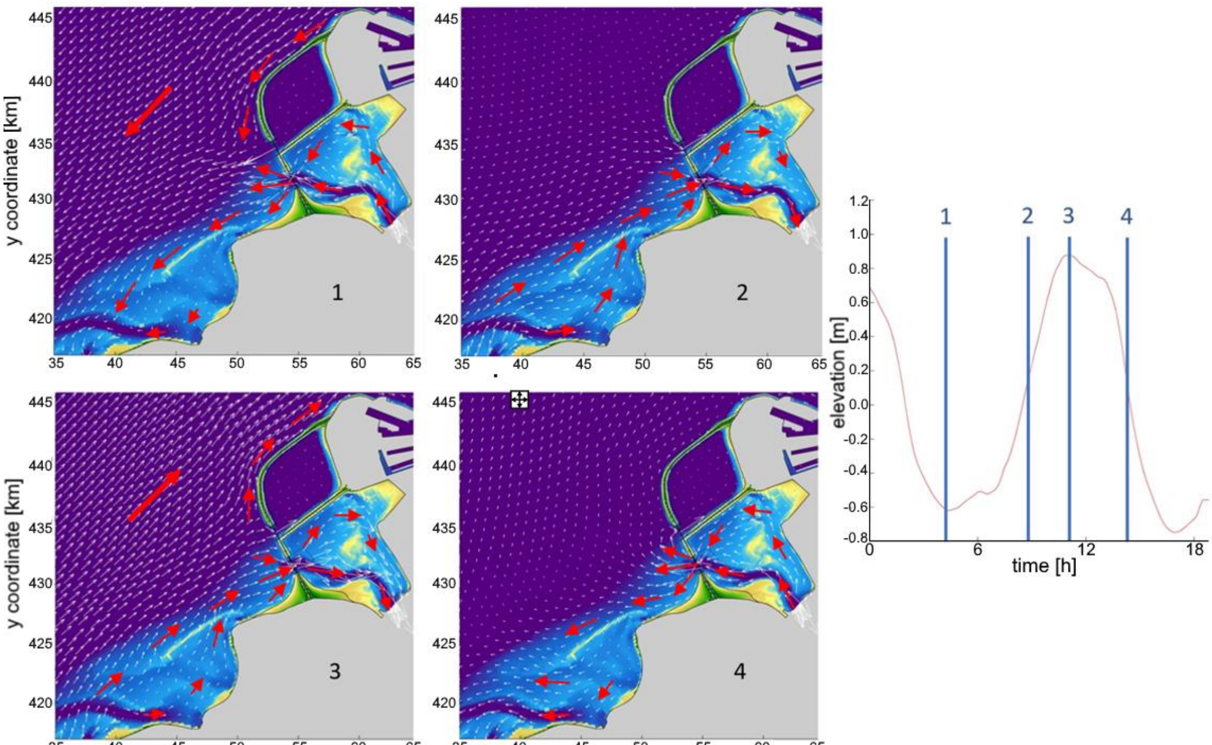


FIGURE 30: I.MODEL1B FLOW PATTERN OF FOUR TIDAL STAGES

The initial influence of the Delta21 project is simulated by Model1B. In this model the Haringvliet estuary is open and the Haringvliet outer delta is surrounded by the Delta21 boundaries. The flow patterns during the four stages of I.Model1B are shown in Figure 30. Comparing the flow pattern of each stage to the patterns observed in I.Model0 several differences can be seen.

Considering the two outer deltas, the Haringvliet flow patterns changed to cross-shore while the flow patterns in the Grevelingen outer delta are more or less the same during all stages. The tidal lake is filled and emptied via the tidal inlet. During ebb, the flow inside the tidal lake is directed anti-clockwise, around the Hinderplaat, and seaward. During flood, the flow pattern is exactly opposite. Further, at the tidal inlet this results in a converging and diverging flow patterns (see Figure 30).

In the Dutch SW coastal area, at sea maximum ebb and flood velocities coincide with low and high water. Along the coast and inside basins the maximum flow velocities start to lack behind the high and low water levels. Where offshore locations show a $0^0$ phase lag (see Figure 31), a phase difference up to $-90^0$ occur inside the Haringvliet estuary. Figure 31 shows that maximum flow velocities at the Slijkgat coincide with the maximum flow velocities offshore and high water comes 2 hours after high water at sea. In the present-day situation, high and low water level in the Haringvliet mouth coincide with the high and low water level at sea, while the maximum flow velocities do not, as explained before.

The phase difference between the velocities offshore and inside the estuary are important for the evolvement of the tidal inlet. If the flow velocities of the estuary and the sea are in phase, they enhance each other. The relative dominance of the waves at sea compared to the in and out coming tide becomes important to the symmetry of the ebb-tidal delta and the flow pattern in and around it. The models of Scha and Van den Berg (1993) showed that a large tidal prism leads to a higher relative tidal dominance compared to a small tidal prism. The overall effect can be addressed by averaging the currents over a spring-neap cycle, these so-called 'residual currents' are discussed in Section 5.2.

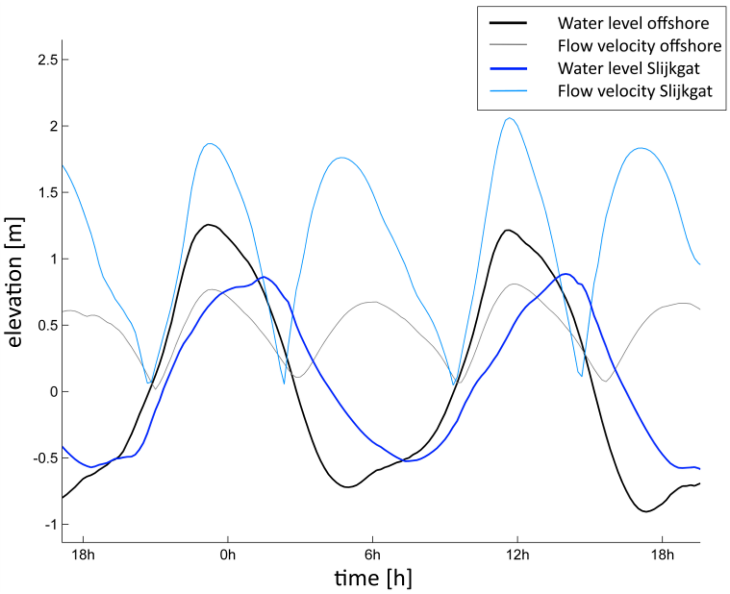


FIGURE 31: COMPARISON OF THE PEAK FLOW VELOCITIES OFFSHORE AND IN THE TIDAL LAKE, THE LOCATIONS OF THE TIME SERIES ARE SHOWN IN FIGURE 27

To resume, a similar process of the tidal squeeze around the corner of Maasvlakte 2 in the I.Model0 scenario can be seen around the NW corner of Delta21. Flow is contracted at this location in both ebb and flood direction. The flow at sea, flowing around the NW corner of the ESL, interacts with the pump station and the outflow of the tidal lake. The way it interacts depends on the working state of the pumping station. If the ESL is being filled, the flow sticks along the boundary of the ESL until the point where it is pushed seaward by the outflow of the tidal lake (see right plot of Figure 32). If the ESL is being emptied, the flow is pushed seaward by the pumping station (see left plot of Figure 32). The flow velocities in front of the pump station are discussed in the next section.

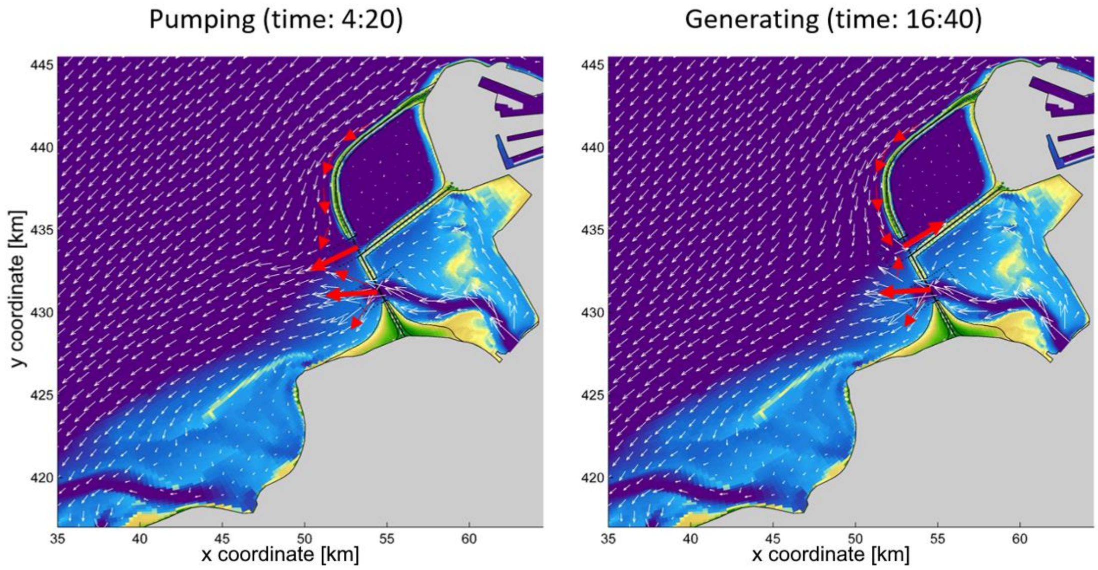


FIGURE 32: DIFFERENCE IN FLOW PATTERN BETWEEN AN EMPTYING ESL (LEFT) AND A FILLING ESL (RIGHT)

#### 5.1.1.2 TIDAL FLOW CHARACTER

The magnitude of the flow velocities can be important since they give insight in the amount of bed shear stress and consequently the expected sediment transport rates. The maximum water level and velocity units are studied and displayed in Table 5. It stands out that the flow velocities near the tidal inlet and inside the channels of the tidal lake increase in the Model1 scenarios. The biggest increase happens during spring tide, then the largest amount of water goes in and out the tidal lake through the inlet. The same principle yields for the channels inside the tidal lake. In the Model1 scenarios, these channels now transport the water in and out the opened Haringvliet estuary whereas in Model0 they only have to discharge the water of the Haringvliet outer delta. In the Grevelingen area, around the Bollen van the Ooster, no significant difference can be discovered between the three scenarios.

TABLE 5: MAXIMUM WATER LEVEL AND VELOCITY UNITS PER SCENARIO, LOCATIONS ARE SHOWN IN FIGURE 27

| | **Model0** | | | | **Model1A** | | | | **Model1B** | | | |
|---|---|---|---|---|---|---|---|---|---|---|---|---|
| *Water level max.* | **Spring** | | **Neap** | | **Spring** | | **Neap** | | **Spring** | | **Neap** | |
| | **HW** | **LW** | **HW** | **LW** | **HW** | **LW** | **HW** | **LW** | **HW** | **LW** | **HW** | **LW** |
| **Hvlt. sluices** | 1.974 | -0.852 | 1.070 | -0.538 | 1.551 | -0.856 | 0.625 | -0.428 | 1.561 | -0.855 | 0.620 | -0.443 |
| **Slijkgat** | 1.922 | -0.926 | 1.062 | -0.582 | 1.598 | -0.861 | 0.524 | -0.441 | 1.609 | -0.858 | 0.523 | -0.458 |
| **Inlet tidal lake** | 1.780 | -1.065 | 1.039 | -0.625 | 1.625 | -1.013 | 0.754 | -0.569 | 1.638 | -1.004 | 0.761 | -0.597 |
| **BvO North** | 1.758 | -1.134 | 1.062 | -0.656 | 1.729 | -1.133 | 1.047 | -0.668 | 1.742 | -1.134 | 1.058 | -0.667 |
| **BvO South** | 1.776 | -1.278 | 1.078 | -0.739 | 1.750 | -1.366 | 1.070 | -0.759 | 7.764 | -1.365 | 1.089 | -0.760 |
| **Outlet pump** | 1.725 | -1.033 | 1.019 | -0.609 | 1.711 | -1.048 | 1.025 | -0.629 | 1.692 | -1.036 | 1.020 | -0.678 |
| | | | | | | | | | | | | |
| *Velocity max.* | **Spring** | | **Neap** | | **Spring** | | **Neap** | | **Spring** | | **Neap** | |
| | **Flood** | **Ebb** | **Flood** | **Ebb** | **Flood** | **Ebb** | **Flood** | **Ebb** | **Flood** | **Ebb** | **Flood** | **Ebb** |
| **Hvlt. sluices** | 0.135 | 0.480 | 0.100 | 0.395 | 2.873 | 1.450 | 2.270 | 1.420 | 2.876 | 1.450 | 2.270 | 1.420 |
| **Slijkgat** | 1.033 | 0.882 | 0.412 | 0.644 | 2.830 | 2.040 | 2.060 | 1.863 | 2.820 | 2.020 | 2.050 | 1.874 |
| **Inlet tidal lake** | 0.651 | 0.360 | 0.340 | 0.248 | 2.720 | 2.544 | 1.652 | 1.930 | 2.763 | 2.490 | 1.660 | 1.950 |
| **BvO North** | 0.836 | 0.481 | 0.479 | 0.374 | 0.777 | 0.518 | 0.473 | 0.409 | 0.765 | 0.565 | 0.423 | 0.410 |
| **BvO South** | 0.813 | 0.785 | 0.517 | 0.468 | 0.780 | 0.554 | 0.498 | 0.364 | 0.782 | 0.534 | 0.477 | 0.365 |
| **Outlet pump** | 0.754 | 0.584 | 0.458 | 0.411 | 0.081 | 0.148 | 0.073 | 0.102 | 1.259 | 1.933 | 1.381 | 1.828 |

The biggest difference in flow velocities, between the I.Model0 and I.Model1B scenarios, are observed at the location of the ESL pump station (see Figure 33). I.Model1B, that includes the ESL pump system, shows a significant increase in flow velocity. However, as explained before, the actual appearing flow velocities at this location highly depend on the working state of the ESL pump system and the stage of the tide. During ebb flow, the flow is accelerated when the ESL is being emptied. The opposite happens during flood, where the outgoing flow is blocked by the tidal currents. The highest velocities occur during the night, when the ESL is being emptied. Model1A shows that without the ESL pump station the flow velocities become very low in front of the pumps. This can be explained by the counteracting flows of the tidal inlet and around the NW-corner of the ESL.

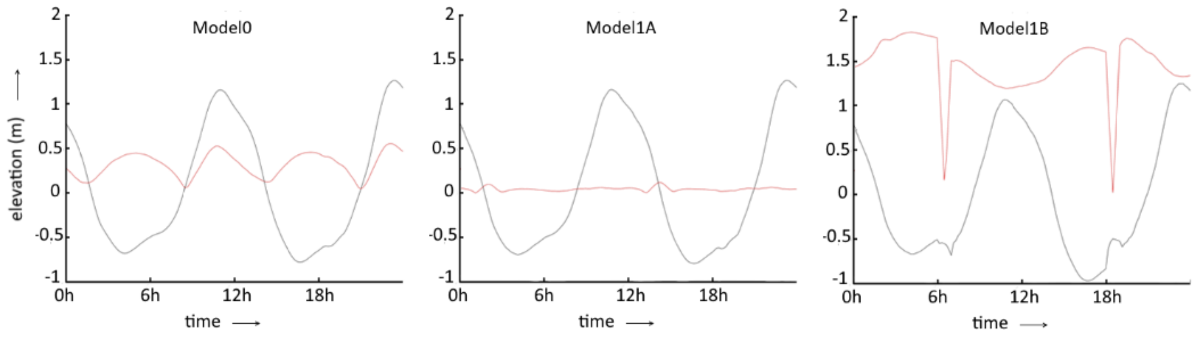


FIGURE 33: FLOW VELOCITIES (RED) AND WATER LEVEL (BLACK) AT OUTLET OF THE PUMP STATION, LOCATION IS SHOWN IN FIGURE 27

### 5.1.2 Wave-driven currents

After the closure of the two estuaries, waves have been a dominant driving force for the morphodynamics in the area (see Section 2.2.2). Further, literature showed that land reclamations like Delta21 could influence the propagation of waves and introduce shadow zones. Additionally, the relative importance of the waves can influence the symmetry and orientation of sandbanks, ebb-tidal deltas and channels. The change in wave-driven currents is treated in this section.

#### 5.1.2.1 Flow patterns

As stated before in Section 2.4.2, waves induce both cross-shore and longshore currents. Obliquely incident waves cause longshore currents along the Grevelingen and Haringvliet ebb-tidal deltas while normal incident waves cause cross-shore currents. The simulations of the individual wave conditions showed that the strongest longshore currents occur for larger obliqueness. This corresponds to the theory of Bosboom and Stive (2015), that states that maximum velocities happen for offshore wave angels of $\phi_0 \approx 45^0$. Other currents can be induced by setup differences or wind-driven currents.

Looking at the wave-driven currents of III.Model0 and III.Model1B in Figure 34, a prevailing longshore current is present in north-eastern direction in both model scenarios. Further, in general it looks like the wave-driven flow follows the coastline in both model scenarios. In the Delta21 scenario (Model1B) this results in almost no wave-driven currents inside the tidal lake and increased northern directed currents starting just westward of the Bollen van de Ooster. A remark has to be made regarding the fact that wave-, wind- and tide-driven currents cannot be seen separately since they affect each other, nonetheless it gives insight in the mechanisms behind the flow patterns.

Considering the combined wave- and tide-driven residual currents in Appendix C, there are no significant differences in the residual flow directions caused by the waves. This can be explained by the results as shown in Appendix C.5 Residual flow magnitudes, in which the residual flow magnitudes of the wind-, the tide- and the wave-driven currents are presented. Wave-driven currents are in the order of 0.02 to 0.05 m/s while tide-driven residual currents are much stronger (0.1 to 0.2 m/s). The influence of the waves is limited to the seaward areas of the two estuaries while the tidal currents cover the nearshore areas. The influence areas of the different processes is addressed in more detail in Section 5.3.

The longshore flow is related to the obliquely incident waves breaking on the foreshore of the outer deltas (see Figure 34). The residual flow pattern in northern direction is caused by the dominance of SW waves in the nearshore area. These waves induce setup at the eastern land boundaries of the Grevelingen and Haringvliet mouths (see Figure 35). The setup difference between these areas and the North Sea induce return currents in northern direction in order to compensate for the pressure gradient. It results in a strong return current in both model scenarios, at the northern part of the Bollen van de Ooster, caused by the setup in the Grevelingen mouth. In the III.Model1 scenario a large setup in the tidal lake, caused by the SW waves, results in a northern return current in front of the inlet (see Figure 34).

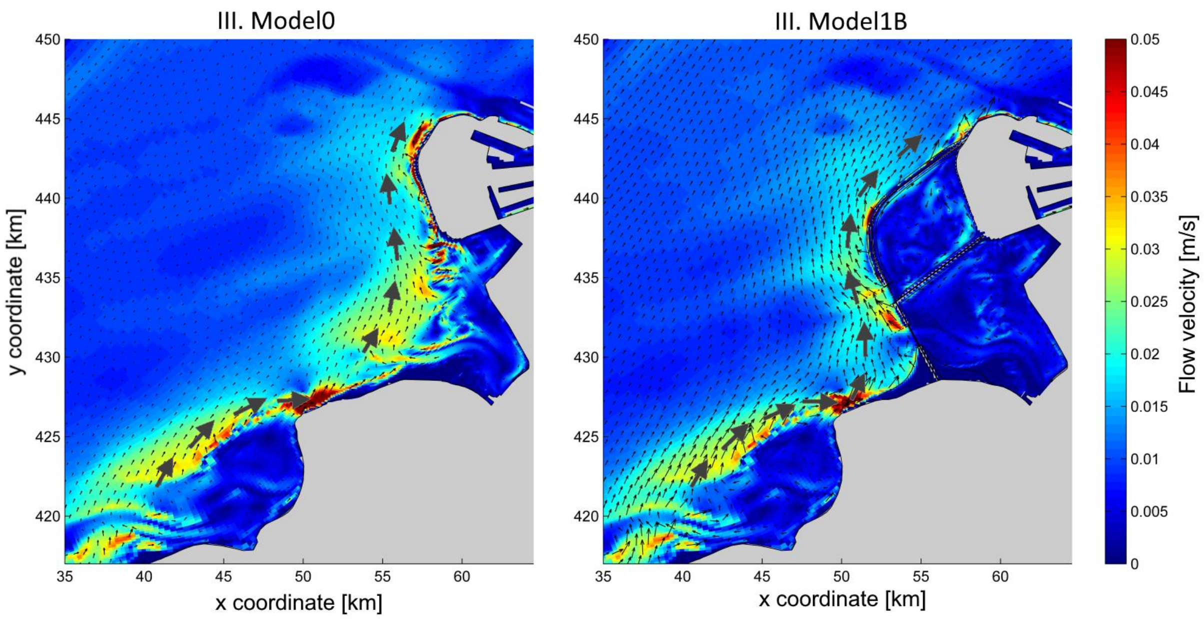


FIGURE 34: RESIDUAL WAVE CURRENTS

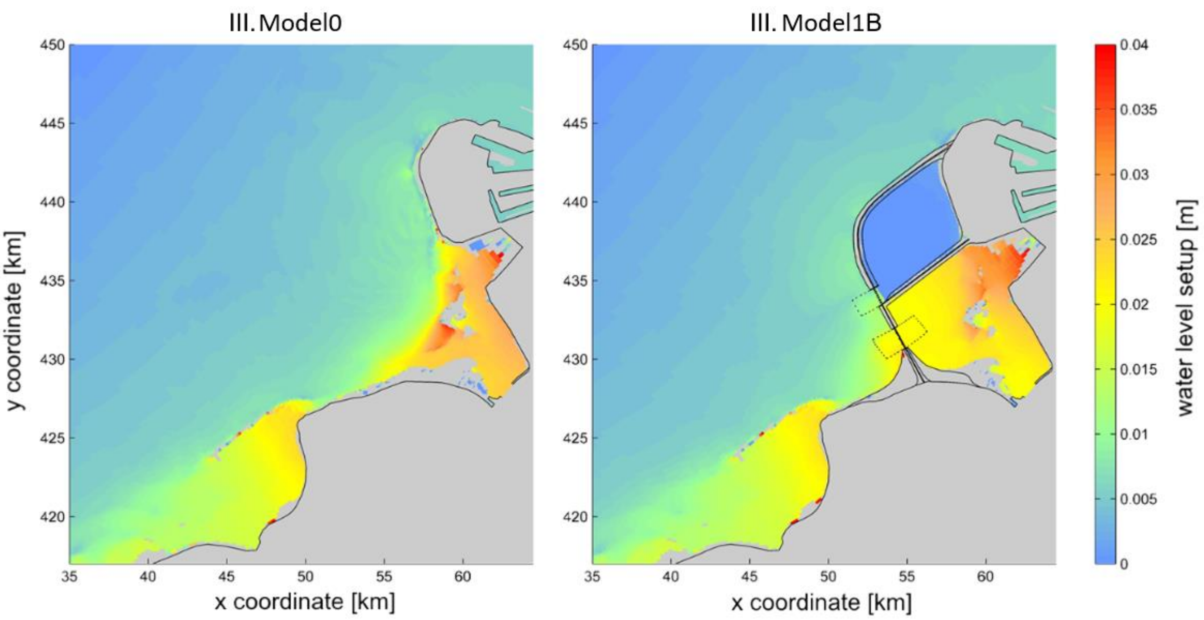


FIGURE 35: RESIDUAL WATER LEVEL SETUP

### 5.1.2.2 WAVE CHARACTERISTICS

As discussed in Section 2.3.3, a WNW wave direction prevails in the coastal area. Figure 36 shows the same prevailing wave direction for both scenarios. At the foreshore of the shallow outer deltas, the wave height decreases with depth and the Bollen van de Ooster and the Hinderplaat form a natural wave barrier. Here offshore wave heights strongly reduce by a factor 2-4. The figure shows that the rapid decrease of wave height happens at the foreshore, this is the location where most of the waves break. The same location shows the strongest longshore currents. The sheltering function of the Bollen van Ooster does not change in the Delta21 scenario. By contrast, the sheltering function of the foreshore of the Hinderplaat is completely taken over by the Delta21 barrier.

In the present-day scenario (III.Model0), an area of high wave heights occur at the North Western tip of Maasvlakte 2. In the Delta21 scenario, this area seems to be more spread out over the entire northern dune line of Delta21. Some local effects happen at the location of the outlet of the pump station and the inlet of the tidal lake, likely caused by the opposite directed outflow currents.

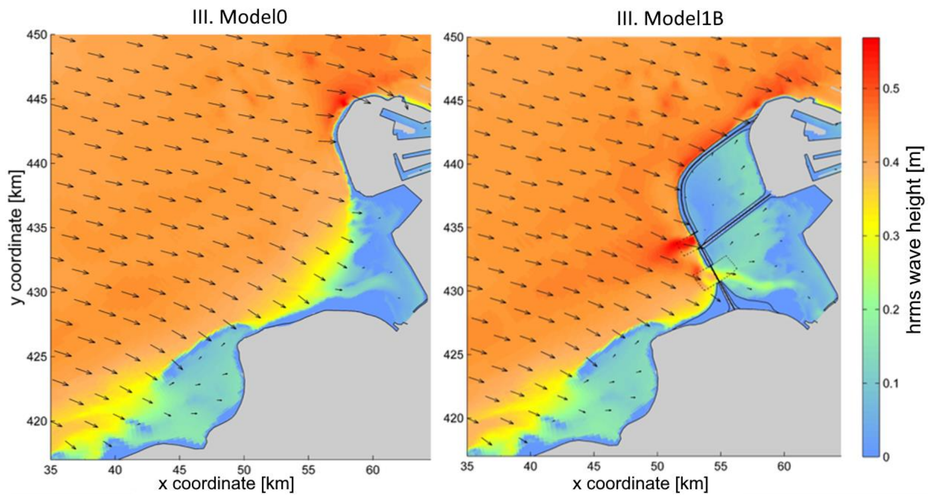


FIGURE 36: WAVE VECTOR AND WAVE HEIGHT OF THE REDUCED WAVE CLIMATE

Figure 37 shows the evolution of the wave height for south westerly waves and north easterly waves. For NE wave directions a shadow zone arises at the southwest side of Delta21, in the outlet area of the pump station and the tidal inlet. For SW waves this is not the case and waves can, to some degree, penetrate into the tidal lake. Inside the shadow zone wave heights are reduced and therefore NE waves have less influence on the longshore currents and the setup-driven currents in the area. Hence, SW waves dominate the residual currents.

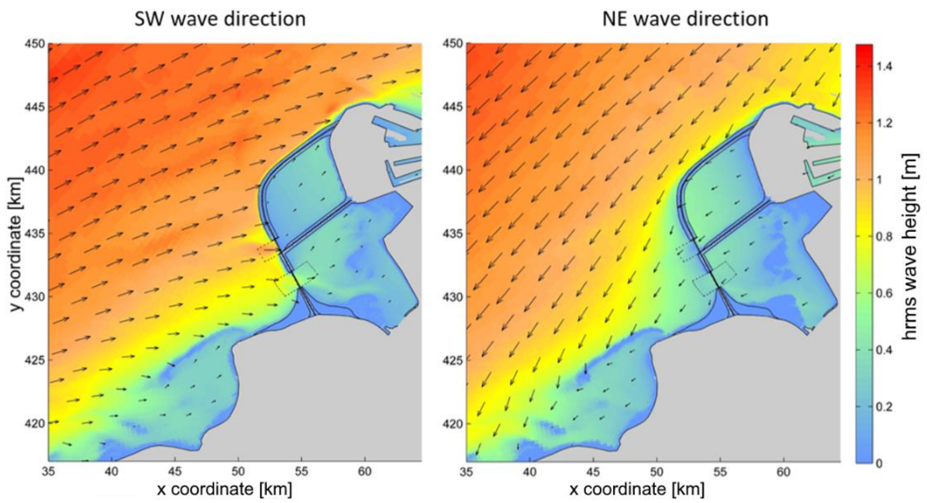


FIGURE 37: III.MODEL1B WAVE HEIGHT EVOLUTION OF DIFFERENT WAVE DIRECTIONS

## 5.3 Residual currents

The flood or ebb dominant character of the flow velocities can differ between spring and neap tide. By averaging the Eulerian velocities over a full spring-neap tidal cycle, using Fourier analysis, one can find the residual currents. The residual currents give insight in the actual flow character at a certain location. Figure 38 and Figure 39 show the residual flow map of respectively III.Model0 and III.Model1B. In general a flood dominant character is present over a full spring-neap tidal cycle. This results in a longshore flow in northern direction along the Brouwersdam and partly over the Bollen van de Ooster. In III.Model0 a mixed character is present in the Haringvliet outer delta. The Slijkgat is ebb dominant and seaward flow dominates the northern part of the delta. The ebb dominance of the Slijkgat can be related to the river discharge flowing through the channel, that is strongest during ebb and especially dominant during a neap tidal cycle (see Table 5). Outside the Hinderplaat the flow is longshore directed. These outcomes correspond to the findings of Colina Alonso (2018) who studied the development of the Haringvliet after its closure in 1957. As concluded, cross-shore tidal currents changed to a longshore flow pattern after closure.

The III.Model1B residual flow patterns show the same longshore flood dominance in the Grevelingen outer delta and outside of the Delta21 boundaries. There the longshore wave-driven currents dominate the residual flow pattern. This longshore pattern is strengthened by setup-driven currents. The setup differences between the Grevelingen mouth, the tidal lake and the North Sea causes a northern flow along the western coastline of Delta21. In contrast, inside the tidal lake the tidal cross-shore currents dominate.

Further, seaward of the tidal lake an ebb flow dominates while just landward of the inlet a flood dominant character is present. Inside the tidal lake a mixed flow character is present mainly caused by the irregular bathymetry of the lake. At high water, the inter-tidal areas in the NE are flooded and a landward flow pattern is present. These areas are emerged at low-water and the seaward flow can only go through the deeper parts, in particular the Slijkgat. At the Haringvliet sluices the flow is landward again, caused by a flood dominant character of the tide in the Haringvliet estuary.

A difference between III.Model1A and III.Model1B is only observed in front of the ESL pump station where a clockwise circular flow pattern remains in the III.Model1B results. The pattern shows landward flow from the north and seaward flow perpendicular to the coast. The detailed flow pattern of this location is shown in Figure 65 of Appendix C. This figure also shows the interaction between the longshore current and the cross-shore currents. It shows that the longshore wave-driven current deflects the cross-shore currents of the tidal inlet and the pump station. This phenomenon is discussed in more detail in Section 5.4.1.

Along the corner of the ESL a net northern longshore directed flow is present while along the northern ESL dune line a southern directed flow can be seen. In Figure 65 of Appendix C the detailed flow pattern at this location is shown. The process is similar to the flow mechanism at Maasvlakte 2 in III.Model0. Flood- and ebb-driven flow is contracted because of Maasvlakte 2 sticking into the North Sea. Likewise, the NW corner of Delta21 bulges out and along with the flood dominant character of the tide, causing the northern flow around the corner.

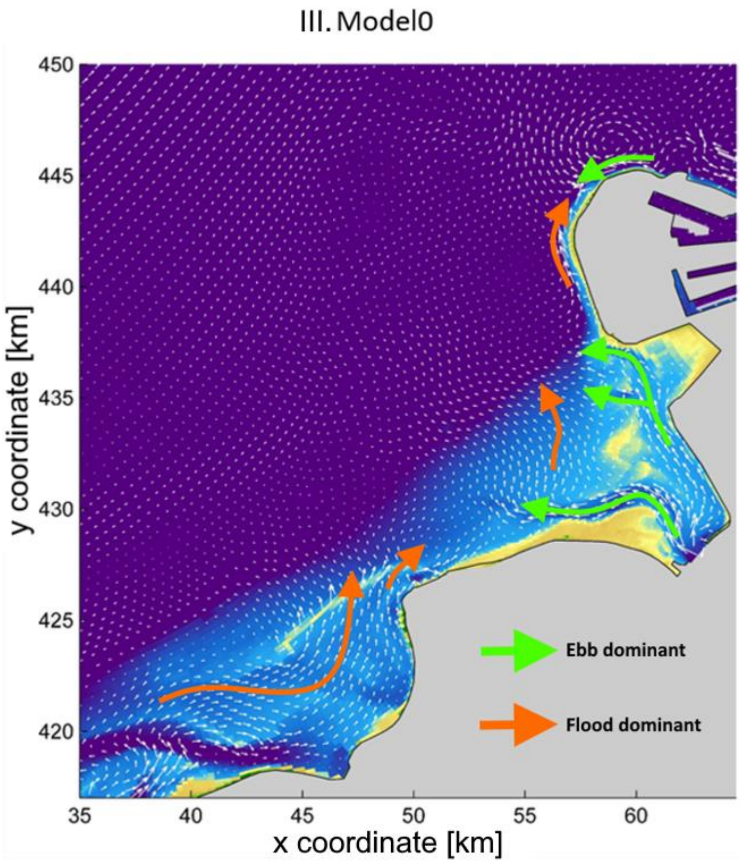


FIGURE 38: RESIDUAL CURRENTS OVER A SPRING-NEAP CYCLE, III.MODEL0

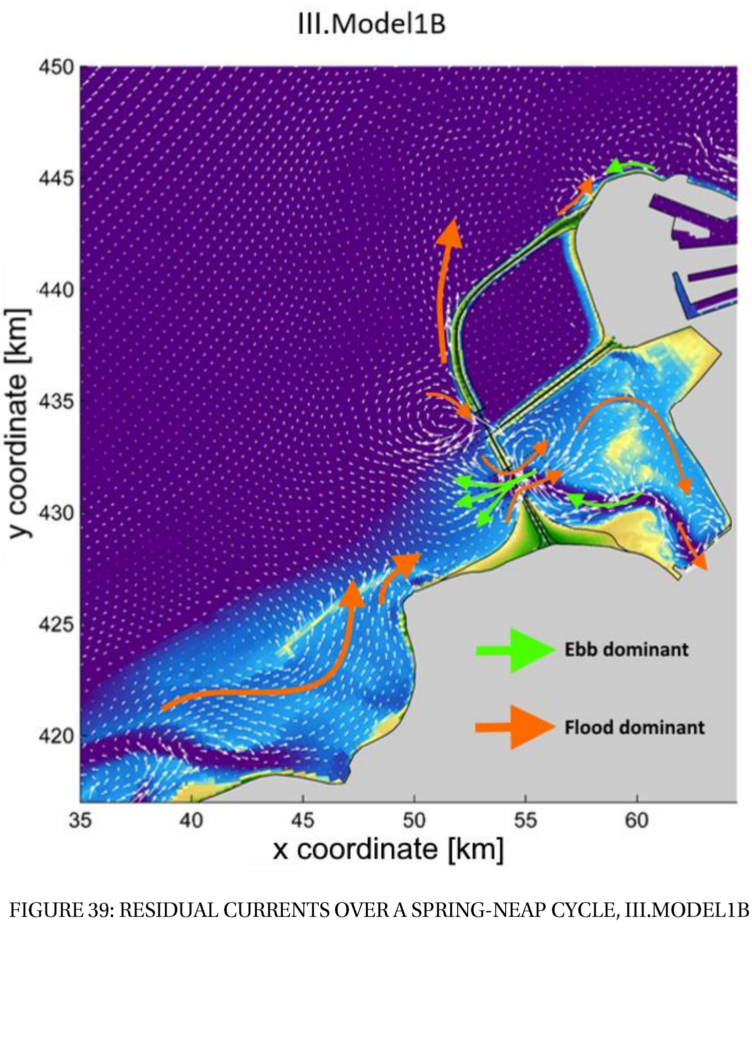


FIGURE 39: RESIDUAL CURRENTS OVER A SPRING-NEAP CYCLE, III.MODEL1B

## 5.4 SEDIMENT TRANSPORT CHARACTERISTICS

So far, the hydrodynamics inside the research area have been studied. This knowledge is important for the understanding of the sediment transport characteristics. Moreover, the transport of coarse sediment (sand) is thought to respond instantaneously to the flow velocity (Bosboom and Stive 2015). This section describes the sediment transport characteristics via a top-down approach. First, the general transport patterns of the entire research area are considered. Then, the transport patterns and characteristics at some important locations are studied. The section ends with the sedimentation and erosion patterns.

### 5.4.1 RESIDUAL TRANSPORT PATTERNS

Figure 40 shows the residual sediment transport patterns of the two model scenarios. Similar to the residual currents the prevailing direction of the transport, or 'net transport direction', is NE. Further, the net transport is the average transport of all wave conditions averaged over the full spring-neap tidal cycle. Therefore, Figure 40 shows that the longshore transport in northern direction has been dominant over the southern directed transport, this does not mean that southern transport does not happen. A longshore transport is not present in the tidal lake, there it follows the cross-shore character as observed in the flow patterns.

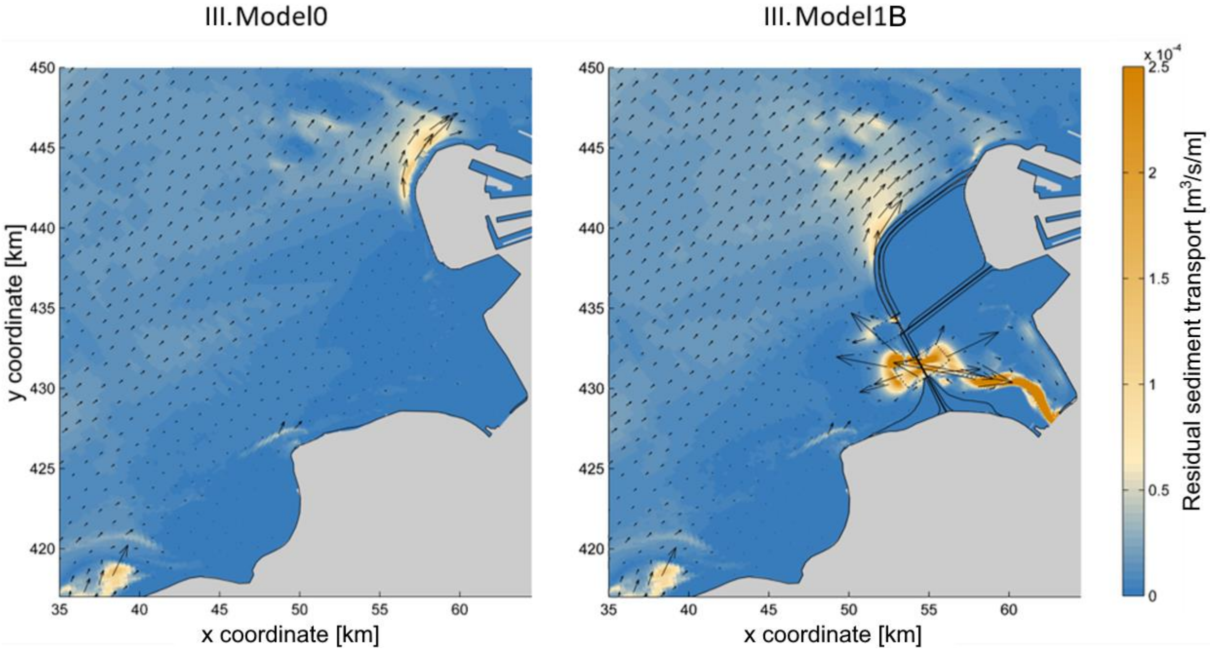


FIGURE 40: RESIDUAL SEDIMENT TRANSPORT PATTERNS

An analysis on sediment transport rates is done with the use of Detran (DElft TRansport ANalyzer). With this tool, sediment transport rates are calculated through arbitrarily chosen transects. The total transport through a certain transect is calculated based on the mean total transport and scaled over a certain time period. Figure 41 shows the annual net sediment transport rates through the chosen transects. The calculated transport rates however, do not represent the exact amount of transported sediment in a year. Further, the transport rates are used to give insight in the order of magnitude and the differences between certain locations.

#### 5.4.1.1 SOUTHERN AREA

Similar to the flow patterns, at the Grevelingen outer delta no significant difference in transport rates can be distinguished between the two scenarios. In contrast to the Grevelingen, a substantial difference can be observed in the Haringvliet outer delta. The cross-shore seaward residual flow pattern in front of the pump station and the tidal lake cause westward sediment transport in the Delta21 scenario (III.Model1B). In the present-day scenario (III.Model0), net sediment transport in the Haringvliet is directed eastward. Further, transport along the Grevelingen shore and the Bollen van de Ooster is opposite to the cross-shore transport in III.Model1B. The longshore transport is pushed seaward and results in bypassing at the east side of the

Bollen van de Ooster (see Appendix D.2 Additional results regarding sediment transport and Figure 65 of Appendix C). The bypassing is related to the setup-driven flow pattern which is in northern direction. This affects the cross-shore transports of the tidal inlet and the pump station at the seaside. There the transport is deflected in downdrift direction.

Figure 43 shows the sediment transport gradients along different paths. Path B shows the increasing sediment transport in seaward direction in front of the pump station. Increasing sediment transport rates is often related to erosion, whereas decreasing sediment transport rates leads to sedimentation. Therefore it is expected that erosion happens close to the pump station More seaward residual flow velocities decrease and sediment can settle, there sedimentation can be expected.

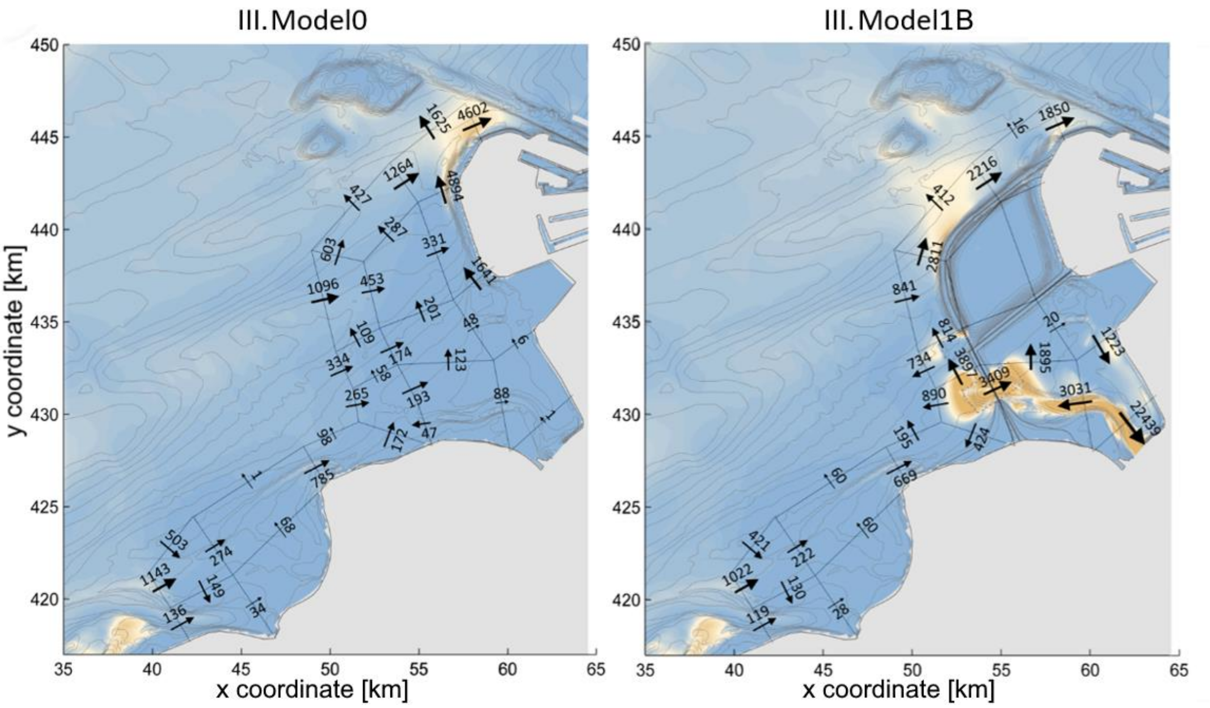


FIGURE 41: ANNUAL NET SEDIMENT TRANSPORT THROUGH TRANSECTS IN M³ (X100)

#### 5.4.1.2 NORTHERN AREA

North of the pump station the transport pattern changes to longshore again. In the present-day scenario a similar northern longshore transport is present along the western dike of Maasvlakte 2. Both transports can be related to the high flow velocities in the areas caused by tidal squeeze. At the northern tip of Maasvlakte 2 a net eastern directed transport is present in both scenarios. However, the transport is significantly higher in III.Model0. The transport pattern in III.Model1B follows the shape of the Delta21 corner but decreases along the northern Delta21 dune line. Path A in Figure 43 depicts the sediment transport along the NW corner of Delta21. The net sediment transport direction is to the north, sediment transport increases until the corner, after that it decreases.

#### 5.4.1.3 TIDAL LAKE

Figure 42 shows the detailed sediment transport pattern in the tidal lake. As became clear from the analysis on flow patterns, the tidal inlet represents the most dynamic area. The strong exchange of water through the inlet leads to high sediment transport rates in the area. Ebb-driven transport at the seaside is the direct response to the ebb dominant flow. Similarly, flood-driven transport prevails at the lake side. Path C in Figure 43 shows the sediment transport gradients through the inlet. In the middle of the inlet the increase in sediment transport is strongest and the transport direction is outward. After 300 to 500 m the rates decrease again. Inside the tidal lake, a clockwise directed transport can be recognized. The clockwise sediment transport pattern originates from a flood dominance at shallow areas. Conversely, along the deeper southern part, in the centre of the Slijkgat, the ebb-driven transport dominates. The flood dominance of the Haringvliet estuary, causes landward transport in the southmost area of the tidal lake.

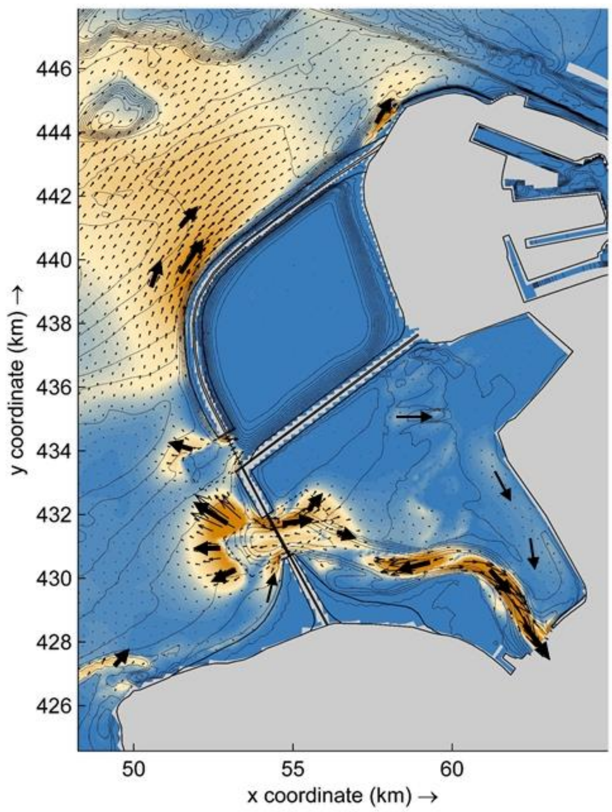


FIGURE 42: DETAILED NET SEDIMENT TRANSPORT PATTERNS OF THE III.MODEL1B SCENARIO

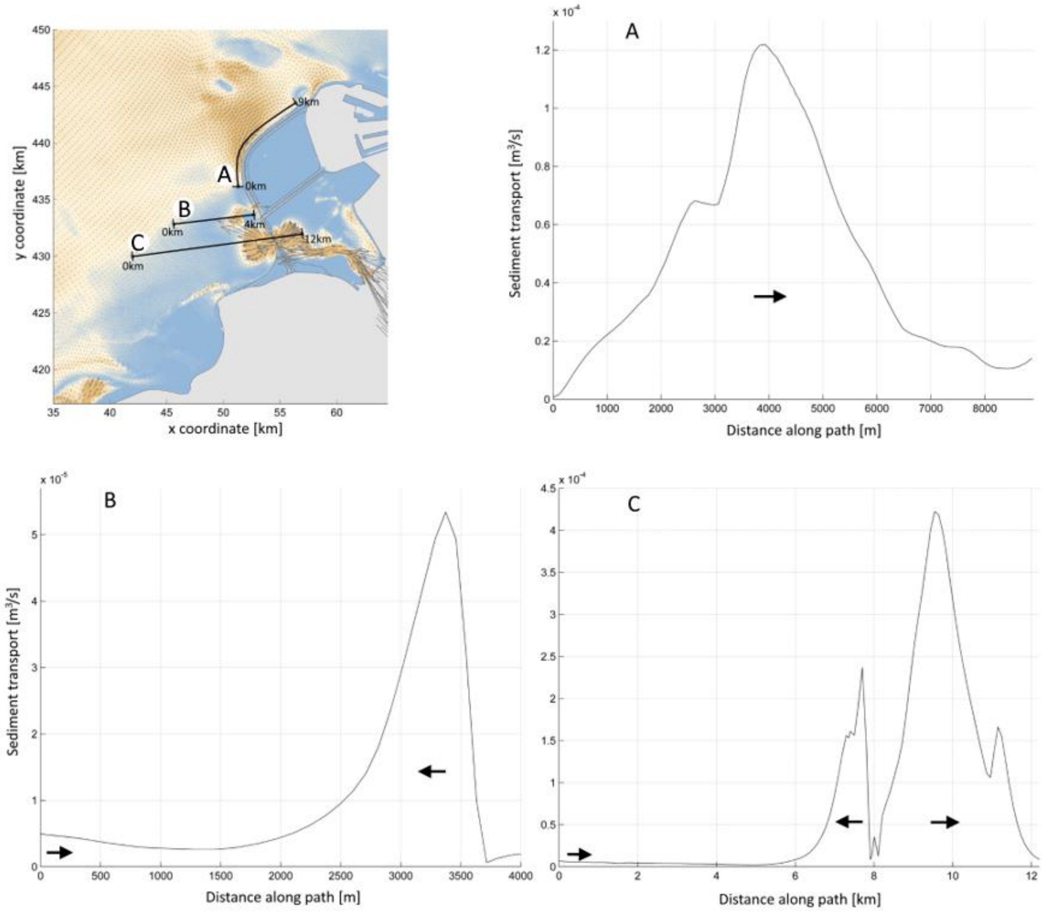


FIGURE 43: SEDIMENT TRANSPORT GRADIENTS ALONG PATHS A, B AND C

#### 5.4.1.4 INFLUENCE AREAS

In the previous sections it was discovered, by separating the wave-driven currents from the tide-driven currents, that the residual flow direction of both the tide and the waves are in northern (flood) direction. Again the same remark has to be made regarding the fact that wave- and tide-driven currents, and their related sediment transport, cannot be seen separately. Yet, analysing their individual influence can be useful for the understanding of the mechanisms behind the transport. With the use of the previously discussed Detran analysis, the influence areas of the various driving mechanisms have been studied. From this analysis and the residual flow analysis, it can be concluded that waves do not significantly cause different transport patterns but they enhanced the already existing tide-driven transport. Looking at the influence areas of the different driving mechanism in Figure 44, it is clear that the tidal lake is completely dominated by the tide (III.Model1B). In III.Model0 the waves dominate the sediment transport at the foreshore of the Grevelingen and the Haringvliet but in the III.Model1B scenario waves hardly affect the Haringvliet anymore. The western foreshore of Delta21 is affected by cross-shore tide-driven flow and the pump-driven flows and longshore wave-driven flows, which makes it a highly dynamic area. The northern foreshore of Delta21 is influenced by the tidal squeeze around the corner, the same mechanism that is present around Maasvlakte 2 in the III.Model0 scenario.

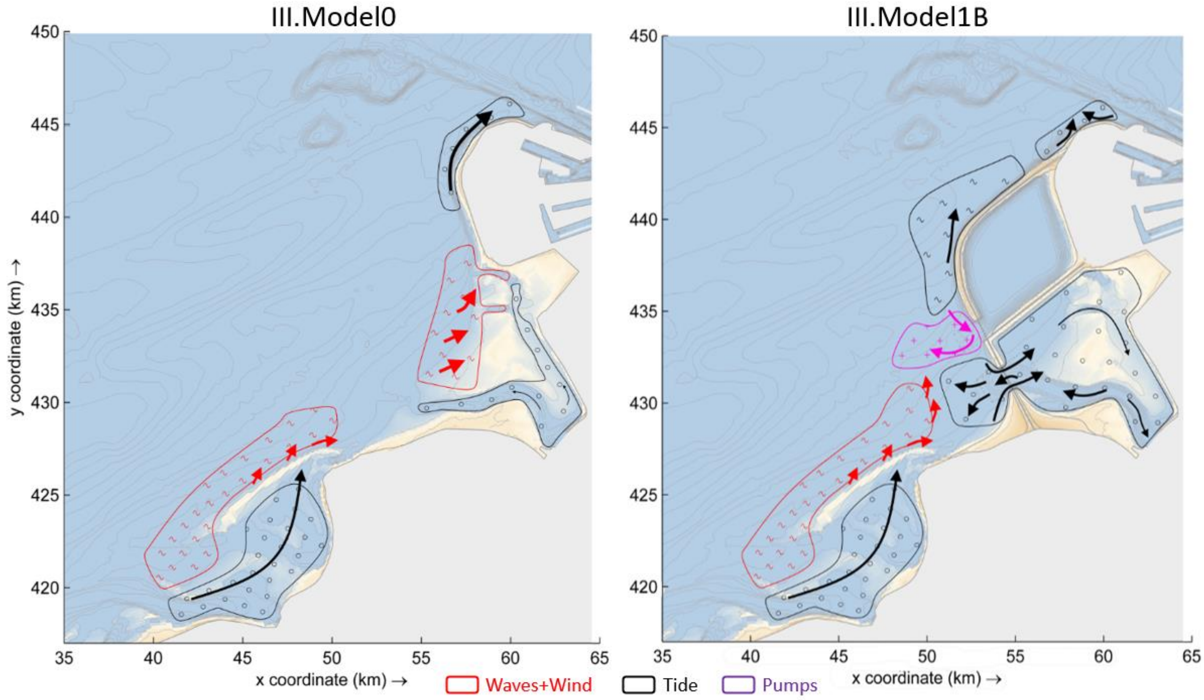


FIGURE 44: INFLUENCE AREAS OF THE VARIOUS DRIVING MECHANISMS

### 5.4.2 INITIAL SEDIMENTATION AND EROSION PATTERNS

Figure 45 shows the initial sedimentation and erosion patterns of the present-day scenario and the Delta21 scenario. Sedimentation and erosion are related to the gradients in sediment transport rates. In the present-day scenario only small changes happen to the seabed, especially in the Haringvliet delta. There is ongoing erosion happening at the corner of Maasvlakte 2 and elongation at the northeast side of the Bollen van de Ooster. Comparing the two scenarios, initially there are no significant changes to the morphology of the Grevelingen outer delta other than the already existing evolution. The major differences are found in the Haringvliet outer delta and at the northern part of the research area.

The strong exchange of sediment between the tidal lake and the outside area result in an ebb-tidal delta at the seaside of the inlet and a flood-tidal delta at the lake side of the inlet. Erosion in the middle of the inlet is the result of the high flow velocities and increased sediment transport at the location. The Slijkgat can be described as a mixed area of both sedimentation and erosion. The area experiences a mixed flood and ebb dominance, it results in the formation of channels and flats. The Hinderplaat is exposed to the changing dynamics of the transport at the south side. The clockwise transport around the north side causes minor changes to its morphology.

At the seaside of Delta21 a cross-shore transport, originating from the pump-driven flow, results in erosion around the bed protection. The eroded sediment nourishes the area more offshore where transport rates decrease again. Besides, the interaction between the pump-driven flow and the flow at the tidal inlet causes the formation of a small channel between the pump station and the tidal inlet. This channels is also used by the flood current that enters the tidal inlet from both the north and the south. A similar flood channel is present at the northern side of the pump station. However, this is caused by the inflow of the ESL. All in all there is a strong similarity between the sedimentation and erosion patterns of the pump station and the ebb-tidal delta. However, the morphodynamics of the ebb-tidal delta occur at a larger scale.

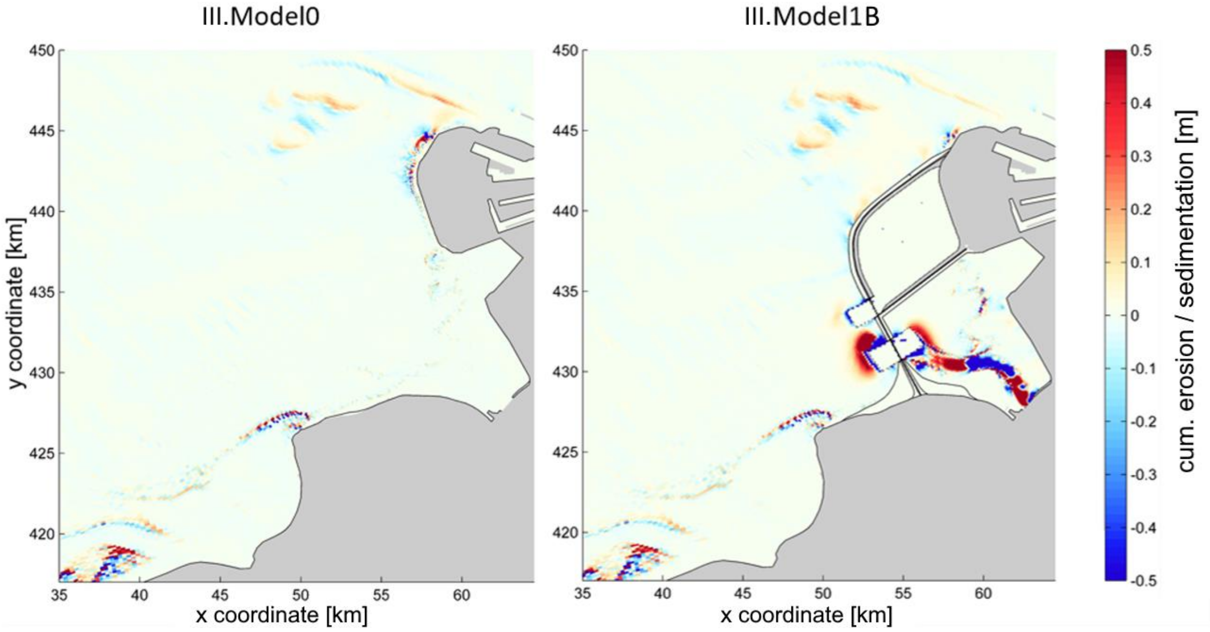


FIGURE 45: INITIAL SEDIMENTATION AND EROSION PATTERNS

Around the NW corner of Delta21, the sediment transport rates increase by the influence of wave- and tide-driven currents. The net transport is in northern direction and the increase causes erosion at the tip of the corner. North of the tip the transport rates decrease and due to the circular pattern caused by the flow separation, sedimentation at the north side is the result. This phenomenon is mainly caused by waves coming from SW that enhance the northern transport. The NE waves cause the exact opposite pattern, meaning that erosion happens at the north side of the corner and sedimentation at the south. Other areas, especially the tide dominated areas, do not show significant differences between the sedimentation and erosion patterns of the two dominant wave directions (see Figure 73 of Appendix D).

The erosion at the Maasvlakte 2 disappears in the III.Model1B scenario, only a small part of it remains due to tide-driven sediment transport around the corner. The detailed flow pattern in the area gives insight in the driving mechanism behind the transport and is shown in Figure 66 of Appendix C. However, details of this area are outside the scope of this study.

# CHAPTER 6

# CONCEPTUAL MODEL

## 6.1 INTRODUCTION

Based on the findings of the modelling study in Chapter 5, a conceptual model is elaborated in this chapter. This conceptual model summarizes the processes and visualises the initial morphological changes of the different scenarios. Besides, it provides the expected morphodynamics for the first years after implementation of the Delta21 plan based on expert judgement using the knowledge from both the literature review and the analysis of Chapter 5.

## 6.2 CONCEPTUALISING THE EXPECTED RESPONSE TO DELTA21

In this conceptual model the visualisation of the hydraulic and morphodynamic processes and the evolution of these systems in presence of Delta21 is presented. The visualisation is done for the initial situation, i.e. in the period directly after implementation of Delta21, using the results from Chapter 5 and for the situation 5 years after implementation. The latter is based on model results that used the expected 5 year bathymetry. This bathymetry is composed using the results as presented in Chapter 5 and a morphodynamic 'tide only' simulation. The conceptual model provides the comparison of the 5 year results with the results of the initial situation. In this way, the expected change of the system is conceptualized so that it gives answer on the following sub-question:

*To what extent will Delta21 initially change the morphological trend, in response to the initial change of the large scale and multi-year average processes?*

### 6.2.1 EXPECTED TREND INSIDE THE TIDAL LAKE

Prior to the closing of the Haringvliet and Grevelingen estuaries, the tidal propagation was mostly cross-shore directed and water levels offshore and inside the estuaries were out of phase. After closure the tide started to propagate in longshore direction and by reducing the tidal prisms, the cross-shore flow patterns disappeared. Following the characteristics of a short basin, water levels are now more or less in phase with the offshore water levels. The significant reduction of the tidal prisms caused the seaward extent of the tidal dominance to disappear. Waves started to 'bulldoze' the former ebb-tidal deltas onshore and created shore parallel sandbars like the Bollen van de Ooster and the Hinderplaat. The construction of the Maasvlakte 2 triggered sedimentation of the Haringvliet mouth, landward of the Hinderplaat, by sheltering the area from NW waves.

In the presence of Delta21 the coastal system of the Voordelta, particularly the Haringvliet mouth, changes significantly. The open Haringvliet estuary returns the tidal motion and the cross-shore flow patterns in the area. Similar to the situation prior to the closing of the Haringvliet, the water level inside the Haringvliet mouth, i.e. the tidal lake, is out of phase with the offshore water level. Following the characteristics of a long basin, friction causes the velocity to lag behind the water level inside the estuary. However, the flow velocity in the tidal lake is almost in phase with the offshore flow velocity.

The opening of the Haringvliet sluices increases the tidal prism from 15 $Mm^3$ to 237 $Mm^3$. The increased tidal prism introduces ebb and flow currents inside the Haringvliet mouth, i.e. the tidal lake. The tide dominates in this area and the influence of waves and wind are strongly reduced by the Delta21 barrier. Initially currents in the dredged Slijkgat are strong (peak: 2.8 m/s), during both ebb and flood. The entering water finds its path through the channel and clockwise around the Hinderplaat until it enters the Haringvliet estuary at the sluices (see Figure 48). The ebb flow shows a similar pattern in seaward direction and anti-clockwise around the Hinderplaat. The residual flow patterns show a flood dominance at the sluices, caused by a tidal asymmetry.

The system adapts to the new equilibrium. The adaption time is expected to follow a logarithmic decreasing character (Bosboom and Stive 2015). The morphodynamic model results of the 5 year simulation show the same logarithmic character. The flow velocities are expected to decrease over time as the channels are deepened and their conveying area increases (see Figure 46). Most of the water will be transported through deeper parts of the channel, i.e. the centre of the channels and at the outer sides of the corners. The deepened Slijkgat is likely to act as the main channel and flow patterns around the Hinderplaat will disappear. Due to the tidal asymmetry, most of the channel will be flood dominant. Inside the channel there will be different paths for flood and ebb due to meander effects in opposite directions. The former Slijkgat transports the ebb flow, while the dominant dredged Slijkgat transports the flood flow. This meander action causes sedimentation at the inner sides of the corners and erosion at the outer sides (see Figure 50 and Figure 51).

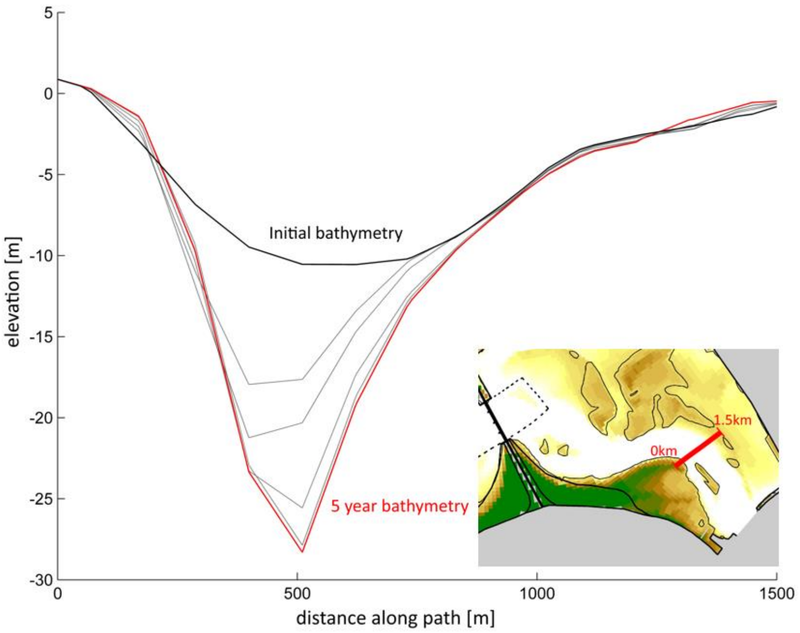


FIGURE 46: EXPECTED MORPHOLOGICAL EVOLUTION OF THE SLIJKGAT CHANNEL

### 6.2.2 EXPECTED TREND AT THE TIDAL INLET

The exchange of water at the tidal inlet causes strong currents at both sides. In the residual flow patterns a flood dominance is present at the lake side and an ebb dominance at the seaside. The seaward extent of the tidal influence is limited by the influence of the wind- and wave-driven longshore current prevailing along the Grevelingen delta and directed northeast. The cross-shore flow patterns show deflection in northern direction until a longshore pattern prevails at the north side of the pump station. The balance between the offshore wave dominance and the nearshore tide dominance determines the eventual seaward extent of the cross-shore action near the inlet. Initially the seaward area of the inlet can be characterized as highly dynamic. There are strong differences in flow velocities and sediment transport rates that result in significant sedimentation and erosion.

The cross-shore transport through the inlet, driven by the tidal currents, decreases with distance causing sedimentation at both sides of the inlet. Over time it results in the formation of an ebb-tidal delta at the seaside and a flood-tidal delta at the lake side. Most of the sediment comes from the eroding Slijkgat inside the tidal lake and in the Haringvliet estuary itself. Another part comes from the erosion at the outer sides of the bed protection. As flow velocities decrease over time, due to the eroding channels, the amount of available sediment decreases as well. This means that the growth of the ebb- and flood-tidal delta, as well as the scour holes, weakens over time (see Figure 47). Model results show an expected sedimentation decrease of the flood-tidal delta from 0.2-0.4 m/year to 0.08-0.12 m/year after 5 years. For the ebb-tidal delta this is 0.6-1.2 m/year to 0.12-0.28 m/year. This decrease over time of both sedimentation and erosion is expected at all locations and follow a logarithmic character. Other results are shown in Table 6.

Figure 47 shows that the ebb- and flood-tidal deltas migrate away from the inlet. The orientation of the ebb-tidal delta and its ebb channels are controlled by the governing wave energy (Scha and Van den Berg (1993), see *Intermezzo* in Section 2.4.2). Waves dominate at the foreshore and part of their energy is dissipated by breaking on the ebb-tidal delta front. Wave breaking causes a shore-directed component of wave radiation stress gradients, which is not fully compensated by the wave-induced setup in front of the inlet (Bertin, Fortunato et al. 2009). This mechanism causes the 'bulldozing' effect that pushes shoals landward. The 'bulldozing' effect together with the orientation of the residual longshore wave- and wind-driven currents cause an asymmetry of the ebb-tidal delta and the ebb channels in NW direction. Model results show that the ebb-tidal delta is migrating in that direction. It further shows that after 5 years the influence area of the tide extents further seaward (Figure 49). The size of the influence area at the seaside of the inlet increases from about 10.8 $km^2$ to about 16.3 $km^2$ after 5 years. But, residual hydrodynamic and morphodynamic processes decrease in intensity.

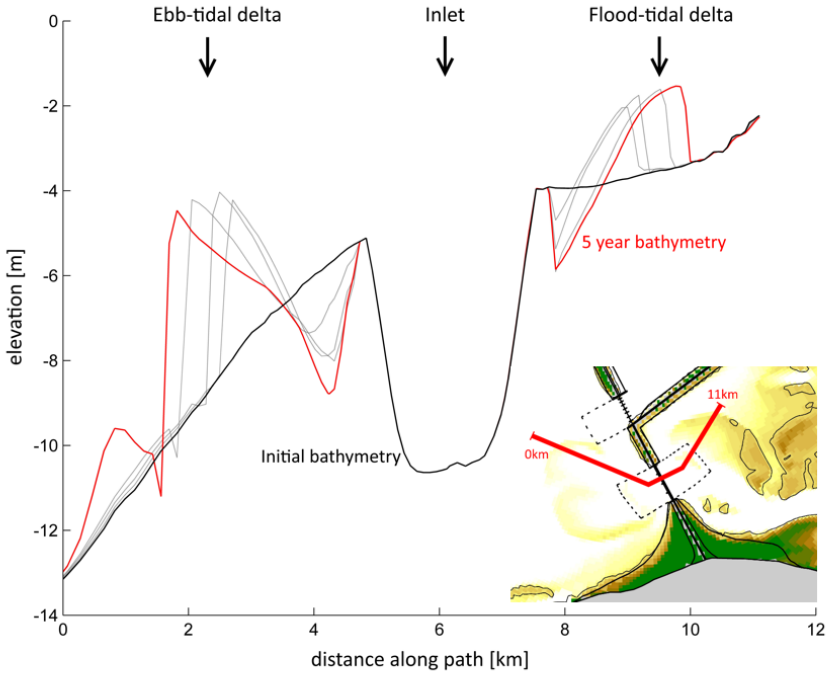


FIGURE 47: EXPECTED MORPHOLOGICAL EVOLUTION OF THE INLET AREA

### 6.2.3 EXPECTED TREND AT THE PUMP STATION AND ALONG THE NORTH SIDE OF DELTA21

The pump station empties and fills the ESL. The flow direction changes every 12 hours which introduces different interaction patterns between the tide and the pump flow. Strongest currents are found during ebb when the directions of the pump flow and the ebb flow coincide. This leads to an influence area that exceeds the seaward extent of the cross-shore flow at the inlet (see Figure 48). The longshore wave- and wind- driven currents, being in north-eastern direction, cause the seaward front of the flow pattern to be deflected northwards. This results in a clockwise residual flow pattern in front of the pump station.

Strong cross-shore currents cause erosion at the seaward side of the bed protection, similar to that of the tidal inlet. This results in a scour hole that both deepens and grows seaward over the years (see Appendix E). The available amount of sediment settles northeast of the scour hole and creates a small shoal. Similar to this mechanism a scour hole develops at the northwest corner of Delta21. Tide-, wave- and wind- driven currents are strong around this corner, comparable to the mechanisms behind the scour hole at Maasvlakte 2. Net sediment transport is in north-eastern direction and decreases along the northern Delta21 dune line, causing sedimentation in the nearshore area. The growth of both the scour hole and the sedimentation show again a logarithmic character (see Appendix E).

TABLE 6: SEDIMENTATION/EROSION RATES PER LOCATION AT T= 0 YEARS AND T= 5 YEARS

| Location | Sedimentation/erosion | 0years | 5years |
|---|---|---|---|
| **Ebb-tidal delta north** | Sedimentation | 0.6-1.2 m/year | 0.12-0.28 m/year |
| **Ebb-tidal delta south** | Sedimentation | 0.2-0.4 m/year | 0.08-0.12 m/year |
| **Flood-tidal delta** | Sedimentation | 0.2-0.4 m/year | 0.08-0.12 m/year |
| **Delta21 corner** | Erosion | 0.8-1.0 m/year | 0.16-0.3 m/year |
| **Delta21 north** | Sedimentation | 0.1-0.5 m/year | 0.02-0.04 m/year |
| **Tidal inlet** | Erosion | 0.9-1.2 m/year | 0.09-0.2 m/year |
| **Pump station** | Erosion | 0.2-0.4 m/year | 0.03-0.08 m/year |
| **Pump station** | Sedimentation | 0.2-0.5 m/year | 0.08 m/year |
| **Slijkgat** | Sedimentation | 0.8-3.7 m/year | 0.1-0.18 m/year |
| **Slijkgat** | Erosion | 0.8-1.6 m/year | 0.1-0.16 m/year |

### 6.2.4 EXPECTED TREND AT THE GREVELINGEN

Similar to the Haringvliet estuary, the tidal propagation in the Grevelingen changed to longshore after the closure. This resulted in a coast parallel flow pattern during both ebb and tide. Maximum flow velocities along the coast are out of phase with the North Sea velocities. Further, the residual currents show a north-eastern directed flow caused by a flood dominance. While the tide still dominates the remaining part of the Grevelingen ebb-tidal delta, waves became more important for the evolution of the morphology at the seaward foreshore as they ‘bulldozed’ sediment landward.

In the presence of Delta21 no significant changes to the forcing mechanisms can be distinguished at the Grevelingen. The tidal influence at the tidal inlet does not reach the Grevelingen mouth. The net sediment transport direction is NE and the effect of NE waves is limited due to the sheltering effect of Delta21. All in all it means that disturbances in the Grevelingen mouth are negligible. Along the coast of Goeree a flood flow into the tidal lake prevails. The influence of this flood flow is again limited but may have an influence on the northern part of the Bollen van de Ooster. However, the accuracy of the model is not high enough to make reliable predictions of the evolution of this part of the sandbank. This part is also under the influence of setup induced return currents in north-eastern direction. These return currents are not different compared to the present-day scenario but the dynamics might change over the years while the influence of the ebb-tidal delta grows. Further research on this area is recommended.

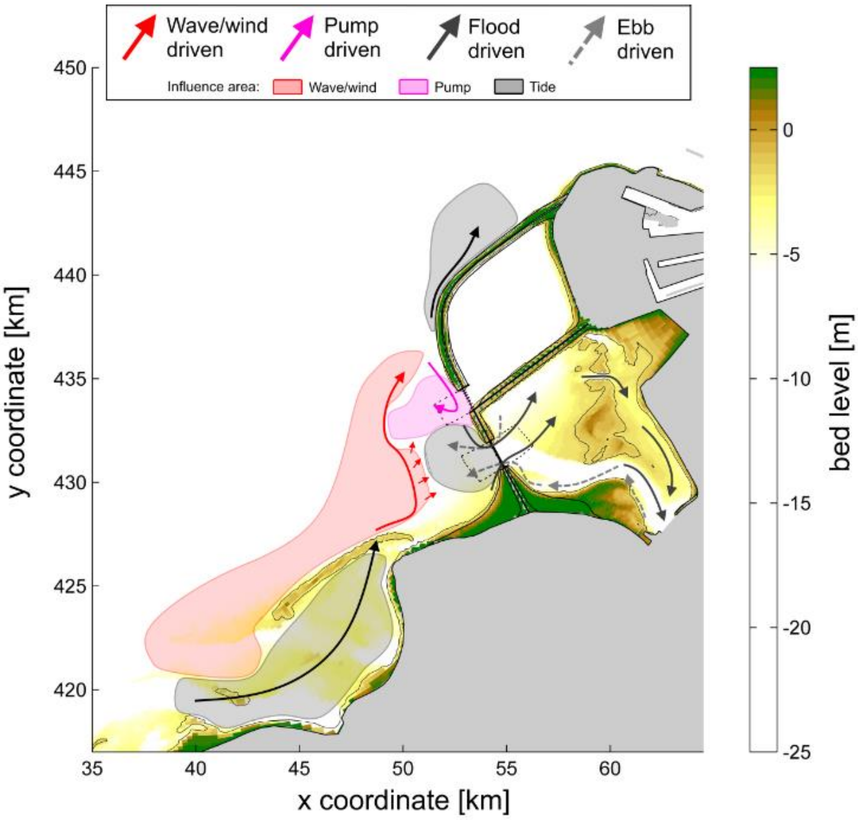


FIGURE 48: CONCEPTUALIZED INITIAL HYDRAULICS

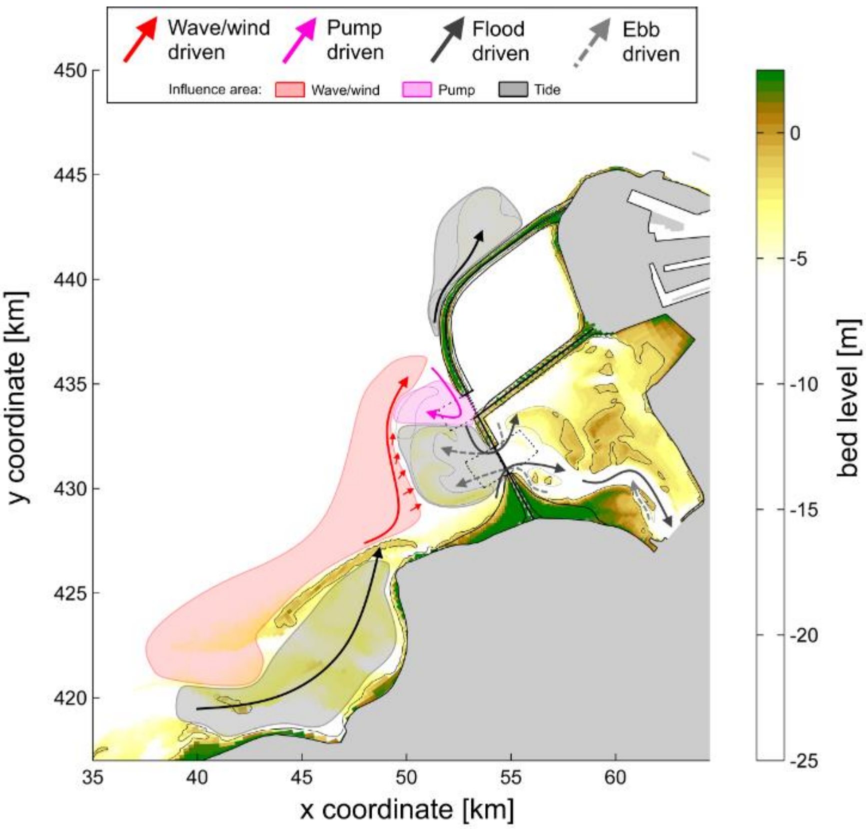


FIGURE 49: CONCEPTUALIZED HYDRAULICS AFTER 5 YEARS

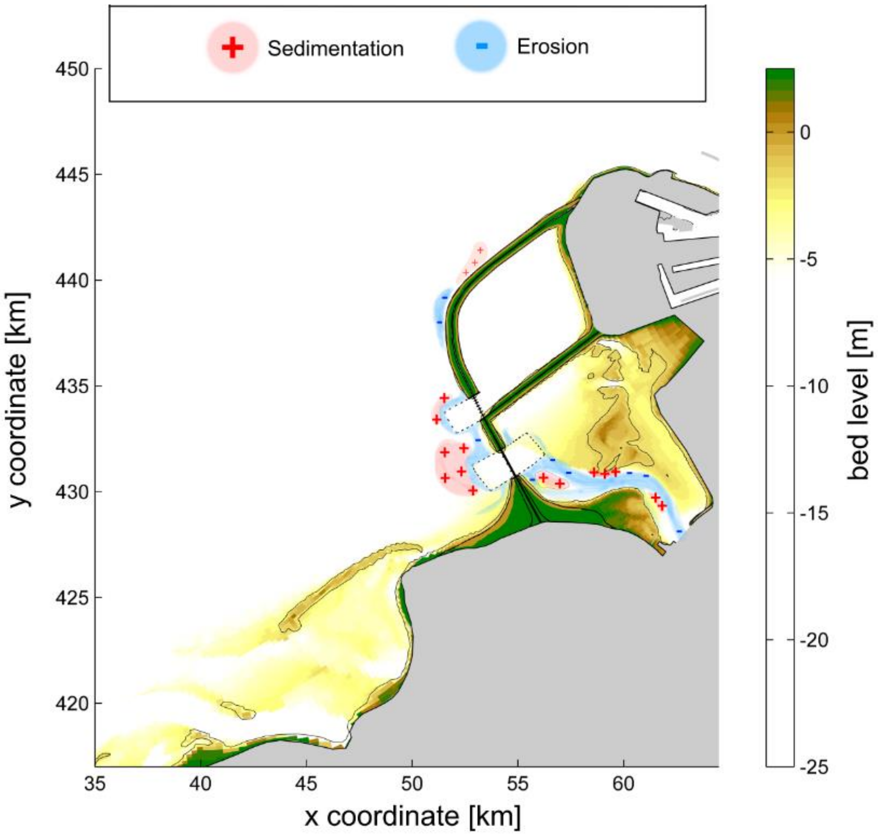


FIGURE 50: CONCEPTUALIZED INITIAL MORPHODYNAMICS

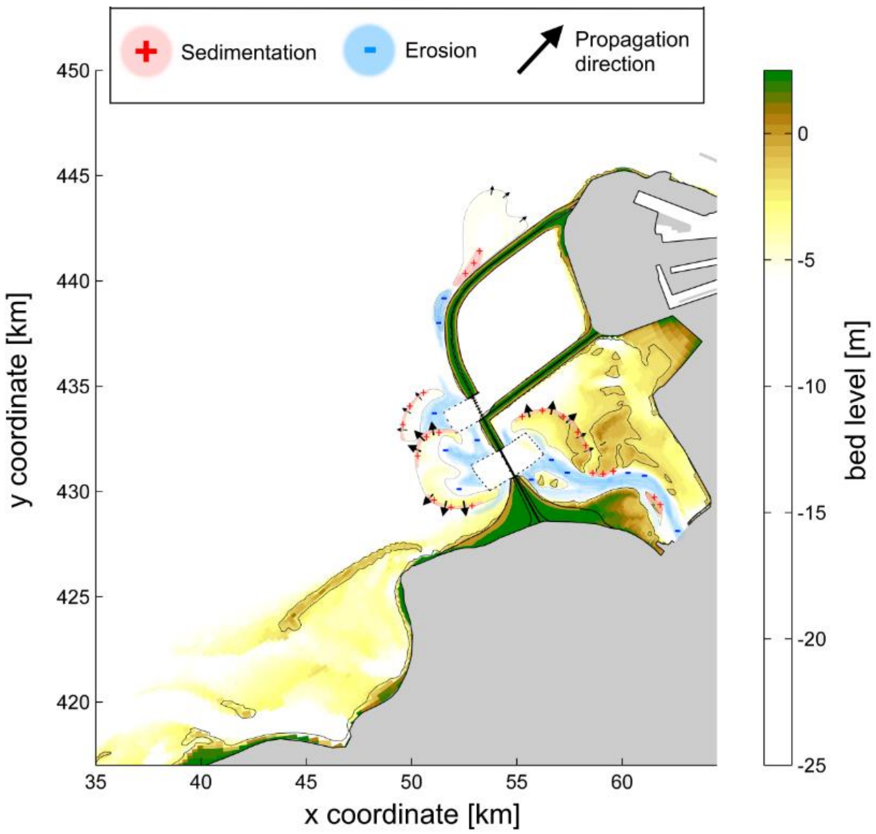


FIGURE 51: CONCEPTUALIZED MORPHODYNAMICS AFTER 5 YEARS

# DISCUSSION

This chapter presents a critical reflection on the research. In particular, it provides a discussion on the limitations of the model and their relation to the results. It also gives more insight into the used model techniques and the setup of the model before establishing the conclusions.

## MODEL LIMITATIONS

To start with, the aim of this research was to give insight in the large scale multi-year average hydraulic and morphodynamic changes in response to the Delta21 interventions. Therefore, a resolution of approximately 120x120 $m^2$ was chosen, in order to limit computation times. However, the bathymetry in the Voordelta is very irregular. Sandbanks like the Hinderplaat and the Bollen van de Ooster have bathymetric characteristics that require a higher grid resolution. Hence, the results from this model do not allow to look into the detailed dynamics around sandbars.

Further, since this study focussed on the changes of the multi-year average processes, extreme events were not taken into account. Storms, extreme setup, extreme discharge events and other similar circumstances can however influence the short-term hydrodynamics and morphodynamics which can influence the morphology on itself. The long-term hydrodynamic and morphodynamic processes can therefore be influenced by these extreme events. Conversely, a significant influence of these events on the large scale dynamics of coastal systems (e.g. basins, estuaries, deltas) have a relatively low probability of occurrence.

The available data used for the boundary conditions did not always cover matching periods in time. For instance, tidal data from 2001 is used on a bathymetry of 2015. This might introduce artificial sedimentation and erosion patterns since the morphology is not in balance with the imposed hydraulics. However, water levels have been verified with datasets of Rijkswaterstaat (see Appendix B) and sedimentation and erosion patterns did not show large artificial fluctuations. Moreover, the model has been considered to act as a tool to obtain insight in the Delta21 system. The III.Model0 scenario did not represent the exact present-day situation of the hydraulics and morphodynamics of the system, yet acted as a qualitative benchmark to other scenarios.

Further, computational time restrictions do not allow for large amounts of wave conditions. Besides, the available wave data was not space varying while the wave boundaries covered up 120km. Along with the significant reduction of the wave climate to 12 conditions, it might introduce a large uncertainty of the nearshore wave imposed processes. Further, waves have a large influence on sediment concentration in the nearshore and have had a substantial effect on the morphology in the past. However, reducing the amount of wave conditions allowed for the investigation of the large scale dynamics, which fitted the purpose of this research. Moreover, a large dataset of over one million datapoints covering more than 7 years of wave data was used for the reduction of the wave climate. Other than that, the combination with the wind and the setup seemed to be of great importance to the residual currents as well. The wind and setup data were however, similarly to the wave data, acquired from only one offshore location. Nonetheless, detailed wave, wind and setup simulations were not within the scope of this research but, seen their importance, can be of significant importance to future morphodynamic research of Delta21.

Besides, the modelling study did not focus on 3D gravitational circulation effects since these effects are assumed to be less relevant in the study on large scale hydrodynamics of coastal cells and deltas compared to the more dominant two dimensional horizontal processes. Hence, 3D current patterns like eddy formation in shadow zones of structures, current patterns around shoals, curvature-induced flows through channels and gradients over the vertical axis in e.g. salinity have not been studied.

Furthermore, the grain size distribution in the study area has been schematized using a single $D_{50}$ of 160 μm. Most of the sediment in the Haringvliet mouth exists of sand particles, however, especially the channels contain finer mud particles. Model results showed large erosion in the Slijkgat channel as a results of the transport of the schematized non-cohesive sand particles. In reality, a cohesive mud layer could have influenced the sediment transport rate, initially resulting in milder erosion. But, since the initial bathymetry used for the Delta21 scenario consisted of the deepening of the Slijkgat channel, this influence is assumed to be negligible. Yet, results should be treated with care.

Further, the Haringvliet boundary condition proved to be one of the most influential boundary conditions for the dynamics in the research area. For this research the data for this boundary was acquired from the research of Piña (2020). They modelled the entire Haringvliet estuary combined with the Delta21 interventions at the Haringvliet mouth. The data of the boundary conditions covered a period of one spring-neap cycle and made use of a single discharge regime. Besides, during extreme discharge events in the past, significant changes happened to the morphology of the Haringvliet mouth (Colina Alonso 2018). Consequently, the model used in this research cannot give insight in the influence of extreme discharge events on the morphology of the tidal lake. Furthermore, this model is not able to simulate long term fluctuations of the hydraulics of the Haringvliet estuary, while this might be of great importance to the dynamics inside the tidal lake. However, the model does give a good insight in the initial response to the yearly average processes in presence of Delta21.

For this study a morphostatic modelling approach was chosen. In a morphostatic simulation the feedback loop between morphological bed changes and hydrodynamic forcing does not exist. This means that the bathymetry is fixed and only the initial sedimentation/erosion (ISE) can be determined. This reduces the complexity of the model but also the reliability of long-term predictions. Besides, only one grain size was used to represent the sediment inside the research area. These choices were made in order to reduce simulation time but above all to increase the reliability of the initial morphodynamic patterns. Using morphodynamic simulations requires intensive calibration and validation in order to increase the model reliability, which is not within the scope of this research. Since Delta21 is still in its design stage, this research aims to provide the basic preliminary changes to the hydraulic and morphodynamic characteristics of the system. A morphostatic model approach using one grain size fits this objective.

### RESULT INTERPRETATION

Based on its limitations, model results as presented in this report must be interpreted qualitatively instead of quantitatively. An example is the analysis of the individual influence of the different forcing mechanisms. These processes do not entirely act independent of each other, since high waves coincide with high wind speeds and increased water level setup. Further, the contribution mechanism of waves and wind to sediment transport compared to the transport mechanisms of the tide are significantly different. Waves mostly contribute in bringing sediment into suspension whereas the tide is responsible for most of the transport of sediment in the horizontal axis. Colina Alonso (2018) found that the relative contribution to the flow pattern of wind seemed to be considerably larger during more energetic wave conditions. This finding suggest a non-linearity between the different mechanisms which makes it difficult to achieve quantitively correct results when studying their individual influence. As a matter of fact, qualitative research has often been used in studies on complex situations in which processes are not known in advance. In such situations the qualitative results are far more important for telling the story compared to quantitative results. A qualitative research method therefore perfectly fits the purpose of this study.

Additionally, this research studies the initial, short-term, response of the system. The studied flow patterns and initial sediment transport rates proofed to be good indicators to debate the feedback of the system to the various multi-year averaged conditions and on a large scale. The analysis are however limited to the large scale which leaves the small scale dynamics (sandbanks, channels, etc.) yet unanswered. It also limits the possibilities to investigate the long-term feedback of the changed morphology, therefore hydraulics and morphodynamics should be based on expert judgement instead of relying on model results. Consequently, this is how the analysis of the expected morphodynamics, as shown in Chapter 6, has been elaborated.

Lastly, the model results relate to the Delta21 design as proposed on April 2020 by Lavooij and Berke (2020). As explained before, hydraulic and morphodynamic processes and characteristics are highly sensitive to the initial bathymetry they are acting on and driven by. Further modification of the design might change these characteristics which could lead to other conclusions.

# CONCLUSIONS

In this chapter the conclusions of this research are presented by answering the research questions formulated in Chapter 1. These questions were triggered by the main objective of this study which was to understand the initial impact of the Delta21 plan on the morphodynamics of the Northern Voordelta.

*What hydraulic and morphodynamic processes caused the evolution of the Northern Voordelta since the closure of the Haringvliet and Grevelingen estuaries?*

The closure of the Haringvliet and Grevelingen deltas in 1970 and 1971 respectively, caused the tidal prims to reduce strongly. The tidal propagation into the estuaries disappeared and changed from cross-shore to longshore in the remaining ebb-tidal deltas seaward of their closure dams. A change of the tidal propagation meant a significant change of the flow patterns. Prior to the closing cross-shore ebb and flood flow patterns prevailed, after closures this changed to a shore parallel flow pattern through the ebb-tidal deltas. The reduction of the tidal prism caused a strong decrease of the flow velocities (30 to 90%) in the ebb and flood channels. A decrease in tidal prism means a decrease in offshore directed ebb-driven sand transport and a smaller cross-sectional area of the ebb- and flood channels (Wang, De Ronde et al. 2009). The reduced flow velocities and the change toward longshore directed tidal currents led to the reduction of the seaward extent of the tidal dominance. The surface area of the seaward part of the ebb-tidal delta decreased along with the average depth in that area. Waves became dominant in the evolution of the morphology in the area. By 'bulldozing' the offshore sandbars in landward direction, the morphology of the ebb-tidal deltas changed. This resulted in shore-parallel sandbars like the Bollen van de Ooster and the Hinderplaat. The erosion of the ebb-tidal delta front in the Grevelingen mouth, together with the longshore tide- and wave-driven currents being in flood directions, resulted in a large sediment supply for the Haringvliet mouth and the adjacent coastline of Goeree. During this period big land reclamations were completed at the north side of the mouth, protecting it from NW waves and strengthening the siltation process of the Haringvliet mouth. Both the Grevelingen and Haringvliet mouths showed a large sedimentation pattern in the channels landward of the shore-parallel sandbars and erosion of the ebb-tidal delta front seaward of these bars.

*What are the present-day characteristics of the large scale multi-year average hydraulics and morphodynamics and what mechanisms are dominant inside the research area?*

Nowadays a longshore tidal propagation prevails which results in shore-parallel flow patterns. While the water levels offshore and along the coast are in phase, the flow velocities are not. Residual currents show a flood dominance in the Grevelingen mouth. In this mouth the direction is more or less shore parallel whereas it has an offshore direction in the Haringvliet mouth. This is mainly caused by the shape and bathymetry of the Haringvliet and the ebb dominant river discharge through the Slijkgat. On top of the Hinderplaat, the flow is flood dominant since the inter-tidal sandbank is only submerged when the flow is in landward direction.

Further, tidal propagation around the Maasvlakte 2 causes 'tidal squeeze', where flow is being contracted in both ebb and flood direction. The flood dominant character of the tide causes a residual flow in NE direction around the Maasvlakte 2. That area and the landward areas of both ebb-tidal deltas are dominated by the tide-driven currents (see Figure 52). The tidal dominance extents no more than the shore parallel sandbars Bollen van de Ooster and Hinderplaat. Seaward of these sandbars the wave- and wind-driven currents dominate and show a longshore NE residual direction. This is caused by the prevailing WNW direction of the waves and SW direction of the wind. The wind and waves cause setup at the east side of both mouths. It results in a northern, seaward directed, return current at the northeast seaward boundary of both ebb-tidal deltas.

The model results, representing the large scale multi-year average residual sediment transport patterns in the area, in general show high similarity to the residual flow patterns. Residual sediment transport rates are relatively low (0 to $0.5 \cdot 10^{-4}$ $m^3/m/s$), suggesting a system that is close to its equilibrium. Further, model results of sedimentation and erosion patterns reveal that erosion at the tip of Maasvlakte 2 and elongation of the Bollen van de Ooster at the NE tip are the most dynamic areas for morphology. However, in comparison to the situation right after the closure in 1971, the morphodynamic action is negligible. After the nineties the rate of change in morphology decreased in both mouths, acting towards the new dynamic equilibrium.

*What will the initial large scale multi-year average characteristics of the hydraulic and morphodynamics be and what mechanisms will initially be dominant inside the research area in the presence of Delta21?*

In the presence of Delta21 the longshore propagation changes towards a cross-shore propagation into the tidal lake and the opened Haringvliet estuary. The tidal prism increases from 15 $Mm^3$ to 237 $Mm^3$ and the Haringvliet starts to follow the characteristics of a long basin instead of a short basin. Similar to the situation before closure, water levels in the mouth are out of phase with the offshore water levels. Further, flow velocities inside the mouth lag behind the water levels while at sea they coincide. Comparing the flow velocities in the mouth with the offshore flow velocities, maximum velocities are roughly in phase.

The increased tidal prism introduces cross-shore ebb and flood currents inside the Haringvliet mouth, i.e. the tidal lake. Initially currents in the dredged Slijkgat increase up to 150% (peak velocity: 2.8 m/s), during both ebb and flood. The entering water finds its path through the channel and clockwise around the Hinderplaat until it enters the Haringvliet estuary at the sluices. The ebb flow shows a similar pattern in seaward direction and anti-clockwise around the Hinderplaat. The residual flows at the tidal inlet show an ebb dominant character at the seaside and a flow dominant character at the lake side. The shallow and inter-tidal parts are flood dominant since these parts are only affected during a submerged state at high water. The deeper parts are affected by the Stokes drift and ebb flow dominates. The Haringvliet estuary landward of the sluices is flood dominated caused by tidal asymmetry. Tide-driven currents dominate in the tidal lake since the influence of waves and wind are strongly reduced by the Delta21 barrier (see Figure 52).

Further, seaward of the tidal lake wave- and wind-driven currents cause a longshore flow prevailing in NE direction. A setup difference between the tidal lake and the North Sea causes a residual current in northern direction along the western coastline of Delta21. Model results show that the cross-shore flow activity does not affect flow patterns in the Grevelingen mouth (see Figure 52). However, the SW offshore area NE of the Bollen van de Ooster is affected by the cross-shore tidal activity in front of the tidal inlet and cross-shore pump-driven flow. The flow of the pump station interacts with the tidal flow near the inlet. The tidal flow dominates the flow pattern in the area since the discharge (peak: $2.9 \cdot 10^4$ $m^3/s$) is significantly higher than the pump discharge ($1.0 \cdot 10^4$ $m^3/s$). The longshore wave- and wind-driven currents are affected by the cross-shore activity and their influence is pushed seaward (see Figure 52). The same area is also sheltered from NW wave activity, therefore western wave directions dominate the direction of wave-driven currents in the area.

Around the NW corner of Delta21 a similar 'tidal squeeze' process happens as is the case for Maasvlakte 2 nowadays. As a result, net sediment transport rates increase around the corner. Increased transport also happens in front of the pump station where offshore directed flow velocities are relatively high. The most dynamic area is through the tidal inlet and inside the tidal lake. The high flow velocities there cause strong residual sediment transport in offshore direction outside the inlet and in landward direction at the lake side of the inlet. Highest residual sediment transport rates can be found in the Slijkgat. Compared to the present-day situation the area is significantly more dynamic with residual sediment transport rates ranging between 0 and $4.5 \cdot 10^{-4}$ $m^3/m/s$.

The strong gradients of the sediment transport lead to both sedimentation and erosion. The morphology of the Slijkgat does not fit to the acting hydraulics and it will therefore erode, despite the initial deepening of the channel to -10m NAP. At locations where sediment transport rates decrease again, sedimentation happens. This will result in the formation of both an ebb-tidal delta seaward of the inlet and a flood-tidal delta landward of the inlet. Both are supplied by sediment coming from the Slijkgat. Further, a strong sediment transport gradient leads to erosion in front of the pump station. The released sediment settles in the seaward area where flow velocities and bed shear stresses decrease. A similar process happens around the NW corner of Delta21 where the increase in flow velocity causes a positive gradient in sediment transport which leads to erosion. At the north side transport rates decrease again and sedimentation can be expected. The scour hole results from the 'tidal squeeze', this is identical to the process that happens around Maasvlakte 2. In presence of Delta21 the flow contraction around Maasvlakte 2 does not disappear, the process is simply shifted towards the Delta21 corner.

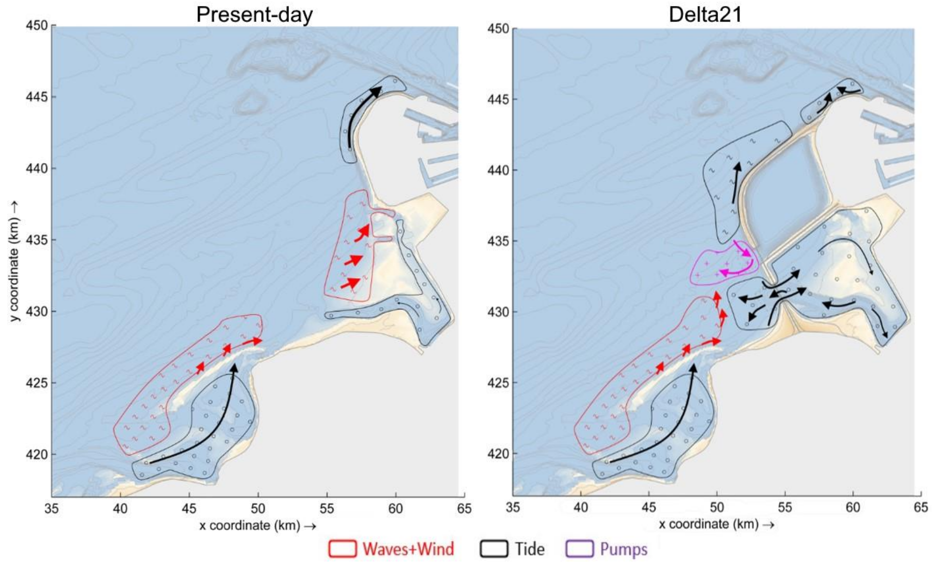


FIGURE 52: CHANGE OF INFLUENCE AREAS OF THE VARIOUS DRIVERS

*To what extent will Delta21 initially change the morphological trend, in response to the initial change of the large scale and multi-year average processes?*

In the presence of Delta21 no significant changes to the driving mechanisms in the Grevelingen mouth can be distinguished. The tidal influence at the tidal inlet does not reach the Grevelingen ebb-tidal delta. The net sediment transport direction is NE and the effect of NE waves is limited due to the sheltering effect of Delta21. All in all it means that disturbances in the Grevelingen mouth are negligible. Therefore, the present-day morphodynamics are more likely to continue in the Grevelingen mouth.

The original morphology inside the Haringvliet mouth (the tidal lake) however will change completely and over the years changes towards a new equilibrium that fits the dynamics of the in- and outgoing tide. This leads to the formation of an ebb-tidal delta and a flood tidal delta, both fed by the eroding Slijkgat. Initially sediment transport gradients are steep since the morphology still has to adapt. The morphological changes are likely to follow a logarithmic character where initial changes happen fast, but sedimentation and erosion rates will lower over time.

Inside the tidal lake, the initial change of the hydraulics and morphodynamics cause erosion of the channels but also sedimentation in the form of a flood-tidal delta. It results in both a smaller inter-tidal storage and deeper channels, which fits the characteristics of a dynamic equilibrium where no particular flood or ebb dominance is presence (Bosboom and Stive 2015). However, the tidal signal shows asymmetry due to a higher flood velocity in comparison to the ebb velocities, i.e. flood dominance. In conclusion, the morphology is adapting and especially inside the tidal lake no particular flood or ebb dominance can be distinguished. It can however shift towards a flood or ebb dominance after a couple of years.

Further, reducing flow velocities caused by flow divergence at both the ebb- and flood-tidal delta fronts cause sedimentation. This inevitably means that both deltas are propagating away from the inlet. Outside the tidal lake, the interaction of waves and tide will determine the seaward extent of the ebb-tidal delta. In the first years this seaward extent will grow (from about 10.8 $km^2$ to about 16.3 $km^2$ after 5 years), while the orientation of the ebb-tidal delta and its ebb channels are controlled by the governing wave energy (Scha and Van den Berg 1993). The orientation of the residual longshore wave- and wind-driven currents cause an asymmetry of the ebb-tidal delta and the ebb channels in NW direction.

Lastly, morphodynamics in front of the pump station and along the Delta21 corner are likely to reduce as the morphology adapts to the new system. These offshore dynamics are different from the dynamics inside the tidal lake where a change in morphology can either act as a positive or negative feedback on the morphodynamics (Bosboom and Stive 2015).

With that the answer is given on the last sub-question. And so, together with the answers on the other sub-questions, the answer on the general research question has been found.

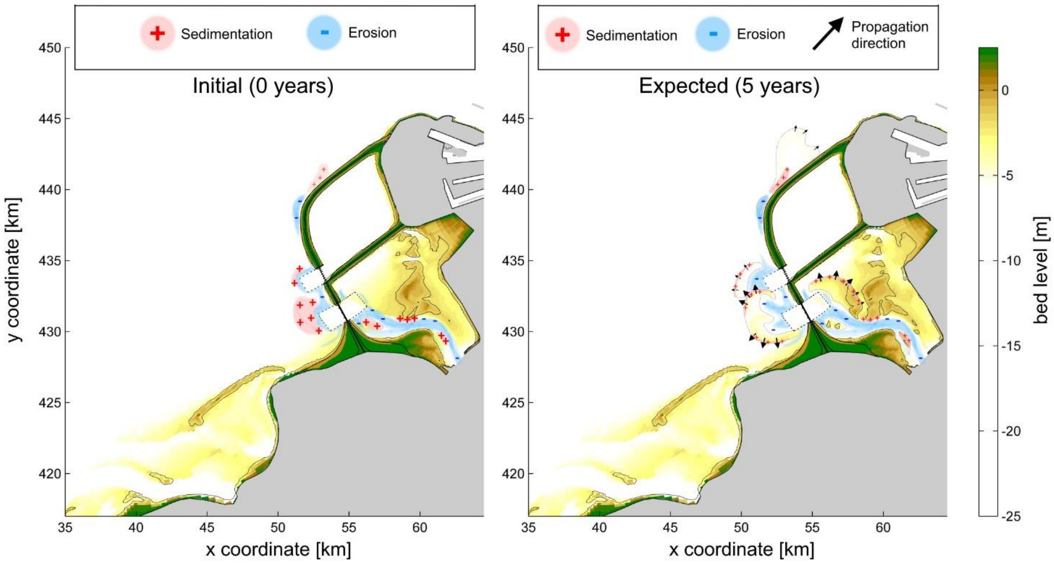


FIGURE 53: INITIAL MORPHODYNAMICS AND EXPECTED MORPHODYNAMICS IN PRESENCE OF DELTA21

# RECOMMENDATIONS

This chapter presents recommendations for further research that followed from either the discussion or the conclusions. First, recommendations regarding research on the revealed processes are addressed. Herein also suggestions are given on the improvement of future research using a Delft3D model. Second, recommendations are given for further research on the Delta21 topic in general.

## FUTURE RESEARCH

This research focussed on the initial response of the hydraulics and morphodynamics of the system. The Delta21 interventions were expected to change the system significantly. Consequently, limitations of the model complexity were unavoidable. Due to the simplifications, this research was not able to focus on several processes in much detail while they could be relevant for the understanding of the response of the system.

- To start with, a study of the long-term response of the system is highly recommended. This is especially needed in the dynamic area of the tidal inlet and the tidal lake since it is important for Natura2000. At the same time, the long-term evolution of the scour hole and the expected sedimentation at the north side will be important for the stability of Delta21 and the maintenance of de Maasgeul respectively. For a long-term response a morphodynamic instead of a morphostatic model approach is recommended. Besides, the effect of sea level rise on long-term morphodynamics should not be overlooked. Unfortunately, including long-term processes like sea level rise once again add complexity to the model. Furthermore, the study of De Vries (2007) on the response of the Haringvliet showed that longer-term predictions, using a morphodynamic model, show a broad uncertainty range. Therefore, long-term morphodynamic studies require extensive calibration and validation work.
- Secondly, important small scale morphological components like sandbanks, ebb- and flood-tidal delta constituents and channels should be studied using a higher grid resolution (10x10$m^2$ or less). This study showed that the morphodynamics of these components will change substantially. The detailed morphodynamics of these morphological components are important for the evolvement of the Natura2000 habitats. Therefore, increasing the resolution of the Delft3D model grid is needed to allow for the study of these components.
- Thirdly, the conclusions of this study can be used to conduct an extended and more reliable reduced wave climate. As concluded in De Queiroz, Scheel et al. (2019), it is best to use the Sediment Transport Bin method, or something similar. Especially for detailed morphodynamic studies on, e.g. the ebb-tidal delta or the development of the north-eastern scour hole, location specific wave reduction is recommended.
- Fourthly, the present model highly schematized the site conditions via the boundary conditions. Extreme discharge events, storm surge and site specific water level setup were not included in the model. Conclusions of this study and former studies showed that these events can have a significant influence on the episodic morphodynamics in the area that may drive bed level changes and therefore change the equilibrium. Further research is recommended wherein these processes are included.
- Fifthly, the revealed processes like the dynamics of the ebb-tidal delta that are influenced by the waves, the tide and the pumping station all at once, should be studied in more detail. Especially considering the possible negative effect Delta21 can have on the northern tip of the Bollen van de Ooster, which is a highly important sandbank in the Natura2000 area. Such detailed studies can however only be performed using a more detailed Delta21 design since its geometry greatly influences the hydraulic processes in and around it. Therefore, smaller scale studies should be done at a later design stage. This design should also include detailed information of the pump discharge regime, the cross-sectional design of the dunes and the nearshore area of Delta21 and the tidal inlet.

# References


Aarninkhof, S. G. J. and T. Van Kessel (1999). Data analyse Voordelta, Grootschalige morfologische veranderingen 1960-1996, WL Delft Hydraulics.

Bertin, X., et al. (2009). "A modeling-based analysis of processes driving wave-dominated inlets." Continental Shelf Research **29**: 819-834.

Bosboom, J. and M. J. F. Stive (2015). Coastal Dynamics 1. Lecture notes CIE4305. Delft, Delft Academic Press (VSSD-uitgeverij).

Colina Alonso, A. (2018). Morphodynamics of the Haringvliet ebb-tidal delta. Civil Engineering. Delft, Delft University of Technology. **Master of Science report**.

Davis, R. A. and M. O. Hayes (1984). "What is a wave-dominated coast?" Marine Geology: 313-329.

De Boom, A. (2016). Modelling hydrodynamics and sediment transport in the Grevelingen outer-delta in response to human interventions. Department of Physical Geography, Utrecht University. **Master of Science report**.

De Queiroz, B., et al. (2019). "Performance Evaluations of Wave Input Reduction Techniques for Modeling Inter-Annual Sandbar Dynamics." Journal of Marine Science and Engineering.

De Vriend, H. J. and J. S. Ribberink (1996). Mathematical modelling of meso-tidal barrier island coasts. Part II: Process-based simulation models. P.L.F. Liu (ed.): Advances in Coastal and Ocean Engineering, Singapore, World Scientific.

De Vries, M. J. (2007). Morphological modelling of the Haringvlietmonding using Delft3D, Universiteit Twente. **Master of Science report.**

De Winter, R. (2008). Exploratory Research into the Maintenance of the Slijkgat, An Analysis of the morphology of the Haringvliet, Delft University of Technology. **Master of Science report**.

Deltares (2014a). Delft3D-FLOW user manual version 3.15, Simulation of multi-dimensional hydrodynamic flows and transport phenomena, including sediments.

Deltares (2014b). Delft3D-WAVE user manual version 3.05, Simulation of short-crested waves with SWAN.

Elias, E. and A. Van der Spek (2014). Grootschalige morfologische veranderingen in de Voordelta. Delft, Deltares.

Elias, E. P. L., et al. (2016). "The ‘Voordelta’, the contiguous ebb-tidal deltas in the SW Netherlands: large-scale morphological changes and sediment budget 1965–2013; impacts of large-scale engineering." Netherlands Journal of Geosciences.

Elias, E. P. L. and A. J. F. Van der Spek (2019). "The long-term impact of closing of an estuary mouth / tidal inlet at its ebb-tidal delta - a conceptual model." Coastal Sediments.

Groenewegen, M. Q. T. (2019). Morphological development of the Bollen van de Ooster, Delft University of Technology. **Master of Science report.**

Huibregtse, W. (2013). Morphological analysis of the beach at the Brouwersdam. Coastal Engineering, Delft University of Technology. **Master of Science report.**

IPCC (2014). Climate Change 2014: Synthesis Report. Geneva, Switzerland, IPCC.

Lavooij, H. and L. Berke (2019). Toekomstbestendige oplossing voor de zuidwestelijke delta. Veenendaal, Delta21.

Lavooij, H. and L. Berke (2020). DELTA21 - Vormgeving april 2020.

Ministerie, v. V. e. W. (2010). Presentatie meetresultaten Debietraai 1 Oosterschelde, 2143m1001, Notitie: ZLMD-10.N.006, Ministerie van Verkeer en Waterstaat.

Noordhuis, R. (2017). Het Haringvliet na de Kier, Deltares.

Piña, M. I. Z. (2020). Stability of intertidal and subtidal areas after Delta21 plan. Civil Engineering. Delft, Delft University of Technology. **Master of Science report.**

Reintjes, C. M. (2002). Morfologische ontwikkeling van de Kwade Hoek en het omringend kustgebied in de Haringvlietmond. Utrecht, Netherlands Institute of Applied Geoscience TNO – National Geological Survey.

Rijkswaterstaat (2016). Beheerplan Natura 2000 Voordelta, Ministerie van Infrastructuur en Milieu, Rijkswaterstaat.

Rijkswaterstaat (2020). Astronomische waterhoogte Brouwershavensche Gat 08.

Rijkswaterstaat (2020). Astronomische waterhoogte Hoek van Holland

Rijkswaterstaat (2020). "Procedure Natura 2000." Natura2000. Retrieved March 20, 2020, from www.natura2000.nl/procedure-natura-2000.

Scha, L. P. and J. H. Van den Berg (1993). "Variation in ebb-tidal delta geometry along the coast of the Netherlands and the German Bight." Journal of Coastal Research **9.3**: pp. 730–746.

Steijn, R., et al. (2001). Bandbreedtje morfologische Effectvoorspelling MV2: Een onderzoek ten behoeve van natuurtypering.

Terwindt, J. H. J. (1964). "De veranderingen in de mond van het Brielse Gat als gevolg van de afdamming." Tijdschrift Koninklijk Nederlands Aardrijkskundig Genootschap **81**: 329-334.

Tönis, I. E., et al. (2002). "Morphological changes of the Haringvliet estuary after closure in 1970." Elsevier, Coastal Engineering **44**: 191-203.

Van Holland, G. (1997). Hydrodynamica en morfodynamica van de monding van het Haringvliet, validatie van modeltechnieken voor een intergetijde gebied. TU Delft, waterloopkunding laboratorium WL. Delft, Delft University of Technology. **Master of Science report.**

Wang, Z. B., et al. (2009). "Responses of the Dutch Coastal System To the (Semi-) Closures of Tidal Basins." Estuaries and Coasts: 203-210.

Wesselink, A. J., et al. (2007). "Dutch Dealings with the Delta." Nature and Culture: 188-209.

# APPENDICES

# APPENDIX A

## A.1 INTRODUCTION

This appendix consists of figures that act as additional information to Chapter 2.

## A.2 WIND ROSES

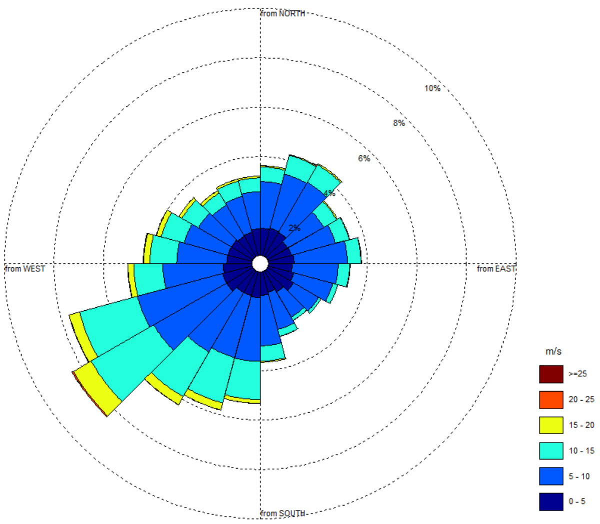


FIGURE 55: WIND ROSE BROUWERSHAVENSE GAT (SOURCE: HUIBREGTSE (2013))

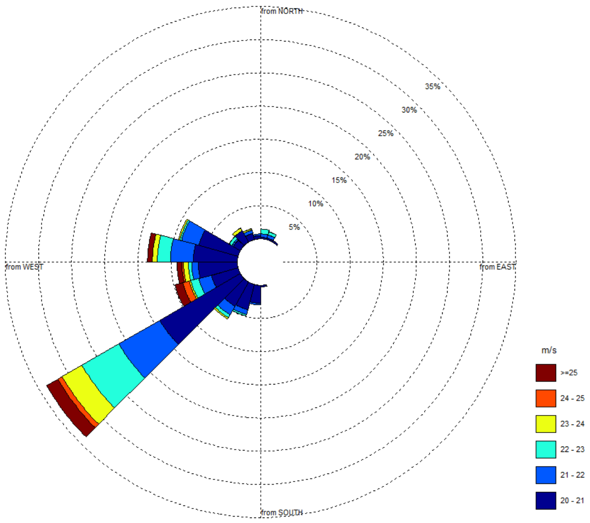


FIGURE 54: WIND ROSE BROUWERSHAVENSE GAT >20M/S (SOURCE: HUIBREGTSE (2013))

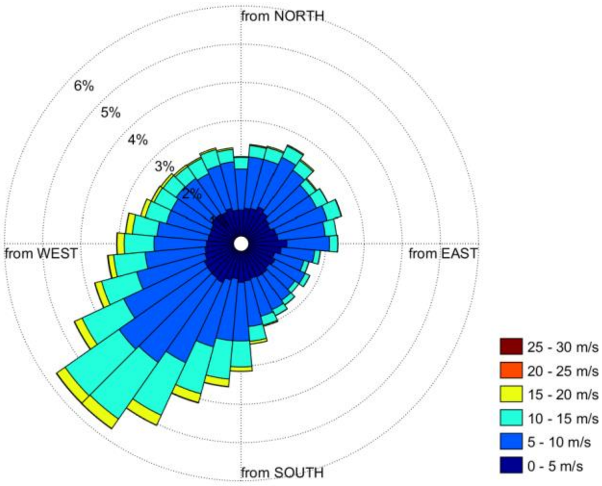


FIGURE 56: WIND ROSE EUROPLATFORM (SOURCE: COLINA ALONSO (2018))

# APPENDIX B

## B.1 INTRODUCTION

This appendix consists of tables that act as additional information to Chapter 4.

## B.2 WAVE CONDITIONS

TABLE 7: WAVE HEIGHT VS. WAVE DIRECTION PROBABILITY

| Wave direction [degrees] | Significant wave height [m] | | | | | | | | | | | | |
|---|---|---|---|---|---|---|---|---|---|---|---|---|---|
| lower | < | 0.5 | 1 | 1.5 | 2 | 2.5 | 3 | 3.5 | 4 | 4.5 | 5 | 5.5 | total |
| upper | 0.5 | 1 | 1.5 | 2 | 2.5 | 3 | 3.5 | 4 | 4.5 | 5 | 5.5 | > | |
| **0 to 15** | 1.61E-02 | 4.00E-02 | 2.09E-02 | 5.36E-03 | 2.05E-03 | 7.44E-04 | 1.93E-04 | 5.43E-06 | | | | | **0.09** |
| **15 to 30** | 1.04E-02 | 2.44E-02 | 1.71E-02 | 5.86E-03 | 2.58E-03 | 7.41E-04 | 1.90E-04 | 1.36E-05 | | | | | **0.06** |
| **30 to 45** | 6.32E-03 | 1.42E-02 | 9.90E-03 | 4.48E-03 | 2.54E-03 | 1.22E-03 | 2.55E-04 | | | | | | **0.04** |
| **45 to 60** | 3.43E-03 | 7.14E-03 | 4.91E-03 | 2.45E-03 | 1.09E-03 | 6.00E-04 | 3.15E-04 | | | | | | **0.02** |
| **60 to 75** | 2.17E-03 | 4.22E-03 | 2.68E-03 | 1.37E-03 | 8.69E-05 | 6.25E-05 | 5.43E-06 | | | | | | **0.01** |
| **75 to 90** | 1.39E-03 | 3.07E-03 | 2.00E-03 | 4.75E-04 | | 1.09E-05 | | | | | | | **0.01** |
| **90 to 105** | 1.16E-03 | 2.70E-03 | 1.38E-03 | 3.53E-04 | 2.44E-05 | 1.36E-05 | | | | | | | **0.01** |
| **105 to 120** | 9.53E-04 | 2.40E-03 | 9.37E-04 | 3.64E-04 | 3.80E-05 | 1.36E-05 | | | | | | | **0.00** |
| **120 to 135** | 6.55E-04 | 1.81E-03 | 5.51E-04 | 1.41E-04 | 6.52E-05 | 1.09E-05 | | | | | | | **0.00** |
| **135 to 150** | 5.32E-04 | 1.83E-03 | 7.41E-04 | 1.00E-04 | 1.63E-05 | 1.36E-05 | | | | | | | **0.00** |
| **150 to 165** | 7.82E-04 | 2.42E-03 | 7.50E-04 | 3.23E-04 | 2.17E-04 | 2.71E-05 | | | | | | | **0.00** |
| **165 to 180** | 1.07E-03 | 3.28E-03 | 1.52E-03 | 6.60E-04 | 2.44E-04 | 5.43E-06 | | | | | | | **0.01** |
| **180 to 195** | 1.31E-03 | 5.46E-03 | 3.05E-03 | 2.01E-03 | 5.51E-04 | 5.16E-05 | | | | | | | **0.01** |
| **195 to 210** | 1.92E-03 | 8.14E-03 | 7.50E-03 | 5.66E-03 | 2.49E-03 | 7.93E-04 | 9.51E-05 | 1.63E-05 | | | | | **0.03** |
| **210 to 225** | 3.19E-03 | 2.00E-02 | 2.34E-02 | 1.97E-02 | 9.61E-03 | 3.86E-03 | 1.28E-03 | 5.08E-04 | 1.22E-04 | 2.72E-06 | | | **0.08** |
| **225 to 240** | 7.34E-03 | 3.65E-02 | 3.66E-02 | 2.96E-02 | 1.71E-02 | 1.12E-02 | 6.00E-03 | 2.22E-03 | 6.87E-04 | 1.30E-04 | 2.71E-05 | | **0.15** |
| **240 to 255** | 8.66E-03 | 2.08E-02 | 1.53E-02 | 8.96E-03 | 6.50E-03 | 3.13E-03 | 1.70E-03 | 7.44E-04 | 3.04E-04 | 1.36E-04 | 1.63E-05 | | **0.07** |
| **255 to 270** | 6.00E-03 | 1.14E-02 | 8.83E-03 | 4.73E-03 | 3.28E-03 | 2.03E-03 | 1.27E-03 | 3.78E-04 | 1.14E-04 | 2.72E-05 | 2.71E-06 | | **0.04** |
| **270 to 285** | 4.94E-03 | 8.82E-03 | 6.08E-03 | 3.98E-03 | 2.77E-03 | 1.33E-03 | 7.93E-04 | 4.40E-04 | 1.98E-04 | 5.70E-05 | 2.17E-06 | 8.15E-06 | **0.03** |
| **285 to 300** | 4.38E-03 | 8.00E-03 | 5.89E-03 | 3.95E-03 | 2.94E-03 | 1.78E-03 | 8.45E-04 | 5.62E-04 | 1.90E-04 | 8.42E-05 | 2.17E-05 | | **0.03** |
| **300 to 315** | 5.13E-03 | 9.63E-03 | 6.26E-03 | 5.20E-03 | 3.13E-03 | 2.10E-03 | 1.02E-03 | 4.56E-04 | 1.11E-04 | 1.25E-04 | 4.35E-05 | | **0.03** |
| **315 to 330** | 6.32E-03 | 1.19E-02 | 9.76E-03 | 5.83E-03 | 3.59E-03 | 2.50E-03 | 1.53E-03 | 7.63E-04 | 5.02E-04 | 2.04E-04 | 4.07E-05 | | **0.04** |
| **330 to 345** | 1.07E-02 | 2.00E-02 | 1.59E-02 | 9.10E-03 | 6.18E-03 | 2.97E-03 | 1.76E-03 | 8.85E-04 | 4.64E-04 | 8.15E-05 | 8.15E-06 | | **0.07** |
| **345 to 360** | 1.78E-02 | 3.72E-02 | 2.51E-02 | 1.20E-02 | 5.97E-03 | 2.14E-03 | 1.05E-03 | 3.04E-04 | 4.07E-05 | | | | **0.10** |
| **total** | **0.12** | **0.31** | **0.23** | **0.13** | **0.07** | **0.04** | **0.02** | **0.01** | **0.00** | **0.00** | **0.00** | **0.00** | **1.00** |

## B.3 MAIN MODEL PARAMETER SETTINGS

TABLE 8: MAIN MODEL PARAMETER SETTINGS OF THE DIFFERENT DELFT3D MODULES

| **Module** | **Parameter** | **Value** | **Description** |
|---|---|---|---|
| **Flow** | $\Delta t$ | 1 min/0.5 min | Timestep |
| | T | 15 days | Simulation time |
| | g | 9.813 m/s$^2$ | Gravitational acceleration |
| | $\rho_w$ | 1023 kg/m$^3$ | Water density |
| | $\rho_a$ | 1.205 kg/m$^3$ | Air density |
| | Roumet | M, Manning | Roughness formula type |
| | Ccofu | 0.024 m$^{1/2}$/s | Uniform bottom roughness in u-dir |
| | Ccofv | 0.024 m$^{1/2}$/s | Uniform bottom roughness in v-dir |
| | Vicouv | 1.0 m$^2$/s | Uniform horizontal eddy viscosity |
| | Dicouv | 0.5 m$^2$/s | Uniform horizontal eddy diffusivity |
| | Rouwav | FR84, Fredsou | Bottom stress formulation due to wave action |
| | Dryflc | 0.1 m | Threshold depth for drying and flooding |
| | Momsol | Cyclic | Advection scheme for momentum |
| | Trasol | Cyclic | Advection scheme for transport |
| **Transport** | MorUpd | False | Update bathymetry during FLOW simulation |
| | CmpUpd | True | Update composition during FLOW simulation |
| | MorStt | 1440 min | Spin-up interval from simulation start time till morphological changes |
| | EqmBc | True | Equilibrium concentration profile at inflow boundaries |
| | TraFrn | vanrijn07 | Sediment transport formula type |
| **Wave** | SpShapetype | JONSWAP | Wave spectrum shape type |
| | PeakEnhancFac | 3.3 | Peak enhancement factor for JONSWAP spectrum |
| | WaterLevel Correction | True | Include surge level |
| | GenmodePhys | 3 | Generation mode of physics |
| | Breaking | True | Include wave breaking |
| | BreakAlpha | 1.0 | Alpha coefficient for wave breaking |
| | BreakGamma | 0.73 | Gamma coefficient for wave breaking |
| | Triads | False | Include triads |
| | BedFriction | JONSWAP | Bed friction type |
| | BedFricCoef | 0.067 | Bed friction coefficient |
| | Diffraction | False | Include diffraction |
| | WindGrowth | True | Include wind growth |
| | WhiteCapping | Komen | White capping formula type |
| | Quadruplets | True | Include quadruplets |
| | Refraction | True | Include refraction |
| | FreqShift | True | Include frequency shifting in frequency space |
| | WaveForces | Dissipation 3d | Wave force computation method |
| | SimMode | Stationary | Computational mode |

## B.4 WATER LEVEL DATASET COMPARISON

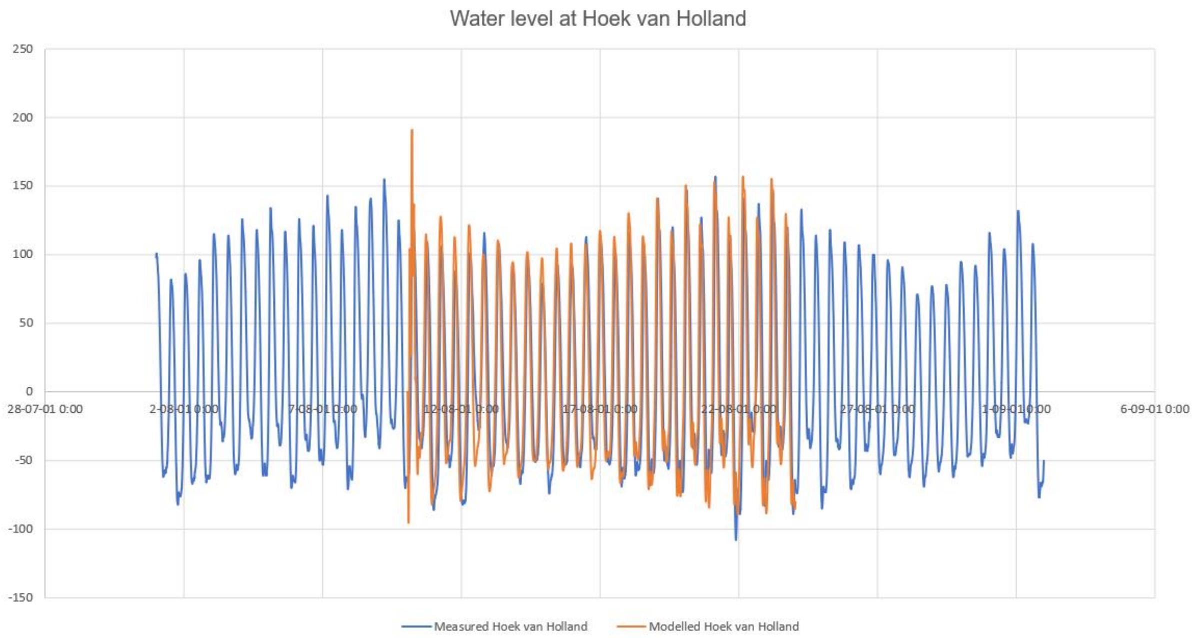


FIGURE 57: COMPARISON OF THE MEASURED AND MODELLED WATER LEVEL AT HOEK VAN HOLLAND (SOURCE MEASURED WATER LEVEL: (RIJKSWATERSTAAT 2020))

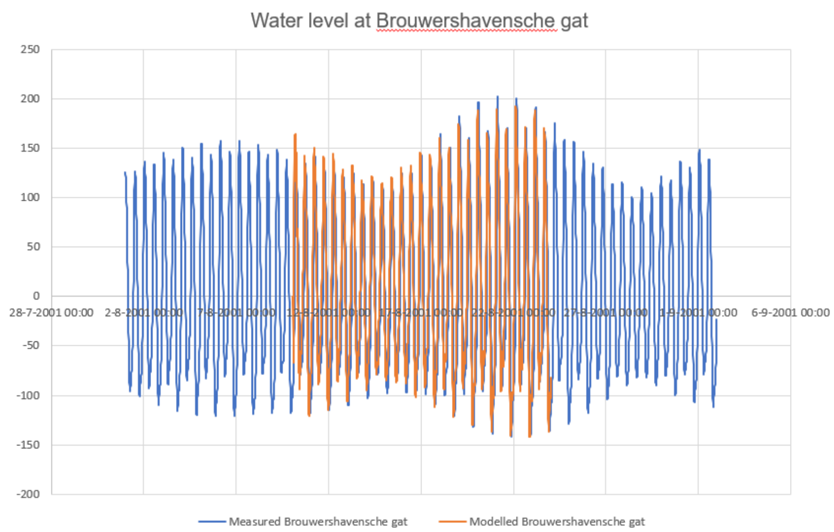


FIGURE 58: COMPARISON OF THE MEASURED AND MODELLED WATER LEVEL AT HOEK VAN HOLLAND (SOURCE MEASURED WATER LEVEL: (RIJKSWATERSTAAT 2020))

# APPENDIX C

## C.1 INTRODUCTION

In this appendix additional simulation results are shown. These results support the findings and results presented in Chapter 5. The additional results in this appendix concern the residual flow patterns.

## C.2 RESIDUAL FLOW PATTERN OF SIMULATION I. TIDE ONLY

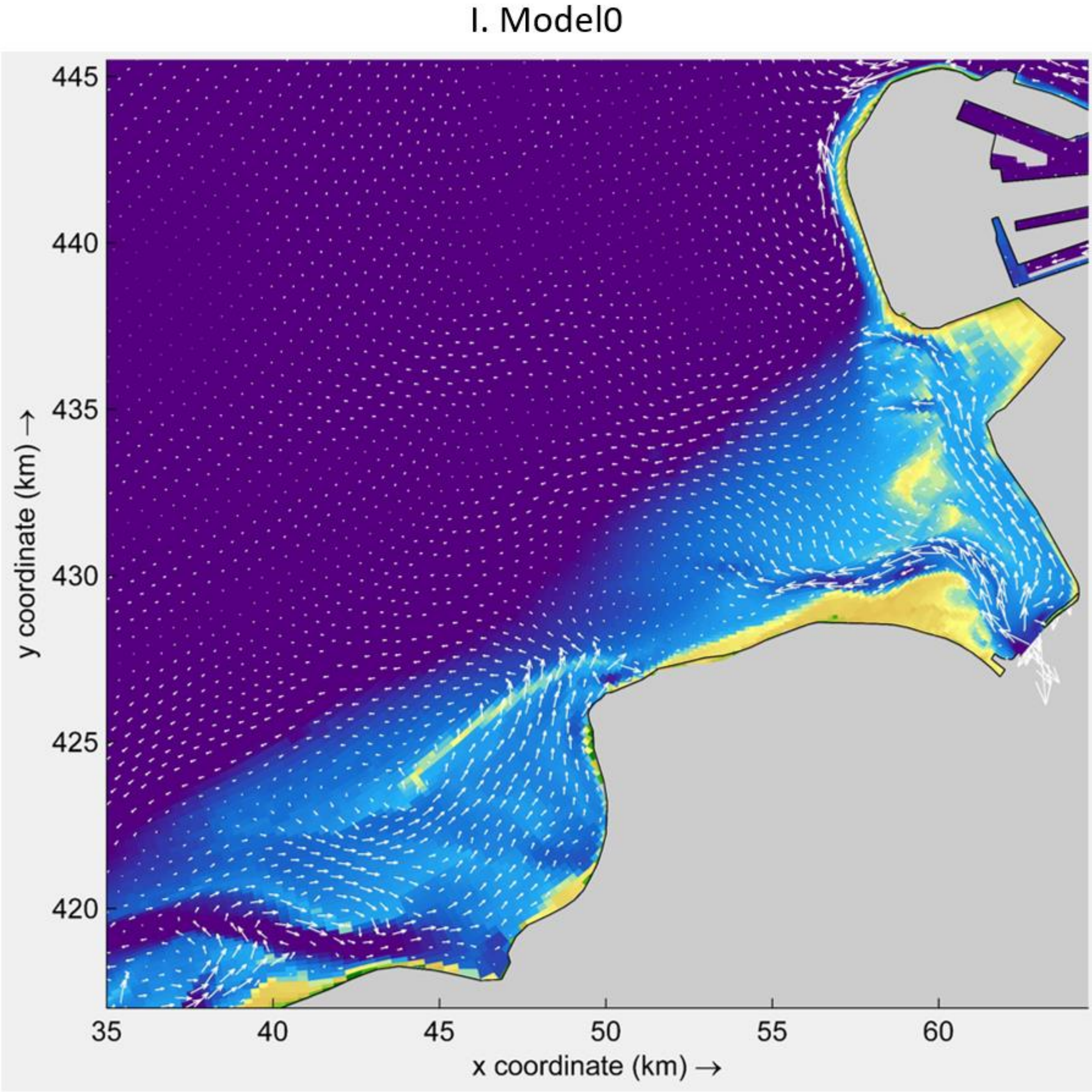


FIGURE 59: RESIDUAL FLOW PATTERN OVER A SPRING-NEAP TIDAL CYCLE, I.MODEL0

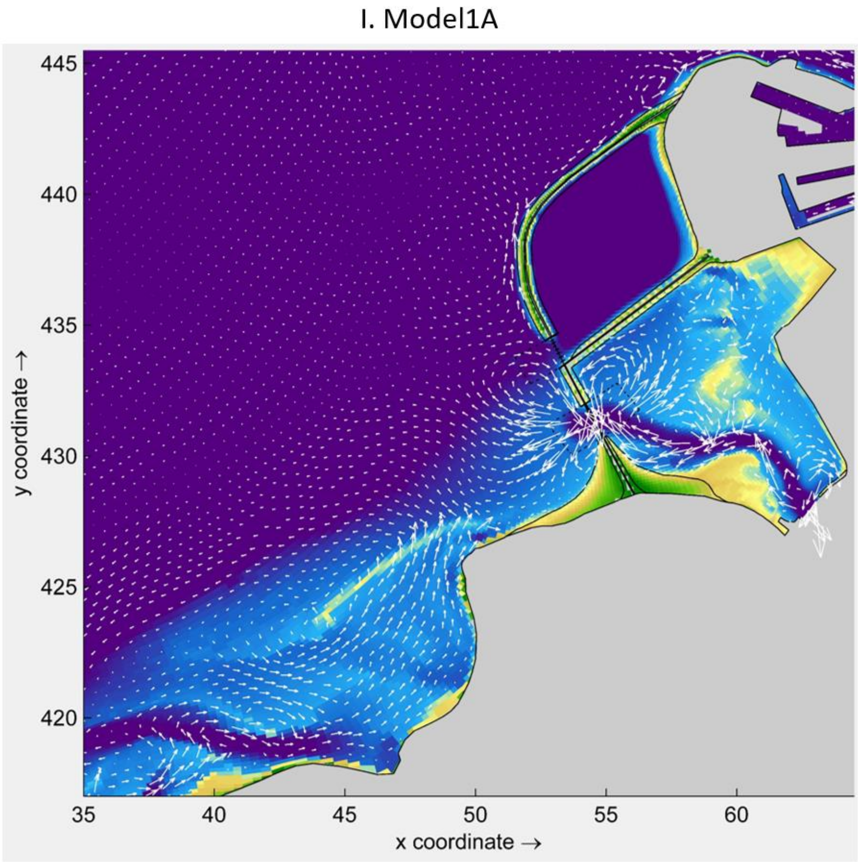


FIGURE 60: RESIDUAL FLOW PATTERN OVER A SPRING-NEAP CYCLE, I.MODEL1A

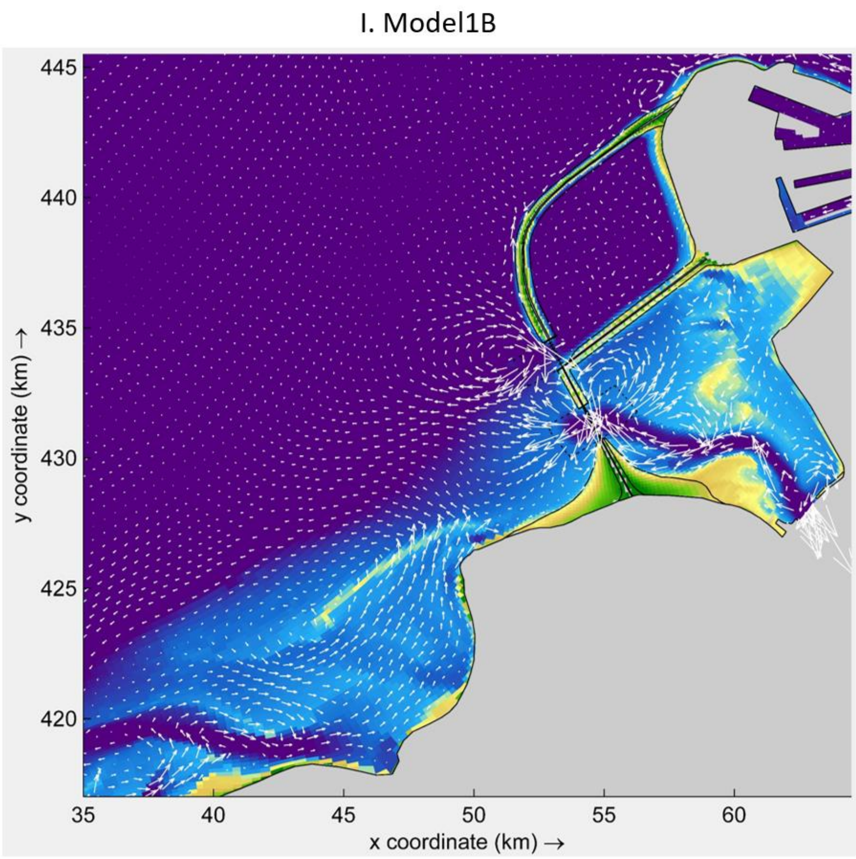


FIGURE 61: RESIDUAL FLOW PATTERN OVER A SPRING-NEAP CYCLE, I.MODEL1B

### C.3 Residual currents of simulation III. All processes

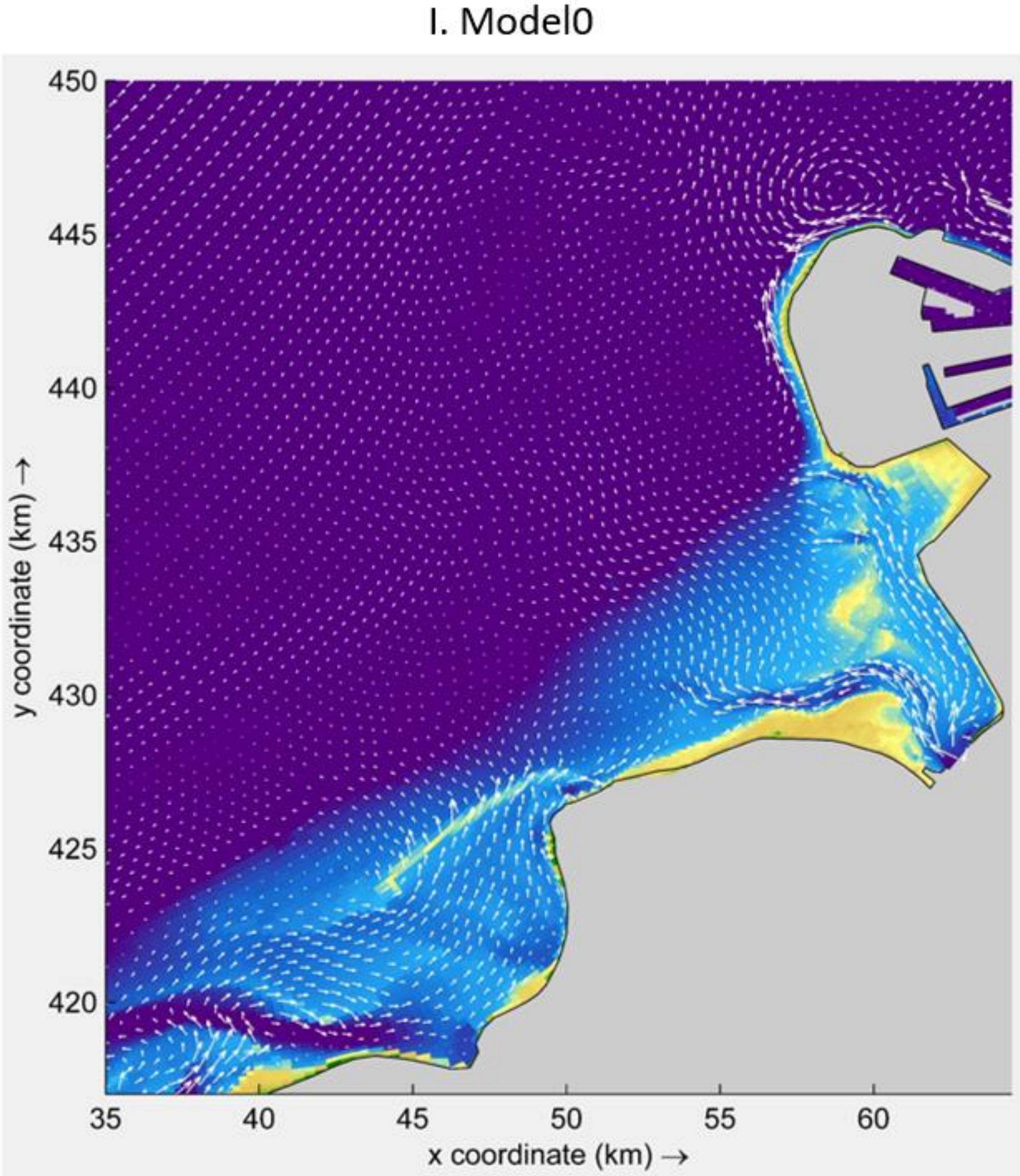


FIGURE 62: RESIDUAL FLOW PATTERN OVER A SPRING-NEAP CYCLE, III.MODEL0

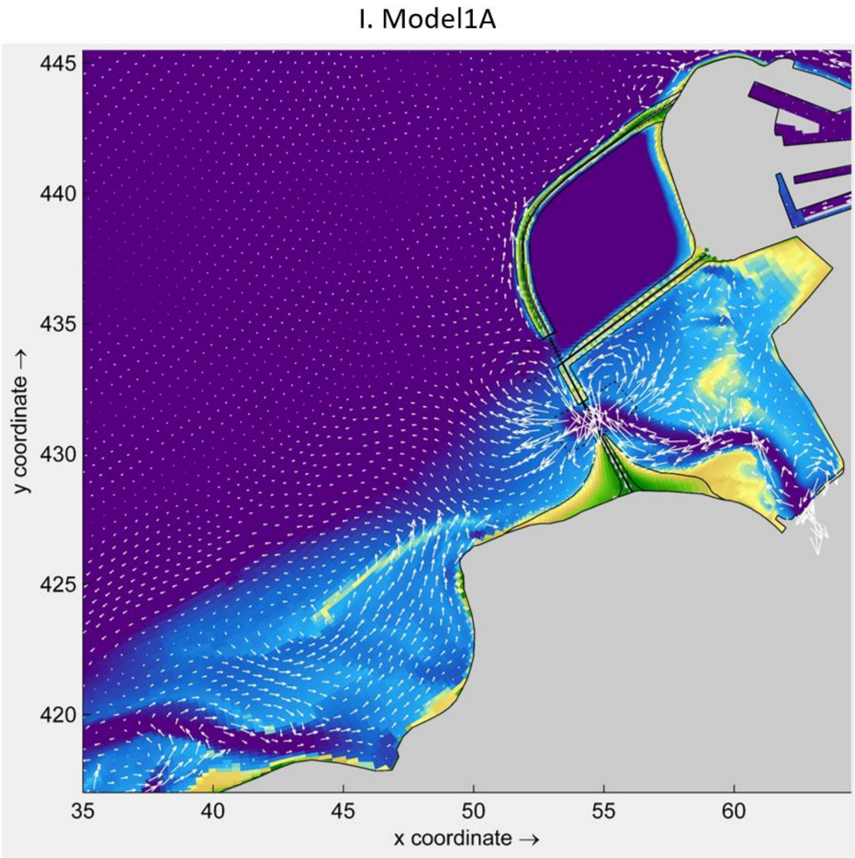


FIGURE 63: RESIDUAL FLOW PATTERN OVER A SPRING-NEAP CYCLE, III.MODEL1A

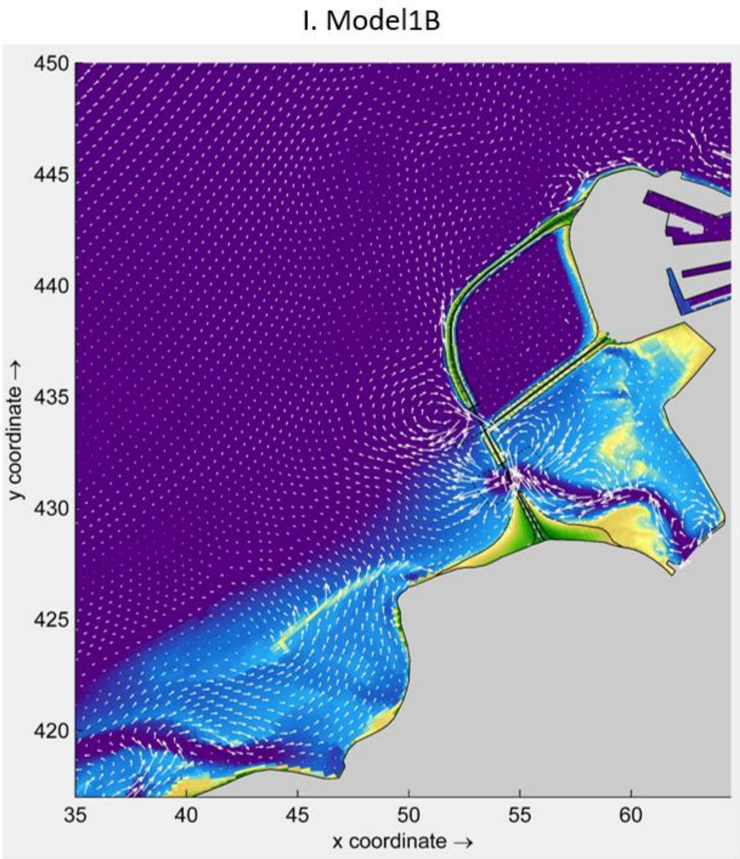


FIGURE 64: RESIDUAL FLOW PATTERN OVER A SPRING-NEAP CYCLE, III.MODEL1B

## C.4 Additional flow patterns

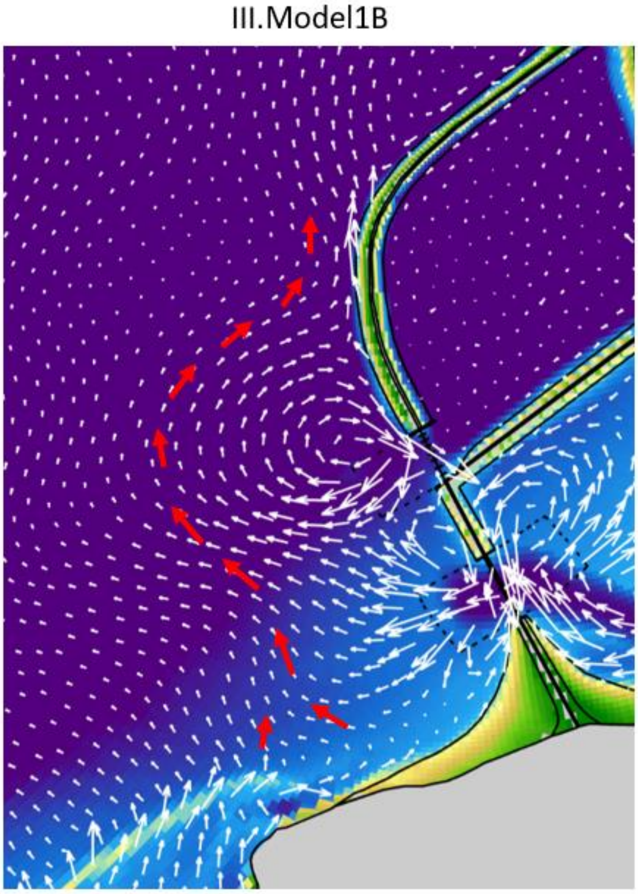


FIGURE 65: BYPASSING EFFECT OF THE LONGSHORE CURRENT

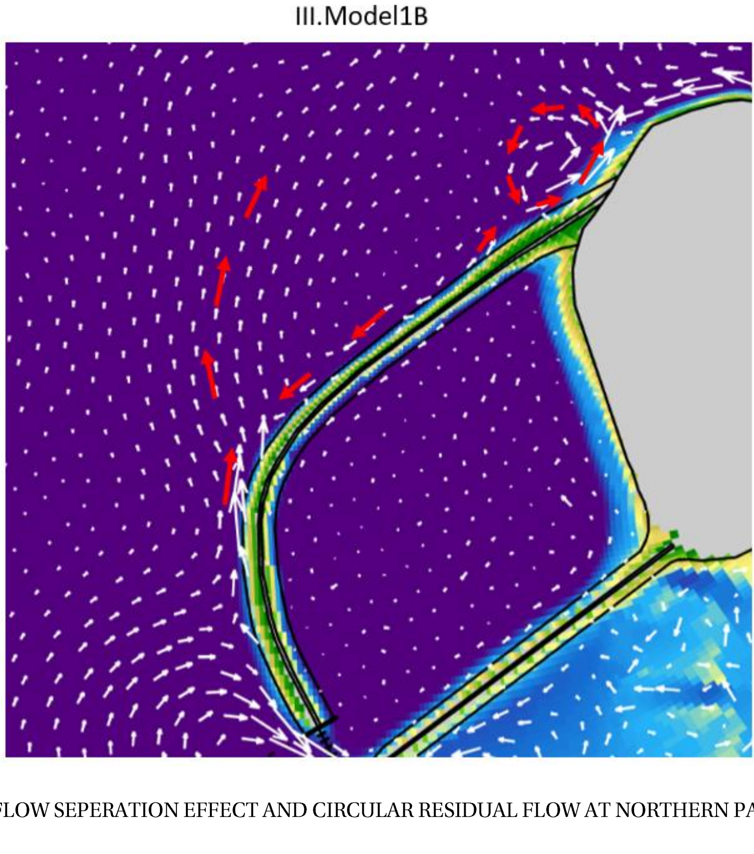


FIGURE 66: FLOW SEPERATION EFFECT AND CIRCULAR RESIDUAL FLOW AT NORTHERN PART DELTA21

## C.5 Residual flow magnitudes

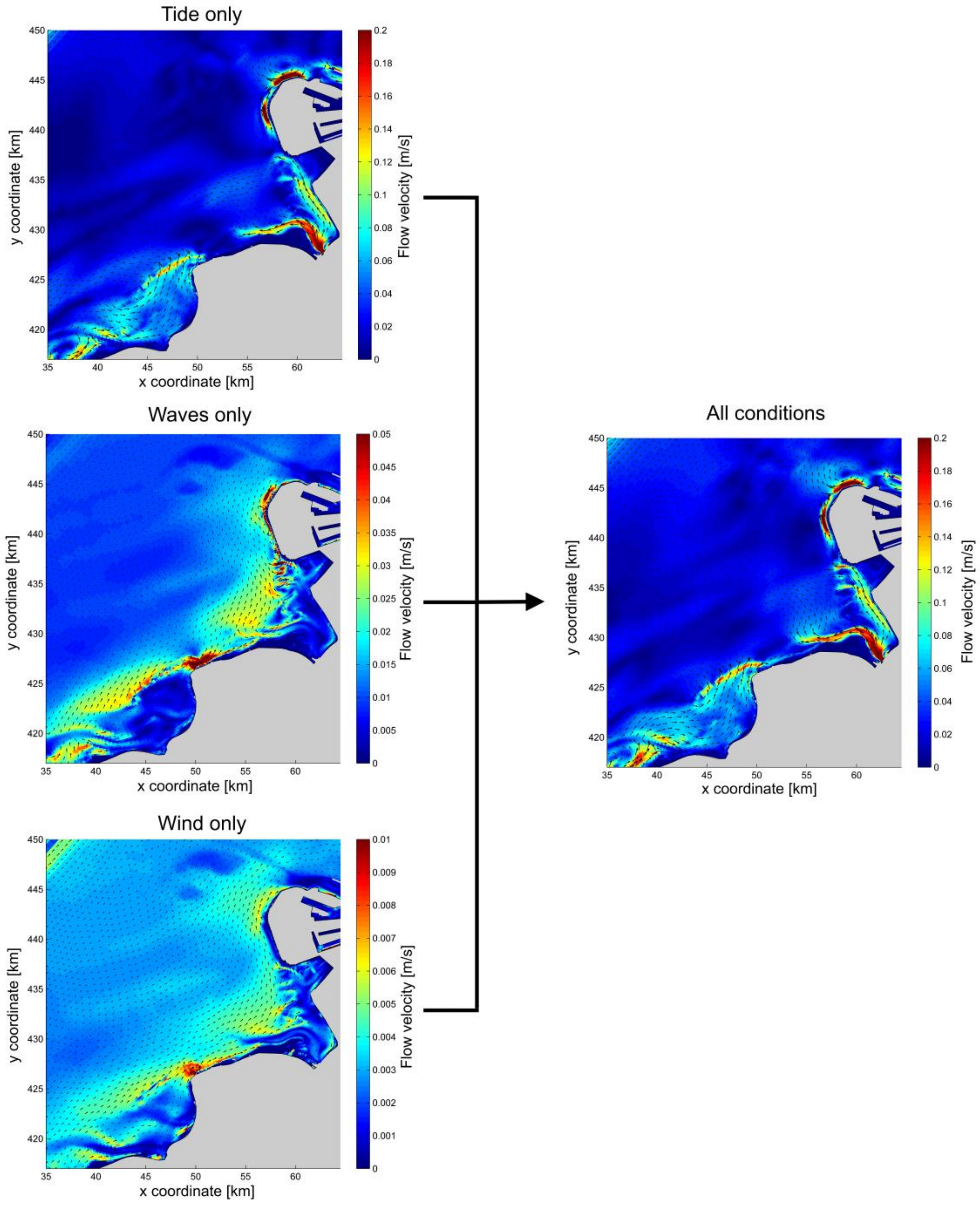


FIGURE 67: RESIDUAL FLOW MAGNITUDES (MODEL0) OF THE THREE ACTING PROCESSES, THE COLOR BARS SHOW THEIR RELATIVE IMPORTANCE TO THE OVERALL RESIDUAL FLOW MAGNITUDES

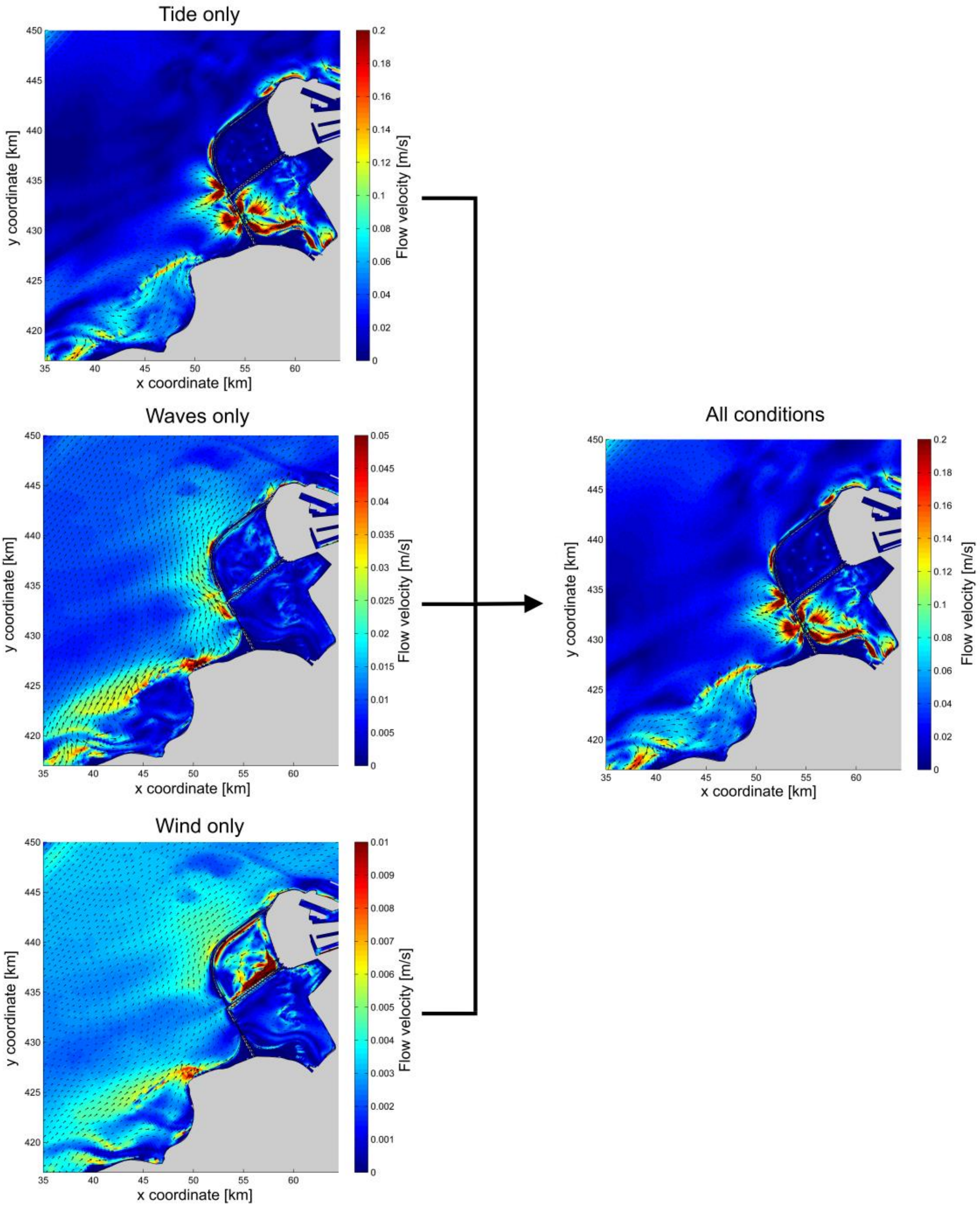


FIGURE 68: RESIDUAL FLOW MAGNITUDES (MODEL1B) OF THE THREE ACTING PROCESSES, THE COLOR BARS SHOW THEIR RELATIVE IMPORTANCE TO THE OVERALL RESIDUAL FLOW MAGNITUDES

# APPENDIX D

## D.1 INTRODUCTION

In this appendix additional simulation results are shown. These results support the findings and results presented in Chapter 5. The additional results in this appendix concern the sediment transport and sedimentation and erosion patterns.

## D.2 ADDITIONAL RESULTS REGARDING SEDIMENT TRANSPORT

Figure 69: Shows the net sediment transport patterns inside the Grevelingen outer delta. Both III.Model0 and III.Model1B results are shown and up until the east side of the Bollen van de Ooster there are no significant differences between the two scenarios.

Figure 70: Shows the net sediment transport patterns at the east side of the Bollen van de Ooster of both III.Model0 and III.Model1B. In the III.Model1B scenario opposing transport patterns can be observed where a net north eastern directed transport is present at the west side and a net western directed transport just outside the tidal inlet. These opposing transports cause an area of small transport rates in between that is directed north. Sediment is bypassed along the seaward side of the tidal inlet and the pump station.

Figure 71: Shows the difference between the transport rates of I.Model1B (tide only) and III.Model1B (all processes). As described in Chapter 6, the waves in III.Model1B do not change the direction of the net sediment transport. The transport rates however, are higher for the simulation with waves.

Figure 72: Shows the net sediment transport rates through the transects of III.Model1A and III.Model1B. III.Model1A does not include the effect of the ESL pump station as can be seen in the low transport rates just in front of that pump station. Including the pump station (III.Model1B), causes a NW directed net sediment transport which can be related to the outflow of the pump station.

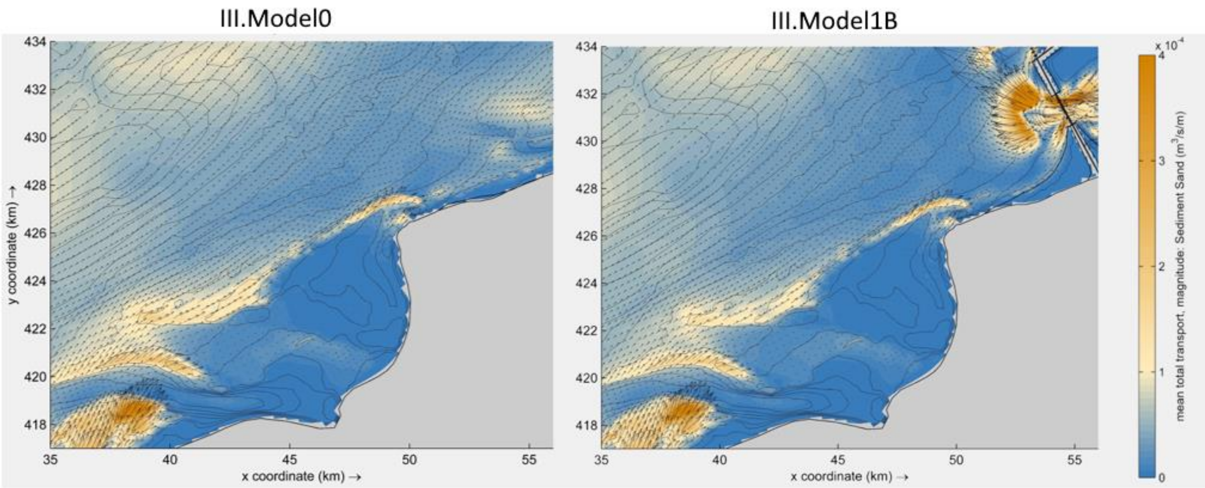


FIGURE 69: DIFFERENCE IN NET SEDIMENT TRANSPORT PATTERNS AT THE GREVELINGEN OUTER DELTA

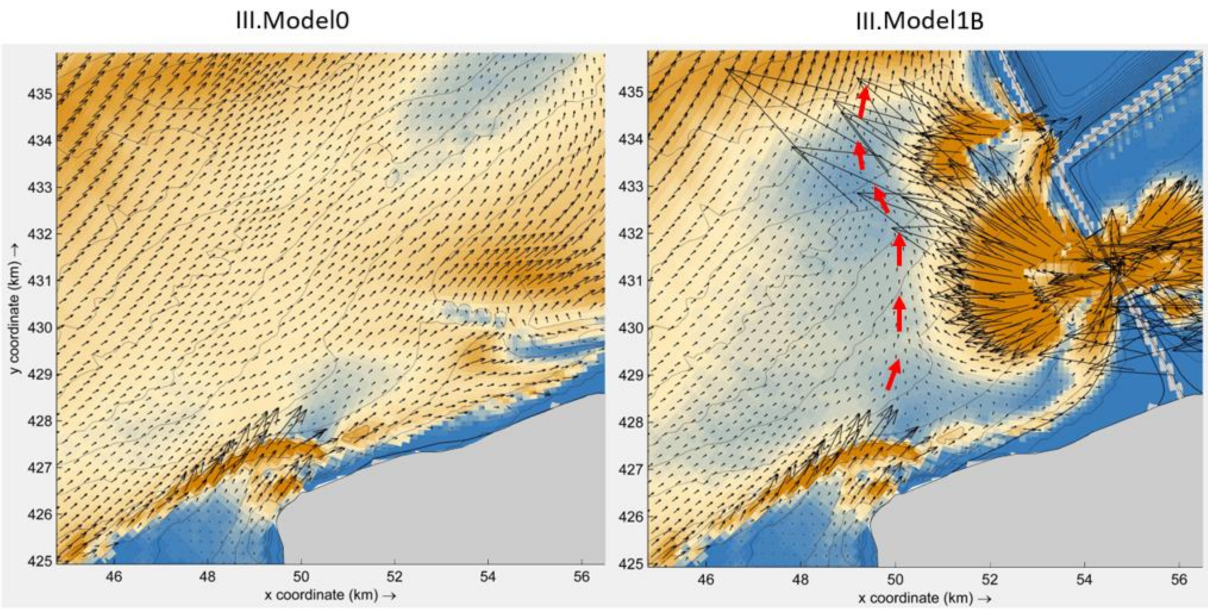


FIGURE 70: BYPASSING EFFECT AT NW SIDE OF THE BOLLEN VAN DE OOSTER

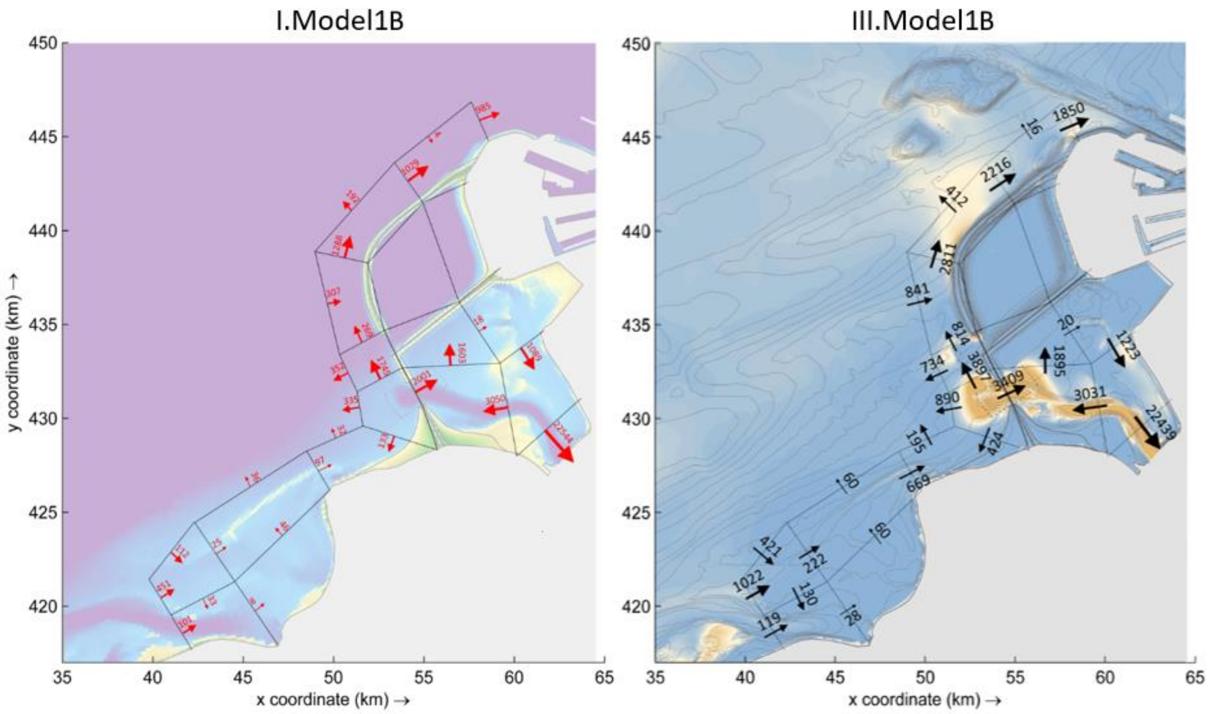


FIGURE 71: DIFFERENCE BETWEEN TIDE ONLY AND TIDE+WAVES

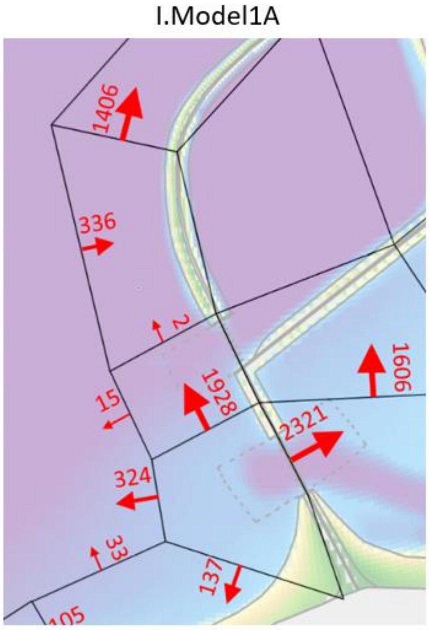


FIGURE 72: EFFECT OF PUMP STATION ON NET SEDIMENT TRANSPORT RATES

## D.3 ADDITIONAL RESULTS REGARDING SEDIMENTATION/EROSION PATTERNS

Figure 73: Shows the initial sedimentation and erosion patterns for the SW waves and the NE waves. The major differences are found around the NW corner of Delta21.

Figure 74: Shows the initial sedimentation and erosion patterns of each wave condition. The wave conditions are plotted from highest to lowest probability of occurrence.

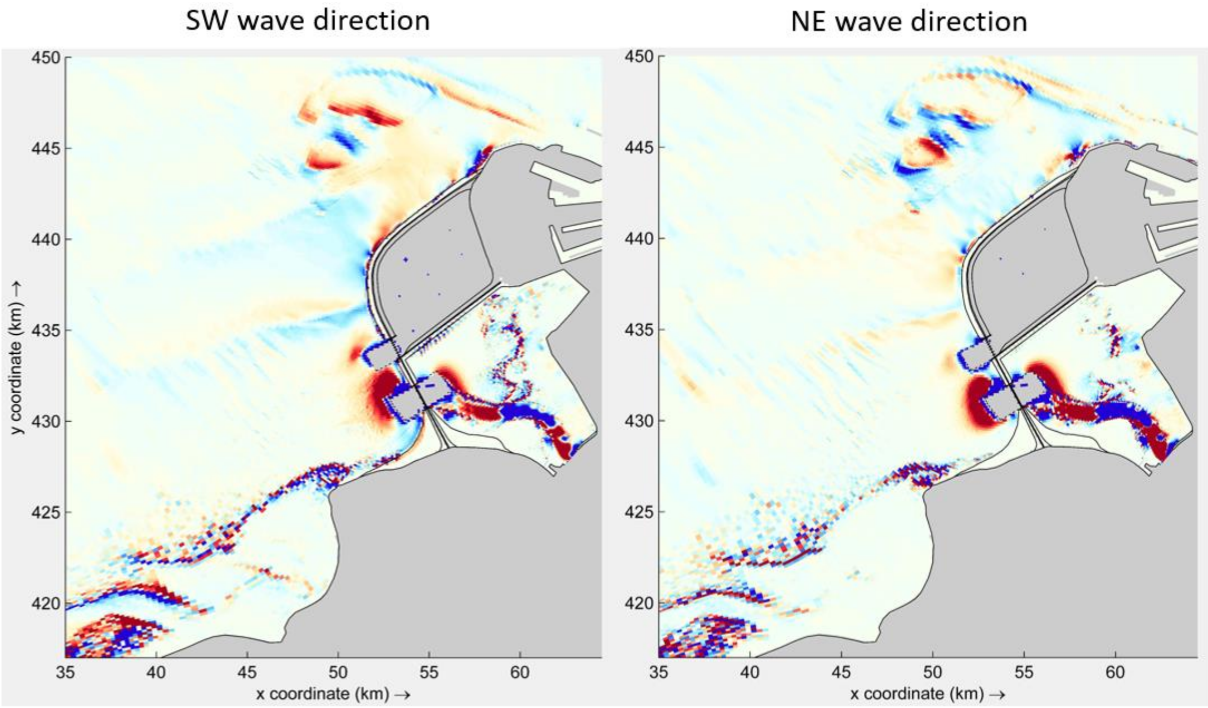


FIGURE 73: ISE FOR SW AND NE WAVE DIRECTION, III.MODEL1B

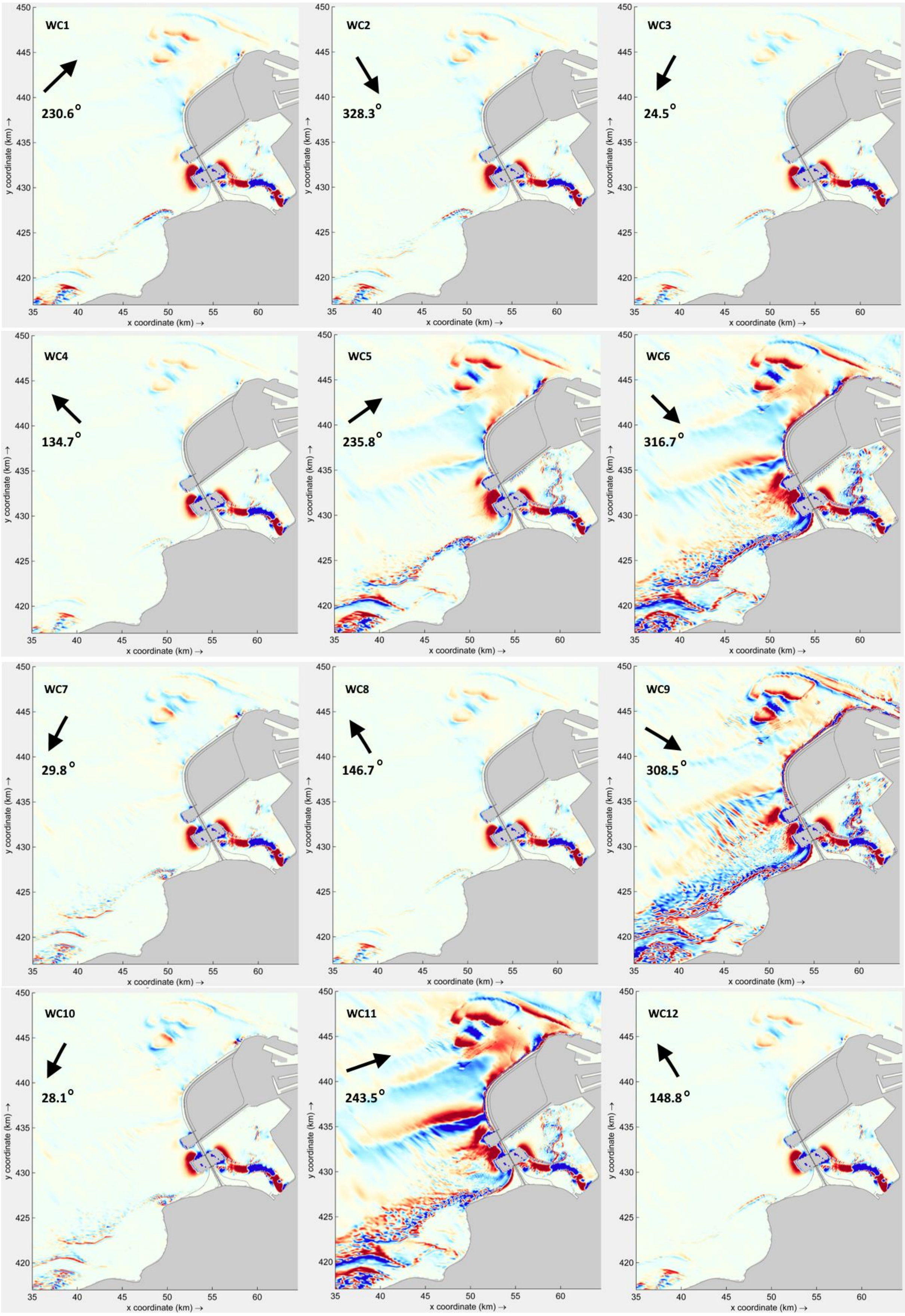


FIGURE 74: SED/ERO PATTERN OF EACH WAVE CONDITION, III.MODEL1B

# APPENDIX E

## E.1 INTRODUCTION

This appendix provides supporting information to the conceptual model as presented in Chapter 6.

## E.2 ADDITIONAL PLOTS REGARDING THE CONCEPTUAL MODEL

Figure 75: Additional plot of the 5 year bathymetry change in front of the pump station. The expected evolution of this area is addressed as part of the conceptual model in Chapter 6.

Figure 76: Additional plot of the 5 year bathymetry change along the NW Delta21 corner. The expected evolution of this area is addressed as part of the conceptual model in Chapter 6.

Figure 77: Shows the change of the residual flow after using the model with the 0 years (relative to the implementation of Delta21) bathymetry and the 5 years bathymetry. The plot acts as supporting information to the conceptual model in Chapter 6.

Figure 78: Shows the change of the residual sediment transport after using the model with the 0 years (relative to the implementation of Delta21) bathymetry and the 5 years bathymetry. The plot acts as supporting information to the conceptual model in Chapter 6.

Figure 79: Shows the change of the sedimentation and erosion patterns after using the model with the 0 years (relative to the implementation of Delta21) bathymetry and the 5 years bathymetry. The plot acts as supporting information to the conceptual model in Chapter 6.

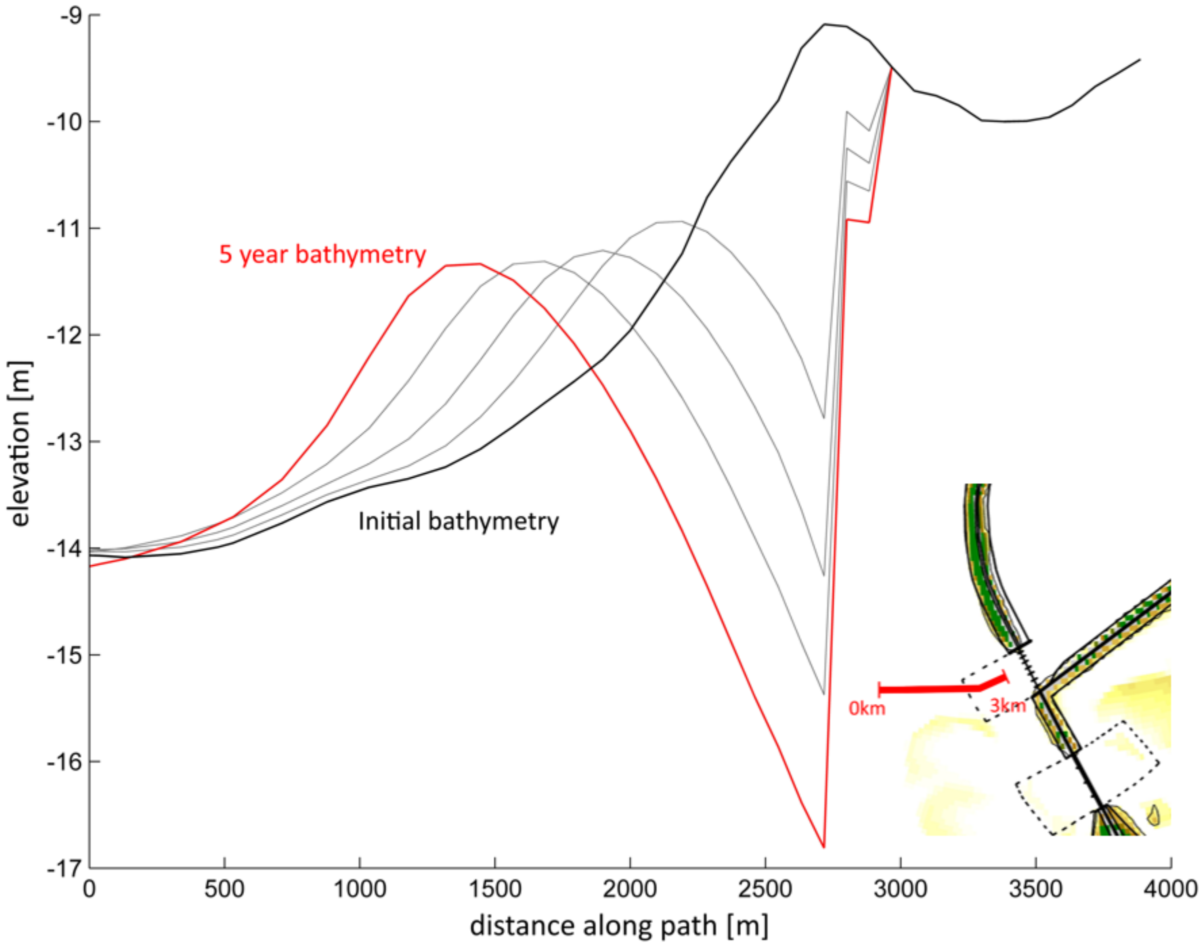


FIGURE 75: EXPECTED MORPHOLOGICAL EVOLUTION IN FRONT OF THE PUMP STATION

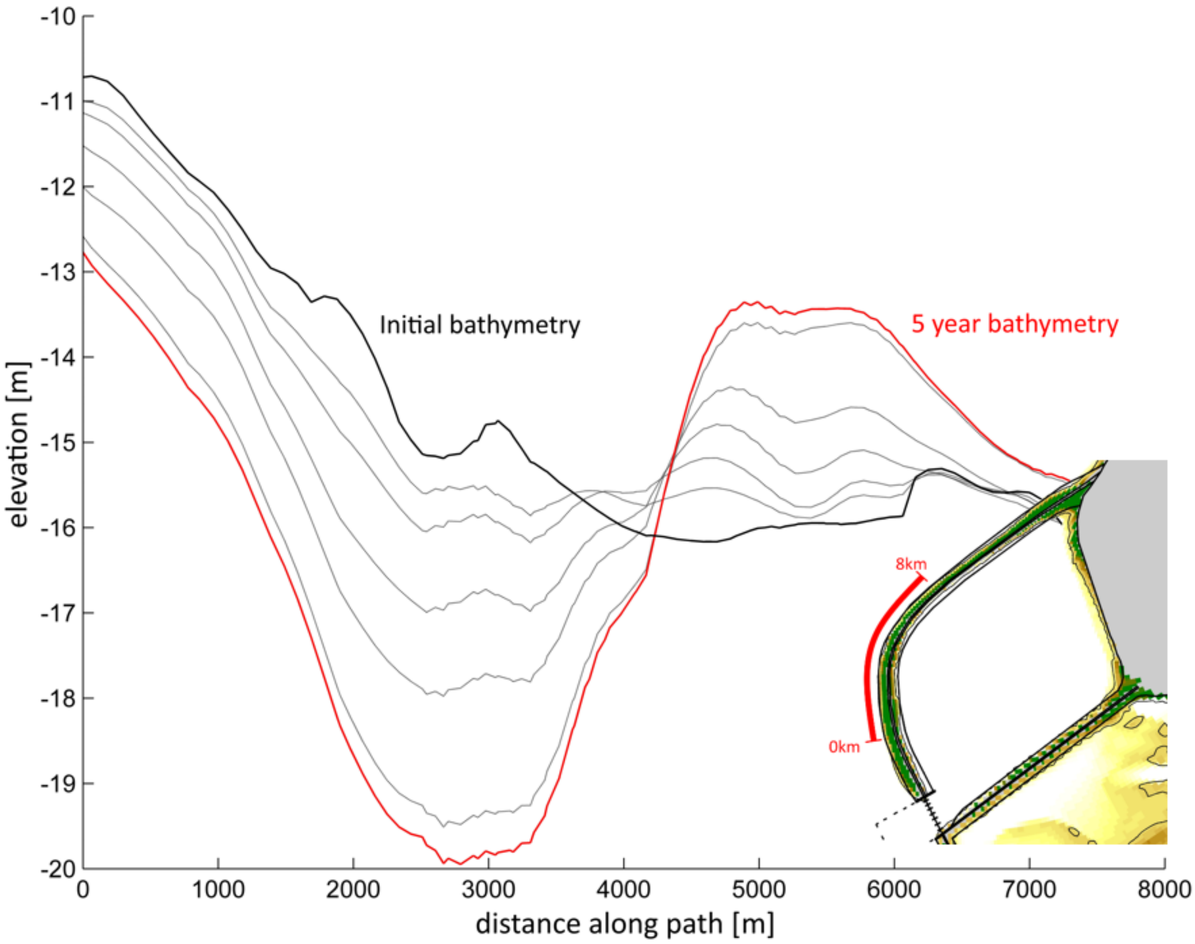


FIGURE 76: EXPECTED MORPHOLOGICAL EVOLUTION ALONG THE NW DELTA21 CORNER

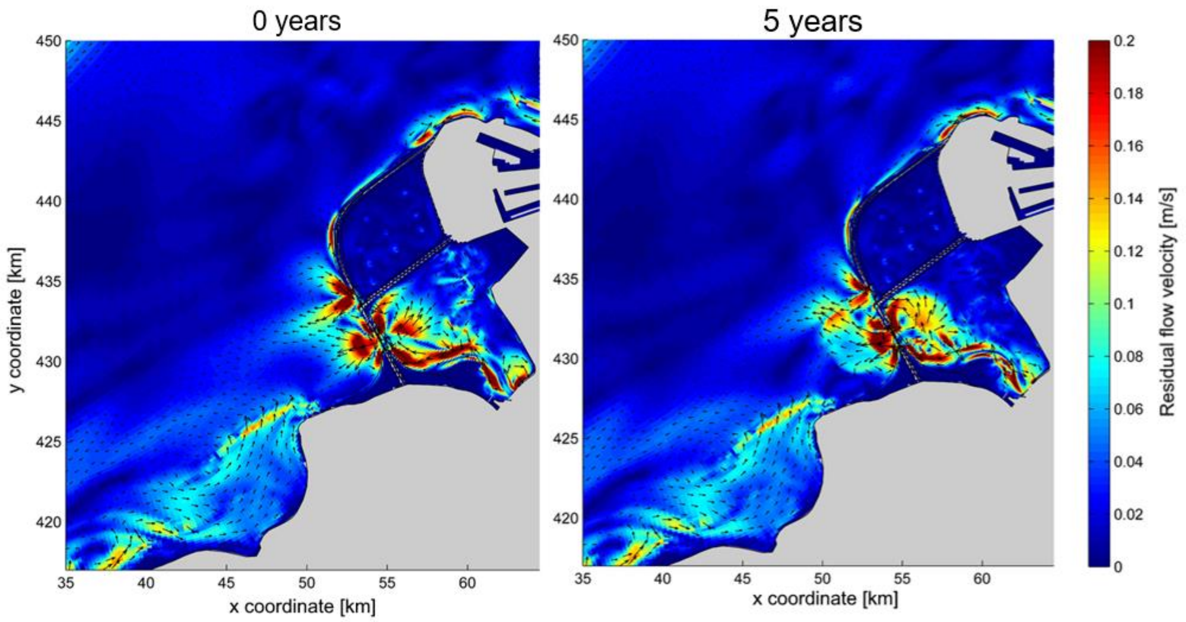


FIGURE 77: EXPECTED CHANGE OF THE TIDAL RESIDUAL FLOW

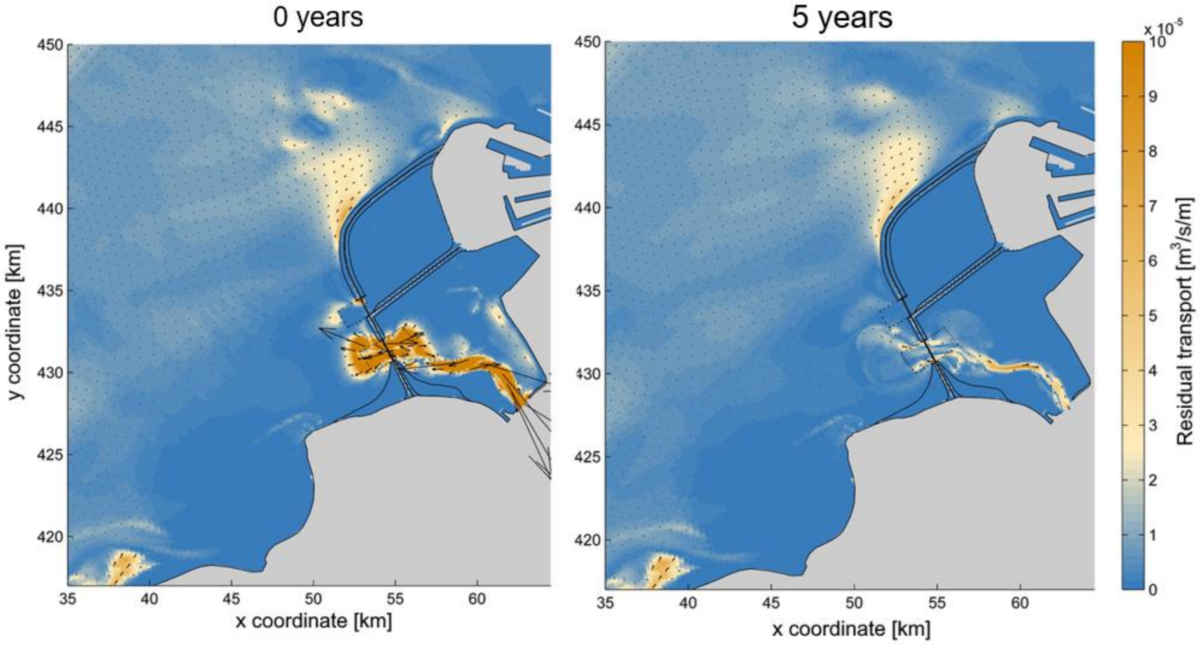


FIGURE 78: EXPECTED CHANGE OF THE TIDAL RESIDUAL TRANSPORT

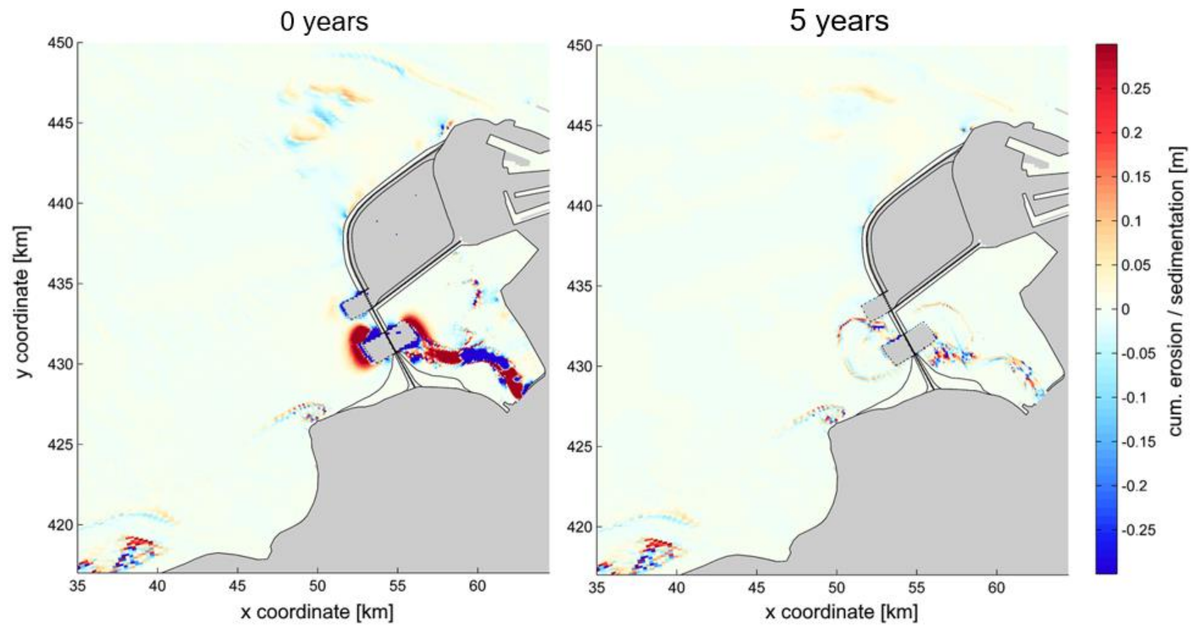


FIGURE 79: EXPECTED CHANGE OF THE SEDIMENTATION AND EROSION PATTERNS